A DETERMINISTIC APPROACH TO TRANSITION TO TURBULENCE IN PLANE SHEAR FLOWS

by

Salim Kunt Atalık

BS. in M.E. Boğaziçi University, 1991

MS. in M.E. Boğaziçi University, 1993

Submitted to the Institute for Graduate Studies in
Science and Engineering in partial fulfillment of
the requirements for the degree of
Doctor
of
Philosophy

Boğaziçi University

1999

ACKNOWLEDGMENTS

I would like to thank to my thesis supervisor Prof. Dr. Akın Tezel for his guidance and support throughout the study. I'm also grateful to the members of the examining committee, Prof. Dr. Erdoğan S. Şuhubi, Doç. Dr. Haluk Örs, Doç. Dr. Osman Börekçi and Yrd. Doç. Dr. Ali Ecder for their careful review of the thesis and corrections. I should also mention that the thesis has partially been supported by Boğaziçi University Research Fund with project code 96HA0626.

Finally, I would like to express my gratitude to my family for their understanding and help throughout my study life.

ABSTRACT

In this work, a parametrical study of the transition to turbulence in two-dimensional shear flows has been conducted. For this purpose, the solutions of the full two-dimensional Navier-Stokes equations have been investigated numerically using spectral methods. In parallel, a new spectral integration algorithm, called the Nonlinear Galerkin Method, stemming from dynamical systems theory and developed for the integration of dissipative evolution equations such as Navier-Stokes equations, has been tested and applied for the study cases. Different nonlinear Galerkin methods have been compared for this purpose with respect to each other in terms of convergence and efficiency and the improvements on the classical Galerkin spectral method have been shown numerically. Transition to turbulence has been analyzed by the parametrical investigation of qualitatively different solutions in the phase space of two-dimensional Navier-Stokes equations for bounded and unbounded shear flows with one nonhomogeneous direction. The applications were plane channel (Poiseuille) flow and oscillatory plane Poiseuille flow for the bounded flow case, and temporally growing mixing layer and plane jet flows for the unbounded flow case.

With this work, we aim to contribute to the enlightening of the structure of the phase space of two-dimensional Navier-Stokes equations as well as to the testing of a new integration algorithm which seems to be promising in the direct numerical simulation of Navier-Stokes equations.

ÖZET

Bu çalışmada, kayma akışlarında, iki boyutlu türbülansa geçiş mekanizmasının parametrik bir incelemesi yürütülmüştür. Bu amaçla, iki boyutlu Navier-Stokes denklemlerinin sayısal çözümlerinin spektral yöntemlerle araştırılmasına gidilmiştir. Buna paralel olarak, dinamik sistemler teorisinden yola çıkılarak, Navier-Stokes denklemleri gibi yitimli evrim denklemlerinin integrasyonu için geliştirilen, yeni bir spektral integrasyon algoritması, lineer olmayan Galerkin yöntemi, incelenen problemlerde test edilmiş ve uygulanmıştır. Farklı lineer olmayan Galerkin algoritmaları, yakınsama ve etkinlik bakımlarından karşılaştırılmış ve yöntemin klasik Galerkin spektral yöntemine göre sağladığı düzeltmeler sayısal olarak gösterilmiştir. Türbülansa geçiş, bir homojen olmayan doğrultuya sahip sınırlı ve sınırsız kayma akışlarında, iki boyutlu Navier-Stokes denklemlerinin faz uzayında niteliksel olarak değişik çözümlerinin parametrik incelenmesiyle araştırılmıştır. Uygulama problemleri, sınırlı akış durumunda düzlem kanal (Poiseuille) akışı ve salınımlı düzlem Poiseuille akışı; sınırsız akış durumunda ise zamansal büyüyen karışım tabakası ve düzlem jet akışlarıdır.

Bu çalışmayla, iki boyutlu Navier-Stokes denklemlerinin faz uzayının yapısının aydınlatılmasına ve Navier-Stokes denklemlerinin doğrudan sayısal benzetimi için umut verici olduğu düşünülen yeni integrasyon algoritmalarının test edilmesine katkıda bulunmak amaçlanmıştır.

TABLE OF CONTENTS

LIST OF FIGURES

LIST OF TABLES

LIST OF SYMBOLS

$\mathbf{a}$	Vector representing spectral expansion coefficients
$a_{km}(t)$	Time dependent spectral expansion coefficients
a_n	Spectral expansion coefficients for Orr-Sommerfeld eigenvectors
A	Stokes operator
A_{km}	Perturbation constant in subharmonic excitation
A	The global attractor
b	Velocity profile thickness in plane jet flow
B	A bounded subset of Hilbert space
$B(\mathbf{u})$	Vector representing the nonlinear terms
c	Eigenvalue of the Orr-Sommerfeld stability equation
C_{ijk}	Turbulent diffusion correlation tensor
$dist$	Distance function
$E(k)$	Energy spectral density of turbulence
$\mathbf{f}$	Body force or forcing vector
$F(\mathbf{a})$	Vector involving nonlinear terms
h	Channel half-width
H	Hilbert space
$H(y)$	Hermite polynomials
I	The identity operator
k	Wavenumber
K	Turbulent kinetic energy
l	Macroscopic (integral) length scale
l_0	Turbulent length scale
l_d	Viscous dissipation length scale
L	Wave length (Period length)
M	The inertial manifold
M	Linear matrix
N	Number of degrees of freedom
N	Linear matrix

p	Kinematic pressure field
p'	Fluctuating pressure field
$\overline{p}$	Mean kinematic pressure field
P	Mean pressure gradient
P_m	Projection operator
Q	Nondimensional total flux in oscillatory Poiseuille case
Q_L	Laminar flux
Q_m	Projection operator
Q_{2n}	Expansion functions for the Orr-Sommerfeld eigenfunction
Q_T	Total flux in channel flow
Re	Integral Reynolds number
Re_P	Reynolds number based on pressure
Re_Q	Reynolds number based on flux
Re_τ	Wall Reynolds number
$S(t)$	Semi-group of nonlinear operators
t	Nondimensional time
$T(y)$	Chebyshev polynomials
$\mathbf{u}$	Velocity vector
u	Streamwise velocity component
u_i'	Fluctuating velocity components
$\overline{u}_i$	Mean velocity components
U	Laminar velocity profile
U_0	Maximum velocity in free shear flows
v	Cross-stream velocity component
V	Centerline velocity in channel flow
V	Volume
$w(y)$	Weight function
$W(y,t)$	Oscillatory part of the laminar velocity profile in channel flow
$\mathbf{y}$	Large scales of motion
$\mathbf{z}$	Small scales of motion
α	Disturbance wavenumber

β	Ratio of the channel half-width to Stokes layer thickness
β_i	Amplification factor
β_r	Circular frequency of oscillation
δ	Stokes layer thickness
δ_i	Initial vorticity thickness
δ_{ij}	Kronecker delta symbol
Δ	Ratio of the amplitude of the oscillatory to steady velocity
ε	The average rate of energy dissipation per unit mass
ε_{ij}	Turbulent dissipation rate correlation tensor
$\phi(y)$	Eigenfunctions of the Orr-Sommerfeld stability equation
$\Phi(y)$	Graph of the inertial manifold
$\Phi_m(y)$	Cross-stream spectral expansion functions
η	Kolmogorov scale
Λ	Ratio of the amplitude of the oscillatory to constant flux
ν	Kinematic viscosity
ν_T	Eddy viscosity
Π_{ij}	Pressure strain rate correlation tensor
θ	Phase shift between fundamental and subharmonic modes
$\Sigma(t)$	Finite-dimensional semi-group of nonlinear operators
τ	Time step
τ_0	Turbulent time scale
τ_{ij}	Turbulent stress tensor
ω	Frequency of the oscillatory flux
Ω	Dimensionless frequency of the oscillatory flux
ψ	Streamfunction

1. INTRODUCTION

In fluid mechanics, there is a general consensus on the fact that the Navier-Stokes equations of motion, derived from local continuum theory, present a good model for fluid motion in both laminar and turbulent flow regimes.

It is possible to show that the smallest scales of motion encountered in turbulent regime are much larger than the molecular scales of motion, hence turbulence is a continuum phenomenon (Tennekes and Lumley, 1972). However, there have been attempts in the literature to re-formulate fluid motion by taking into account the effects of long-range forces and long-range interatomic interactions on the motion and the evolution of the state of the fluid, which are ignored in local continuum physics. Polar theories of first grade have found applications in turbulence. As documented in Eringen (1974), the microfluid theory, first given by Eringen (1964) uncovered new balance laws (conservation of microinertia) and presented the basic equations of polar fluids with deformable directors (micromorphic fluids). Nonlocal fluid mechanics (Eringen, 1972) and nonlocal microfluid mechanics (Eringen, 1973) are the consequent developments in these attempts. However, the mathematical and computational difficulties encountered even in the treatment of the simplest possible continuum formulation as the Navier-Stokes equations of motion, concentrated the efforts of fluid mechanics researchers on the solution of these equations rather than more complicated field equations that polar and nonlocal theories give rise to.

The incompressible Navier-Stokes equations in variational form have at least one solution. In two dimensions the solution is unique. In three dimensions the solution is unique provided the data and the solution itself are sufficiently smooth (Mohammadi and Pironneau, 1994). In turbulence one cannot generally prove this type of regularity for the solution. As stated in Temam (1995), Leray's conjecture (Leray, 1933; Leray, 1934a-b) on turbulence was that the solutions in three dimensions are not smooth, the velocity or the vorticity becoming infinite at some points or on some small sets where turbulence would be located. It has been shown that singularities are local and their Hausdorff dimension is less than one (Caffarelli et al., 1982). So, the uniqueness for Navier-Stokes equations in three

space dimensions remains an open problem related to the regularity of solutions and continuous dependence on the initial data (Temam, 1995).

Besides the above mentioned mathematical difficulties, the numerical treatment of the Navier-Stokes equations, in turbulent regime, even for simplest geometries has difficulties. This is due to the fact that the nonlinearities in the equations give rise to a broad range of spatial and temporal turbulent scales. Estimates on the number of degrees of freedom of a turbulent flow, following the classical approach of Kolmogorov based on physical assumptions and a statistical analysis of the Navier-Stokes equations or the more recent mathematical proof of this same result (Constantin et al., 1983), by using the deterministic Navier-Stokes equations with the proper estimation of the dimension of the attractors in the phase space associated to their solutions are such that this number is of the order of,

$$N \propto (\frac{l}{l_d})^3 \tag{1.1}$$

where l is a typical macroscopic length and l_d is the viscous dissipation length. The largest turbulent scales are directly affected by the external conditions so that their structure and behavior may vary from one flow to another. These scales carry most of the turbulent kinetic energy and they are responsible for the major part of the turbulent diffusion. The smallest turbulent scales, however, are responsible for the major part of the dissipation of kinetic energy in the flow. A numerical simulation, to provide physical insight, has to resolve all scales present in the flow to cover both diffusion and dissipation. This aspect is pursued in the so-called direct numerical simulation approach (DNS), which is obviously related to the available computational resources. The scale disparity between the diffusive and dissipative length scales is a rapidly growing function of the Reynolds number. For incompressible free turbulence (space periodic boundary conditions in each direction), if the largest energy-containing eddies are characterized by an integral length scale l (a characteristic size of the flow region as the diameter of a turbulent jet) and the viscous scales with the Kolmogorov scale η,

$$\eta = (\frac{\nu^3}{\varepsilon})^{\frac{1}{4}} \tag{1.2}$$

where ν is the kinematic viscosity and ε is the average rate of energy dissipation per unit mass in the flow, the scale disparity in homogeneous isotropic turbulence is known to vary as (Tennekes and Lumley, 1972),

$$\frac{l}{\eta} \propto (\mathrm{Re})^{\frac{3}{4}} \tag{1.3}$$

where Re is the integral Reynolds number. The number of grid points to resolve the flow, scales in each direction with the above ratio. Therefore, for a full three-dimensional resolution the necessary number of grid points scales like $(\mathrm{Re})^{9/4}$.

In wall-bounded turbulent flows (with no-slip boundary conditions in at least one direction) where the size of the smallest eddies is determined by the thickness of the viscous wall layer which becomes very small at high Reynolds numbers, a thorough resolution is much more costly. The scale disparity, in that case, grows about linearly with the wall Reynolds number Re_τ which in turn is related to the integral Reynolds number Re based on the integral length scale and bulk velocity, with the empirical relation (Dean, 1978),

$$\mathrm{Re}_\tau \propto \mathrm{Re}^{\frac{7}{8}} \tag{1.4}$$

It follows that the number of grid points in a full three-dimensional simulation varies as $(\mathrm{Re})^{21/8}$.

Another important issue is that a high spatial resolution necessitates a high temporal resolution. If a statistical steady state is to be reached and evaluated, the total time of the simulation should be large enough to provide sufficient samples for all scales since the various scales of motion are not evenly sampled when statistics are taken from the individual realizations (Härtel, 1996).

For compressible flows, computational requirements are more drastic owing to the increase in the number of variables and the complexity of the system equations. Geophysical flows, where large-scale vortices may extend over thousands of kilometers while the dissipative scales are of centimeters or even millimeters in size, constitute an exceptional case since the required number of grid points for such flows has been estimated to be of the order of 10^{24} and this number should be compared to the currently feasible discretizations with the available supercomputers of the order of 10^7 or 10^8 (Härtel, 1996).

The above considerations show that the application of DNS is at present restricted to flows at moderate Reynolds numbers. This situation is not expected to change very much in the near future. The mathematical and computational difficulties associated with the solution of the Navier-Stokes equations imposed since the beginnings of the century, the re-modeling of the physics rather than the solution of the full, unsteady, three-dimensional equations.

1.1. Statistical Approaches

The relevant element of these traditional approaches can be restated as the irregularity condition of the flow in which the various quantities show a random variation with time and space coordinates so that statistically distinct averages exist (Hinze, 1959). In the statistical approach to turbulence, the ergodicity assumption in three dimensions is inherent in all theories developed. This assumption is crucial for statistical regularity and ensures not only the existence of time averages but also their independence from the initial state (Lanford, 1981). We will briefly review two main statistical approaches to turbulence which have been subject to most of the turbulence research during the century: the universal equilibrium theories and Reynolds averaging. The former approach concentrated on the search of a unifying theory of turbulence, the latter approach on the determination of turbulence quantities of engineering interest.

1.1.1. Universal Equilibrium Theories

Following the documentation in Narasimha (1990), the introduction of the Lagrangian auto-correlation function in the context of the dispersion of passive scalars in homogeneous turbulent flow (Taylor, 1921) and the further introduction of the spectrum and the dynamics (von Karman and Howarth, 1938) led to a statistical theory of turbulence in the sense of modern probability theory, by Kolmogorov and his students. In 1941, Kolmogorov suggested that as the energy is transferred from low wavenumbers where it is produced (the production range) to high wavenumbers where it is dissipated due to the viscosity (dissipation range) it would lose detailed information about the mechanism of its production. At the limit of infinite Reynolds number (after infinitely many steps in the energy cascade), the small scales would know only how much energy they were receiving, hence they might be expected to be isotropic (local isotropy) having lost all information about the anisotropy of the energy-containing scales. Thus, he argued that at sufficiently high Reynolds numbers, there exists a range of high wavenumbers where turbulence is in statistical equilibrium, in the sense that energy flux across each wavenumber is constant. This equilibrium range is termed as universal since turbulence in this range is independent of external conditions and is uniquely determined by the rate of energy dissipation per unit mass, ε, and kinematic viscosity, ν. From dimensional reasoning, he predicted that the energy spectral density of turbulence $E(k)$ has the universal form (Leslie, 1973),

$$E(k) = \varepsilon^{2/3} k^{-5/3} f(\nu^{3/4} \varepsilon^{-1/4} k) \tag{1.5}$$

where k is the wavenumber. In the inertial range, the dimensionless function f reduces to a constant, called the Kolmogorov constant. Recently, this law, known as the 5/3 law of Kolmogorov, has been derived directly from Navier-Stokes equations by demonstrating that invariance under a time-dependent two-parameter group of transformations implies that the second-order velocity correlation takes the Kolmogorov form (Foias et al., 1987a).

Kolmogorov hypothesis has been criticized mainly from the fact that it does not account for the intermittency of the dissipative scales. According to the documentation in McComb (1992), this fact has been advanced by experimental investigations (Batchelor and

Townsend, 1949) conducted on the flatness factors of the probabilistic distributions of the turbulent velocity and its derivatives. Although the velocity distributions were found to be approximately normal (Gaussian) as supposed by the original Kolmogorov theory, velocity derivatives distributions were much flatter than a Gaussian distribution implying the existence of an intermittent variable which may jump randomly between a stochastic and a non-stochastic state. This criticism has been countered by various refinements of Kolmogorov scaling (Kolmogorov, 1962; Oboukhov, 1962; Monin and Yaglom, 1975) supposing a log-normal probabilistic distribution of velocity derivatives or by the so-called fractal models of turbulence first proposed by Mandelbrot (1974). Recent experiments show that velocity derivatives distributions exhibit an evident non-Gaussian behavior being close to exponential distributions (a Gaussian core with an exponential tail), hence some of the current research on turbulence are focused on non-Kolmogorov scalings to deal with the non-Gaussian statistical nature of small scales in turbulence (Kraichnan, 1990; She, 1991; Procaccia and Constantin, 1993).

1.1.2. Reynolds Averaging and Closure Modeling

The engineering tool of choice in computing turbulent flows has been the statistically averaged equations and quantities which eliminate the need to completely resolve the flow, but on the other hand, which need the modeling of the closure problem, i. e. of the unknown higher-order correlations in both the mean and turbulent equations, resulting from the averaging procedure. Thus, any flow variable can be decomposed into mean and fluctuating components (Reynolds decomposition),

$$u_i = \overline{u}_i + u'_i \tag{1.6}$$

where the bar denotes the mean part and the prime denotes the fluctuating part. The mean variable can be extracted if a statistically steady or a statistically homogeneous turbulence is assumed. In the former case, a long time average of the flow variable is taken, in the latter case, a volume average is taken. If the flow is neither stationary nor homogeneous then an ensemble mean over all realizations (samples) is required. The ergodic hypothesis assumes that in a statistically steady flow the time average and in a homogeneous turbulent flow the

volume average is equal to the ensemble mean taken over all repeated experiments (Speziale, 1991). If the averaging procedure is applied to the continuity equation and to the Navier-Stokes equations of motion in the incompressible case, then one can obtain the mean continuity equation and the Reynolds-averaged Navier-Stokes equations (RANS) in terms of the mean components of the flow variables which can be expressed in indicial notation as,

$$\frac{\partial \overline{u}_i}{\partial x_i} = 0 \tag{1.7}$$

$$\frac{\partial \overline{u}_i}{\partial t} + \overline{u}_j \frac{\partial \overline{u}_i}{\partial x_j} = -\frac{\partial \overline{p}}{\partial x_i} + \nu \nabla^2 \overline{u}_i - \frac{\partial \tau_{ij}}{\partial x_j} \tag{1.8}$$

where $\overline{u}_i$ denotes the mean velocity components and $\overline{p}$ denotes the mean kinematic pressure (mean pressure divided by the fluid density). These equations have the same form as the Navier-Stokes equations with the exception of the second-moment or the correlation tensor which includes the statistical average of the products of the fluctuating velocity components as,

$$\tau_{ij} = \overline{u'_i u'_j} \tag{1.9}$$

These terms correspond to Reynolds stresses or the turbulent stresses. Since there are more unknowns than equations, the unknowns being the Reynolds stresses, RANS modeling suffers from the so-called closure problem. To close the equations, one has to model the Reynolds stresses, hence Reynolds stress modeling or turbulence modeling has been the main research topic of the statistical approach to turbulence. In mathematical terms, the Reynolds stress tensor is assumed to be a functional of the global history of the mean velocity field as (Speziale, 1991),

$$\tau_{ij}(\mathbf{x},t) = \Im_{ij}(\overline{\mathbf{u}}(\mathbf{x}',s), l_0(\mathbf{x}',s), \tau_0(\mathbf{x}',s); \mathbf{x}, t), \qquad \mathbf{x}' \in V, s \in (-\infty, t) \tag{1.10}$$

where l_0 is the turbulent length scale and τ_0 is the turbulent time scale.

Following the documentation in Speziale (1991), in analogy with the constitutive equations which model stresses in the laminar case, in the latter part of the nineteenth century, Boussinesq (1877) suggested replacing turbulence by a laminar flow with increased viscosity, termed as the eddy viscosity, ν_T. Hence, the oldest Reynolds stress closures are based on the Boussinesq eddy viscosity hypothesis with,

$$\tau_{ij} = \frac{2}{3} K \delta_{ij} - \nu_T \left(\frac{\partial \overline{u}_i}{\partial x_j} + \frac{\partial \overline{u}_j}{\partial x_i} \right) \tag{1.11}$$

in which the isotropic part given by $2K/3$, where $K=\tau_{ii}/2$ (with summation on indices) is the turbulent kinetic energy, can be absorbed into the mean kinematic pressure. The deviatoric part contains the eddy viscosity (with the eddy viscosity $\nu_T \propto l_0^2 / \tau_0$) which multiplies the mean rate-of-strain tensor. It can be shown that the standard eddy viscosity model (1.11) can be obtained by imposing form invariance under the extended Galilean group of transformations to the relation (1.10) and performing a Taylor series expansion of its arguments while keeping the first order terms with the assumption of the complete separation of turbulent and mean scales (Smith, 1971).

The zero-equation model derives its name from the fact that it defines the length and time scales to determine the eddy viscosity with an algebraic relationship rather than a differential one. That assumption, where the Reynolds stress tensor can be characterized by a single length and time scale constitutes an oversimplification since turbulent flows exhibit a wide range of excited length and time scales as mentioned above. As documented in Speziale (1991), the earliest example of such a closure is the Prandtl's mixing-length theory (Prandtl, 1925) in analogy with the kinetic theory of gases. Later, this type of model was generalized to three-dimensional turbulent flows (Smagorinsky, 1963). The more recent examples are Cebeci-Smith (1974) and Baldwin-Lomax (1978) models. Zero-equation models have the disadvantages of the need of an ad hoc prescription of the turbulent length scale and the complete neglect of history effects. The next level of complexity in closure modeling is the half-equation model (Johnson and King, 1985) which derives its name from the fact that it uses an ordinary differential equation to account in a limited way for history effects by solving a transport equation for the maximum turbulent shear stress. Both the

zero- and half-equation models are also two-layer models since they use different relations for the eddy viscosity in the inner and the outer layers of the boundary layer, however, in half-equation models the eddy viscosity transitions in a prescribed functional manner from the inner layer form to the outer layer form (Gatski, 1996).

For higher levels in turbulence modeling, one has to introduce the second moment or the Reynolds stress transport equations which can be obtained from the fluctuating momentum equation resulting from the substraction of the mean momentum equation (RANS) from the direct Navier-Stokes linear momentum equation and using the Reynolds decomposition as,

$$\frac{\partial u'_i}{\partial t}+\overline{u}_j\frac{\partial u'_i}{\partial x_j}=-u'_j\frac{\partial \overline{u}_i}{\partial x_j}-\frac{\partial p'}{\partial x_i}+\nu\nabla^2 u'_i+\frac{\partial \tau_{ij}}{\partial x_j} \tag{1.12}$$

Taking the second moment of the obtained fluctuating momentum equation (1.12) results in the transport equation for the Reynolds stress tensor components as (Speziale, 1996),

$$\frac{\partial \tau_{ij}}{\partial t}+\overline{u}_k\frac{\partial \tau_{ij}}{\partial x_k}=-\tau_{ik}\frac{\partial \overline{u}_j}{\partial x_k}-\tau_{jk}\frac{\partial \overline{u}_i}{\partial x_k}+\Pi_{ij}-\varepsilon_{ij}-\frac{\partial C_{ijk}}{\partial x_k}+\nu\nabla^2\tau_{ij} \tag{1.13}$$

where,

$$\Pi_{ij}=\overline{p'\left(\frac{\partial u'_i}{\partial x_j}+\frac{\partial u'_j}{\partial x_i}\right)} \tag{1.14}$$

$$\varepsilon_{ij}=2\nu\overline{\frac{\partial u'_i}{\partial x_k}\frac{\partial u'_j}{\partial x_k}} \tag{1.15}$$

$$C_{ijk}=\overline{u'_i u'_j u'_k}+\overline{p'u'_i}\delta_{jk}+\overline{p'u'_j}\delta_{ik} \tag{1.16}$$

are the pressure-strain rate correlation, turbulent dissipation rate correlation and third-order turbulent diffusion correlation tensors respectively. It is also possible to write the turbulent dissipation rate transport equation, forming another moment of the fluctuating momentum equation (1.12), in terms of the transport of the scalar dissipation rate ($\varepsilon = \varepsilon_{ii} / 2$, with summation on indices). Obviously, this system of differential equations is not closed either and it requires modeling of the third-order and other type of correlations.

Two constraints have played an important role in the formulation of modern Reynolds stress models: realizability which requires that the model yield positive component energies ($\tau_{\alpha\alpha} \geq 0$, no summation on indices) and frame invariance where time-dependent rotations and translations are accounted for, to extend the model to geometrically complex flows (Speziale, 1991).

One-equation models assume the eddy viscosity to be of the form,

$$\nu_T = K^{1/2} l_0 \tag{1.17}$$

where the turbulent kinetic energy ($K=\tau_{ii}/2$) is obtained from a modeled version of its exact transport equation which derives from the contraction of Reynolds stress transport equation (1.13) and the turbulent length scale, l_0, is specified empirically. To close the system, the turbulent transport and dissipation terms are to be modeled. These models provide for the computation of the turbulent kinetic energy and account for some nonlocal and history effects in the determination of the eddy viscosity. They are superior to zero-equation models in that the time scale of the eddy viscosity is constructed from turbulence statistics rather than the mean velocity gradients, however the empirical specification of the turbulent length scale limits predictive capabilities and universality of these models (Speziale, 1996).

Two-equation models (K-ε, K-l) use two separate modeled transport equations for the turbulent length and time scales. In the most common approach (with the turbulent length scale $l_0 \propto K^{3/2} / \varepsilon$, the turbulent time scale $\tau_0 \propto K / \varepsilon$) the modeled differential transport equations for K and ε are solved. Hence, these models determine both turbulent

length and time scales from turbulence statistics and they represent the minimum acceptable level of Reynolds stress closure (Speziale,1996).

All of the above models, from zero- to two-equation models, use the standard eddy viscosity form (1.11). However, this form is not able to describe properly turbulent flows with body force effects arising from system rotation or from streamline curvature and turbulent flows with flow structures generated by normal Reynolds stress anisotropies such as secondary flows in non-circular ducts. To overcome some of these deficiencies, nonlinear or anisotropic generalizations of eddy viscosity models have been considered by keeping second order terms in the Taylor expansions of the relation (1.10) subject to invariance under the extended Galilean group of transformations and more general representations for the Reynolds stress tensor have been obtained as the nonlinear K-ε model (Speziale, 1987) formulated with a properly invariant anisotropic eddy viscosity model that is nonlinear in the mean velocity gradients. These models have still many of the deficiencies of the simpler two-equation models as the inability to account for component Reynolds stress relaxation effects or body force effects (Speziale, 1991).

Second-order closure models are based on the full solution of Reynolds stress transport equation (1.13). Unlike eddy viscosity models, they are able to account for turbulent flows exhibiting relaxation effects, strong nonlocal and history effects as well as streamline curvature and rotational effects. However, models must be provided for the higher order pressure-strain rate (1.14), turbulent dissipation rate (1.15) and turbulent diffusion (1.16) correlations . The crucial assumption of separation of scales is made this time, at third-moment level. In principle, second-order closures account for more physics, however it has been remarked that they are not as effective in the case of wall-bounded turbulent flows as they are in homogeneous flows (Speziale, 1996).

It should be noted that all of these Reynolds stress models, from zero-equation models to full second-order closures, involve nondimensional constants which are calibrated basing on comparisons with benchmark flows. These benchmark flows are generally near equilibrium homogeneous two-dimensional mean shear flows, hence in the inhomogeneous situation such as wall-bounded flows, ad hoc wall reflection terms have to be incorporated

in the modeling of the high-order correlations (1.14-16) (Speziale, 1996). Another point is that all these closure models are one-point closures in the sense that the averaged products of fluctuating quantities are those in which the two or more quantities in question are evaluated at the same point in space, and thus they do not yield accurate quantitative predictions for a wide variety of turbulent flows where the energy spectrum can change drastically (Speziale, 1990). Following the documentations in Narasimha (1990) and Lesieur (1993), we should also quote two-point closures such as the Direct Interaction Approximation, DIA (Kraichnan, 1959; Kraichnan and Herring, 1978, Nakano, 1988), Eddy-Damped Quasi-Normal Markovian theory, EDQNM (Orszag, 1977) or Renormalization Group Methods, RNG (Yakhot and Orszag, 1986) which are based on statistical perturbation methods to organize the solution of the Navier-Stokes equations as an expansion in powers of the effective Reynolds number and derive systematically the coarse-grained equations of motion for turbulent flows. However, these statistical closure models, in general deal with homogeneous turbulence based on near-Gaussian statistics and suffer from convergence problems related to the perturbation series (Narasimha, 1990; Herring, 1990).

1.2. Towards New Approaches

Besides the well-known limitations of traditional Reynolds stress modeling based on Reynolds averaging quoted in the previous section, the idea of statistical modeling or statistical theories of turbulence has been severely questioned with research conducted since 1960's on the so-called coherent structures which were detected by modern visualization techniques in the experiments. The idea of coherent structures was first articulated by Liepmann (1952) according to the documentation of Liu (1988) and was thoroughly exploited by Townsend (1956). However, as documented in Holmes et al. (1996), their impact on the field originates from the works of Kline et al. (1969) and Brown and Roshko (1974). Although, there is no general consensus on the definition of a coherent structure, it can be viewed as a region of the flow over which at least one fundamental flow variable exhibits significant correlation with itself or another variable over a range of space and (or) time that is significantly larger than the smallest local length and time scales of the flow

(Robinson, 1991). These structures implied that turbulence, traditionally viewed as disorganised phenomena without any structure, thus fully random, might involve organised motion and be with some structure, thus random in appearance only or pseudorandom. The experiments suggest that, turbulence is not a single set of states, but it is a very complex and variable set of states that react in unanticipated ways to a great variety of circumstances thus, it is not meaningful to talk of the properties of a turbulent flow independently of the physical situation in which it arises and it seems not possible to fit many phenomena which vary from flow to flow into a universal turbulence theory, contrary to the earlier implicit assumptions of statistical approaches that the dynamic events comprising turbulence are similar in nature (Bushnell, 1990).

The inability of Reynolds stress closures, due to Reynolds averaging, to even identify the occurrence of coherent vortical structures, has been subject to criticisms as statistical approaches obscured the physics of the flow and made certain questions unapproachable, to the extent that some research funding agencies in US declared that they no longer support work based on Reynolds averaging (Lumley, 1990). It has also been argued that coherent structures obey their own statistics too with respect to their occurrence in the flow, so do not necessarily invalidate all statistical approaches but either new techniques should be used or if statistical approaches are to be used, they should be used in new ways (Lumley, 1990). In this context, high-order moment closures (third and higher) and two-point closures have been suggested as some remedy.

An intermediate way between the statistical solutions and the direct numerical solutions (DNS) of the Navier-Stokes equations, is the large-eddy simulation approach (LES) with which the severe Reynolds number restrictions of DNS are bypassed by directly simulating the large scales only and supplying the effect of the small scales which are not directly simulated, by a so-called subgrid scale (SGS) modeling. This approach is consistent with the observation that large scales are directly affected by external conditions and may vary from flow to flow in contrast to small scales which are more universal in nature. Hence, in LES, large scales are determined deterministically, small scales are modeled statistically. It is generally thought that, as large scales are computed directly, a relatively simple statistical closure than sophisticated Reynolds stress closures might be used for

subgrid scale modeling, such as the Smagorinsky model, mentioned above, which is a zero-equation model. Computationally, LES is less costly than DNS, but in general much more costly than statistical simulations based on RANS (Härtel, 1996).

1.3. Deterministic Approaches

The alternative approach to statistical ones is certainly the deterministic approach. The original Navier-Stokes equations of motion give a deterministic description of the flow and they do not suffer from closure problems. It is clear that any solution of Navier-Stokes equations is also a solution of RANS equations but the converse is not in general true since forced closure at moments of some finite order and the ad hoc procedures adopted for this, are not rigorous consequences of the Navier-Stokes equations (Narasimha, 1990). It is known that the solutions of Navier-Stokes equations exhibit extremely irregular and chaotic behavior with respect to the parameter range, however statistical description studies their smoothened characteristics which vary more regularly, due to the statistical averaging which, in many cases, can lead to a loss of information if applied without care.

As mentioned at the very beginning, the mathematical and direct numerical treatment of the full Navier-Stokes equations pose severe problems. However, the relatively recent use of the dynamical systems theory approach to turbulence or properly saying, to the Navier-Stokes system constitutes a promising alternative in several respects. As documented in Holmes (1990), this theory, which studies the qualitative behavior of parametrized families of deterministic differential equations, has its origins in the work of Henri Poincaré, who proposed that the solutions of differential equations be approached qualitatively by the consideration of the global behavior of large sets of solutions rather than seeking particular analytical or numerical solutions for specified initial data. He developed the basic ideas of invariant manifolds, bifurcation of equilibrium and periodic orbits and recognized the importance of homoclinic orbits in the generation of chaotic motions. While he mainly dealt with Hamiltonian systems, the methods he suggested have found applications in the study of dissipative dynamical systems too. The topological methods he

introduced were largely developed and applied to differential equations by Smale, Arnold and their colleagues (Holmes, 1990).

The first clear connection between dynamical systems and turbulence has been established in the famous work of Lorenz who investigated analytically and numerically a set of three first order nonlinear ordinary differential equations (Lorenz system) obtained by a drastic truncation of the Fourier-Galerkin projection of the coupled Navier-Stokes and heat equations for Boussinesq convection problem in a two-dimensional convecting layer (Rayleigh-Bénard convection problem) (Lorenz, 1963). He found strong evidence for a strange attractor (chaotic attractor), called the Lorenz attractor, for the solutions of the system. Although that attractor was located far beyond the Rayleigh number range in which the truncation was reasonable, this work demonstrated the possibility of a connection between the qualitative solutions of low-dimensional dynamical systems and infinite-dimensional partial differential equations with the observation of the bifurcation of equilibrium and periodic solutions towards very complex and apparently random solutions (chaotic solutions) in low-dimensional nonlinear dynamical systems.

The application of the dynamical systems theory to turbulence has primarily been conducted on the transition to turbulence. Newhouse-Ruelle-Takens (NRT) scenario for the transition to turbulence in fluid systems has been another pioneering work in the field (Newhouse et al., 1978). They proposed a new scenario for the transition to turbulence different from the early scenarios of Landau and Hopf who suggested that the continuous Fourier spectrum of temporal frequencies typical to turbulence might be produced via successive bifurcations from steady to periodic and quasi-periodic flows of increasing complexity as the Reynolds number is increased, remaining however quasi-periodic with increasing number of incommensurate frequencies and turbulent in appearance (Hopf, 1948; Landau and Lifshitz, 1959). In dynamical systems theory language, the resulting fluid flow corresponds to a phase flow on an n-dimensional torus in the state (or phase) space. With the NRT scenario, it has been proposed that a mathematical object called Axiom A strange attractor might exist for the Navier-Stokes equations under appropriate conditions and that solutions attracted to such an object might correspond to turbulence. This scenario stems from the observation that the quasi-periodic flows proposed by Landau and Hopf are not

structurally stable and it suggests that the solutions might be attracted to a structurally stable non-periodic attractor (chaotic attractor) following two or three quasi-periodic (Hopf) bifurcations and arising from the destruction of a three-dimensional torus in the phase space by infinitesimal perturbations, contrary to Landau-type flows which do not suggest the existence of a non-periodic attractor sensitively dependent on the initial conditions. Experimental investigations conducted on Rayleigh-Bénard convection in a small box and Taylor-Couette flow (flow between concentric counter-rotating cylinders) seem to confirm that scenario with the evidence of sequences of bifurcations leading to low-dimensional chaos as the Taylor and Rayleigh numbers respectively are raised above the initial onset of linear instability (DiPrima and Swinney, 1981; Busse, 1981). Power spectra displaying jumps from two or three frequency quasi-periodic motions to broad band chaos were measured. This sudden transition to turbulence where the flow system is highly sensitive to initial conditions (closely related to the ergodicity of the flow with the assumption that time averages are essentially independent of the initial state), is a point which is absent in Landau's hypothesis. Moreover, the power spectrum of such flows exhibits a continuous spectrum (a flat noiselike picture), an indication of chaotic behavior contrary to Landau- type flow which should exhibit a spectrum with sharp peaks at the incommensurate frequencies and their harmonics (Yorke and Yorke, 1981).

Another recent work (Aubry et al, 1988) in the context of the application of dynamical systems theory to turbulence involves the study of the dynamics of coherent structures in the wall region of a turbulent boundary layer and also provides another link between chaos in relatively low-dimensional systems and turbulence in open flows, using low-dimensional sets of ordinary differential equations obtained by the truncation of the Navier-Stokes equations, via Galerkin projection. The system models the nonlinear interaction among the deterministic structures in terms of the time dependent amplitude coefficients of the basis functions which are empirical eigenfunctions derived from correlation measurements using the proper orthogonal decomposition method, POD (Lumley, 1970) with the basic idea stemming from Karnuhen-Loève decomposition theorem. Although the method is far from being a predictive method, since the eigenfunctions are obtained empirically from experiments, it suggests the possibility of a low-dimensional description for an infinite-dimensional differential system which mimics

very important features of the original system. In the literature, there are other recent examples basing on the same idea, intending to develop the mentioned work or devising other low-dimensional systems in which the onset of chaos shows the right kind of dependence on external disturbance and Reynolds number (Narasimha, 1990).

One important issue is the question of the randomness observed in the solutions of a deterministic set of equations such as the Navier-Stokes system, hence the possibility of a reconciliation between a statistical approach and a deterministic one. That question is partially answered by the dynamical systems theory which demonstrates that there are nonlinear dynamical systems whose solutions, because of sensitive dependence on initial conditions, exhibit a weak causality and hence are apparently random.

The general tendency to distinguish between turbulence and chaos lies in the fact that chaos is defined as the time history of a single descriptor of a deterministic dynamical system which undergoes a loss of temporal correlation with a change in some system parameters and that displays sensitivity to initial conditions. Turbulence is defined as the time history of the spatial distribution of a deterministic dynamical system which undergoes a loss of temporal and (subsequently) spatial correlation with a change in some system parameters (Reynolds et al., 1993).

The fundamental picture of the strange attractor theory of turbulence is the following: The mathematical object which accounts for turbulence is an attractor or a few attractors of reasonably small dimensions, imbedded in the very large dimensional phase space of the fluid system. Motion on the attractor depends sensitively on initial conditions and this sensitive dependence accounts for the apparently stochastic time dependence of the fluid (Lanford, 1981). The theory is based upon the mathematical ideas of genericity and transversality. In physical terms, one postulates that phenomena requiring special conditions or exceptional circumstances that are not part of the physical constraints of the system will not be observed (as an example, multi-periodic motion which can be destroyed by small perturbations is non-generic). However, when a physical system embodies a symmetry, then that symmetry may prevent bifurcations from occurring in a generic way. Application of the theory to such situations requires the bifurcations which are generic within the class of

systems embodying symmetry be computed. Hence, there is considerable scope for extending the theory to take into account symmetries of the physical system and exploring multi-parameter systems near points of degenerate bifurcation (Guckenheimer, 1986).

On the theoretical side, much of the recently acquired knowledge about bifurcations of dynamical systems is based upon numerical studies with low-dimensional phase spaces (10-20 ordinary differential equations). However, little is known about the structure of attractors and virtually nothing is known about how dynamical details depend upon dimension. It is reported also that rigorous estimates of attractor dimension indicate any dynamical system which captures all of the relevant spatial scales will be of very high dimension (Temam, 1988). Advances in such areas necessitate a dramatic reduction in complexity by the removal of inessential degrees of freedom. The first real evidence of the possibility of such a reduction came with the experimental discovery of coherent structures as organized spatial features which repeatedly appear (often in flows dominated by local shear) and undergo a characteristic temporal life cycle (Guckenheimer, 1986).

An important new idea in partial differential equations and infinite dimensional dynamical systems in general is the concept of inertial manifolds. Recently, it has been shown (Temam, 1988; Constantin et al. 1989), that a fairly wide class of strongly dissipative partial differential equations not only possess attracting sets of finite Hausdorff dimension but that these sets lie within smooth inertial manifolds: compact, finite dimensional manifolds invariant under the dynamical flow, and attracting all solutions at an exponential rate. Thus, if a suitable coordinate system can be found for the inertial manifold, solutions are asymptotic to those of a finite set of ordinary differential equations on that manifold and so long term behavior is rigorously governed by ordinary differential equations on a flat finite dimensional model space. Essentially, inertial manifolds are global, attracting center manifolds. It is important to note that in this global reduction to finite dimensions, one is not ignoring or truncating the high wavenumber modes, one is using the fact that they are slaved to the low modes. They are present in the inertial manifold which is not flat: its curvature describes the coupling to these higher modes (Holmes, 1990). Inertial manifolds are known to exist for multi-space dimension equations of reaction diffusion type and various one dimensional model equations such as Kuramoto-Sivashinsky and Ginzburg-

Landau equations. Although, the existence of exact inertial manifolds for two and three dimensional Navier-Stokes equations has not yet been asserted, an inertial form has been found in the two dimensional case (Kwak, 1992). Furthermore, approximate inertial manifolds have been introduced and shown to exist in the case of Navier-Stokes equations and methodologies for their construction have been developed. These recently introduced integration algorithms are known as the Nonlinear Galerkin Methods (Temam, 1993).

In this work, we aimed to conduct a deterministic analysis of the Navier-Stokes equations for the investigation of the transition to turbulent regime in the case of plane shear flows. The mathematical formulation for the temporal stability problem for these type of flows is given in Chapter 2. The study cases include the wall-bounded shear flows such as the plane channel (Poiseuille) flow (Section 2.1.1), the oscillatory Poiseuille flow (Section 2.1.2) the unbounded shear flows such as the temporally growing mixing layer (Section 2.2.1) and plane jet flow (Section 2.2.2). In Chapter 3, the spectral methods of solution as the classical Galerkin spectral method (Section 3.1) and the recent nonlinear Galerkin spectral methods (Section 3.2) which bring improvements in terms of convergence and efficiency on the former one and enable the construction of the approximate inertial manifold on which the flow dynamics is described by the inertial form, are presented. The Navier-Stokes equations, for the above flow cases, are therefore reduced to a dynamical system using these methods and the qualitatively different solutions of this system are then parametrically investigated to get insight of the structure of the corresponding phase space. In Chapter 4, the results and discussion on the convergence and efficiency tests of the new nonlinear Galerkin algorithms (Section 4.1) and on the numerical simulations corresponding to the parametrical investigation of the transition to turbulence for the study flow cases (Section 4.2) are presented before concluding in Chapter 5.

2. FORMULATION OF THE FLOW PROBLEMS

For Newtonian incompressible fluid flow, the conservation of mass and the conservation of the linear momentum can be written as,

$$\frac{\partial \mathbf{u}}{\partial t} - \nu \Delta \mathbf{u} + (\mathbf{u}.\nabla)\mathbf{u} + \nabla p = \mathbf{f} \tag{2.1}$$

$$\nabla . \mathbf{u} = 0 \tag{2.2}$$

where $\mathbf{u}$ is the velocity vector, p represents the kinematic pressure field, ν is the kinematic viscosity and $\mathbf{f}$ represents the body force vector per unit mass. The continuity equation (2.2) is known as the incompressibility condition and imposes a divergence free velocity field. The continuity equation can also be interpreted as a condition on the pressure since the pressure can be viewed as an adjusting parameter in the momentum equation to ensure a divergence free velocity field. The above formulation together with the necessary boundary and initial conditions, is also known as the primitive-variable formulation. Although the boundary conditions on the velocity vector can naturally be imposed, the difficulty with this formulation is to impose the boundary conditions on the pressure.

In two dimensions, it is possible to define a streamfunction ψ, related to the velocity components as,

$$u = \frac{\partial \psi}{\partial y}, \qquad v = -\frac{\partial \psi}{\partial x} \tag{2.3}$$

The above definition of the streamfunction automatically satisfies the incompressibility condition and guarantees a divergence free velocity field. Taking then, the rotational of the equations of motion (2.1) one can obtain the compatibility equation for the velocity field in terms of the streamfunction, known as the streamfunction formulation,

$$\frac{\partial}{\partial t}(\nabla^2 \psi) - \frac{1}{\mathrm{Re}} \nabla^4 \psi + \frac{\partial \psi}{\partial y}\frac{\partial}{\partial x}(\nabla^2 \psi) - \frac{\partial \psi}{\partial x}\frac{\partial}{\partial y}(\nabla^2 \psi) = 0 \tag{2.4}$$

The above equation is in nondimensional form and Re represents the nondimensional Reynolds number. To obtain the equation governing the evolution of perturbations to the laminar flow, one can decompose the streamfunction into its laminar and perturbation parts and re-insert into (2.4). Re-defining ψ, as the perturbation streamfunction, we obtain,

$$\frac{\partial}{\partial t}(\nabla^2\psi)-\frac{1}{\mathrm{Re}}\nabla^4\psi+U\frac{\partial}{\partial x}(\nabla^2\psi)-\frac{d^2U}{dy^2}\frac{\partial\psi}{\partial x}+\frac{\partial\psi}{\partial y}\frac{\partial}{\partial x}(\nabla^2\psi) -\frac{\partial\psi}{\partial x}\frac{\partial}{\partial y}(\nabla^2\psi)=0 \tag{2.5}$$

where U, a function of the space and time variables, is the laminar velocity profile. This equation governs the evolution of two-dimensional finite disturbances to the flow. It can be considered as the nonlinear stability equation, since its linearized form for the infinitesimal two-dimensional disturbances, leads to the linear stability or the Orr-Sommerfeld equation for parallel flows. In the derivation of the Orr-Sommerfeld equation (Schlichting, 1979), the superimposed disturbances are taken to be small in the sense that all quadratic terms in the fluctuating components can be neglected with respect to linear terms. The task of the linear stability theory consists in determining whether the disturbance is amplified or whether it decays for a given motion. Substituting the mean flow, upon which two-dimensional disturbances are superimposed in the two-dimensional Navier-Stokes equations and neglecting the quadratic terms in the disturbance components, a system of equations for the disturbance velocity and pressure components can be obtained. Hence, introducing the streamfunction representing a single oscillation of the disturbance (with the assumption that any arbitrary two-dimensional disturbance is expanded in a Fourier series) for two-dimensional parallel flows corresponding to the wavenumber α,

$$\psi(x,y,t)=\phi(y)\exp(i(\alpha x-(\beta_r+i\beta_i)t)) \tag{2.6}$$

where β_r represents the circular frequency of the oscillation and β_i is the amplification factor into the linearized system of equations, one can obtain,

$$(U-c)(\phi''-\alpha^2\phi)-U''\phi=\frac{i}{\alpha\,\mathrm{Re}}(\phi^{iv}-2\alpha^2\phi''+\alpha^4\phi)$$
$$\phi=\phi'=0 \qquad at \quad boundaries \tag{2.7}$$

where c is the ratio $(\beta_r + i\beta_i)/\alpha$. Equation (2.7) is a linear eigenvalue problem where ϕ's are the eigenfunctions corresponding to the eigenvalues c. For a certain Reynolds number, linear instability sets in when the imaginary part of c takes a positive value.

2.1. Wall-Bounded Shear Flow Formulations

For plane channel (Poiseuille) flow, the nondimensionalization in the equation (2.5) is carried out as follows: Space variables x and y are nondimensionalized with the channel half-width h. The Reynolds number Re is defined, with respect to the channel half-width h, the fluid kinematic viscosity ν, and the centerline velocity V as,

$$\mathrm{Re}=\frac{Vh}{\nu} \tag{2.8}$$

The dimensionless laminar velocity profile U in (2.5) is the parabolic velocity profile given as,

$$U=u=1-y^2 \tag{2.9}$$

In the streamwise direction, periodic boundary conditions are imposed. It has been given two justifications for their use (Orszag and Kells, 1980): The instabilities of laminar flows are of small spatial scale so that streamwise boundary conditions are of little effect and the spatial growth of a disturbance in a laboratory coordinate frame appears as temporal growth in an advected coordinate frame, similar to that observed with periodic boundary conditions. Hence, in the streamwise direction, L being the dimensionless period length, we can write,

$$\psi(x,y,t) = \psi(x+L,y,t) \tag{2.10}$$

In the normal direction to the flow, we apply the no-slip boundary conditions. In terms of the streamfunction, it gives,

$$\frac{\partial \psi}{\partial x} = \frac{\partial \psi}{\partial y} = 0 \qquad at \quad y = \pm 1 \tag{2.11}$$

These boundary conditions are not, however sufficient to determine ψ, since they leave an arbitrariness in its value at $y = \pm 1$. This arbitrariness can be removed by choosing either the constant flux or constant pressure gradient formulation. In this study, we use the constant flux formulation.

2.1.1. Plane Channel Flow with Constant Flux Formulation

Using the freedom to add an arbitrary constant to ψ, we can fix its value at the lower boundary,

$$\psi(x,-1,t) = 0 \tag{2.12}$$

There is still an arbitrariness in ψ at the upper boundary. We consider the physical situation in which the total flux Q_T is prescribed for the flow. Then the flux will be equal to the laminar flux $Q_L = 4Vh/3$ and the flux due to the perturbation will be zero. We can set,

$$\psi(x,1,t) = 0 \tag{2.13}$$

and letting $V=3Q_T/4h$, the Reynolds number, in this case, is expressed in terms of the total flux as,

$$\mathrm{Re}_Q = \frac{3Q_T}{4\nu} \tag{2.14}$$

The subscript emphasizes that this Reynolds number is appropriate for flows with time independent flux. Alternatively, another formulation concerning the physical situation in which the total pressure drop over the streamwise length of the channel is maintained constant, could be considered. In this case, the Reynolds number is expressed in terms of mean pressure gradient as,

$$\mathrm{Re}_P = \frac{-h^3 P}{2\nu^2} \tag{2.15}$$

where P denotes the mean pressure gradient (Pugh and Saffman, 1988).

In laminar regime both the flux and the pressure gradient are constant, hence, the two formulations are equivalent. However, in transition and turbulence, the Reynolds numbers based on flux and pressure gradient differ. In general, $\mathrm{Re}_Q \leq \mathrm{Re}_P$. Although, most of the previous numerical work on channel flow were carried out using constant pressure gradient formulation, it has been suggested to base the formulation on constant flux since the flux is experimentally the most accessible quantity (Barkley, 1990).

2.1.2. Oscillatory Plane Poiseuille Flow

In this case, the basic motion of the fluid is forced by the combination of the spatially and temporally constant flux and the time periodic and spatially constant flux. Thus, in that case, following the notation of von Kerczek (1982), the flux can be written in nondimensional form as,

$$Q = 1 + \Lambda \cos(\Omega t) \tag{2.16}$$

where Λ is the ratio of the amplitude of the oscillating component of the flux to constant flux and the dimensionless frequency Ω of the imposed oscillatory flux is defined as,

$$\Omega = \frac{h\omega}{V} = \frac{2\beta^2}{\mathrm{Re}} \tag{2.17}$$

where ω is the frequency of the oscillatory component of the flux, $\beta = h/\delta$ is the ratio of the channel half-width to Stokes layer thickness $\delta = (2\nu/\omega)^{1/2}$. The Reynolds number Re is defined as in (2.8). The laminar velocity profile can be written as,

$$U = u = 1 - y^2 + \Delta W(y,t) \tag{2.18}$$

where $\Delta = \Lambda/\beta^2$ is the ratio of the amplitude of the oscillatory to steady velocity and,

$$W(y,t) = \Re e\left\{\left[\frac{\cosh\beta(1+i) - \cosh\beta(1+i)y}{i\cosh\beta(1+i)}\right]\exp(i\Omega t)\right\} \tag{2.19}$$

where $i=\sqrt{-1}$ and $\Re e$ denotes the real part.

2.2. Free Shear Layer Flow Formulations

2.2.1. Temporally Growing Mixing Layer Formulation

The shear layer is a zone of transition between two parallel streams each with a uniform velocity and both assumed to be in the same streamwise x direction. We consider therefore two parallel streams of the same fluid with the same uniform speed but in opposite senses. Then, we can write the boundary conditions in the cross-stream direction as,

$$\begin{aligned} u &\to U_0 \quad as \quad y \to +\infty \\ u &\to -U_0 \quad as \quad y \to -\infty \end{aligned} \tag{2.20}$$

In the mixing layer flow case, we can not write the exact laminar solution as in the case of channel flow. In the literature, for linear temporal stability problems, a tangent hyperbolic velocity profile which satisfies the boundary conditions and which approximates the profile in the layer, is generaly assumed (Betchov and Criminale, 1967; Pozrikidis, 1997). This base profile is of the form,

$$U = u = U_0 \tanh(\frac{y}{\delta_i}) \tag{2.21}$$

where δ_i is the initial vorticity thickness giving a measure for the thickness of the layer and providing a length scale. The velocity scale is chosen to be U_0 . Then, the time scale would be δ_i / U_0 and the Reynolds number can be defined as,

$$\mathrm{Re} = \frac{U_0 \delta_i}{\nu} \tag{2.22}$$

We should mention that, as the above base profile (2.21) is not an exact solution of the Navier-Stokes equations in the laminar case, the perturbation streamfunction formulation (2.5) will no more represent the exact perturbation problem of the Navier-Stokes equations. This assumption will lead to the loss of some physical aspects of the real problem. We consider the temporal stability problem which studies the temporal growth of disturbances imposed on the laminar flow. In fact, the mixing layer originating in the merger of two streams will develop in the streamwise direction and the spatial stability problem which studies the spatial growth of disturbances can also be implemented using the necessary inflow-outflow boundary conditions in the streamwise x direction. However, the temporally evolving mixing layer can be simulated at higher Reynolds numbers and with better resolution than the spatially growing mixing layer for a given level of computer resources (Metcalfe et al., 1987). Therefore, to formulate the temporal stability problem, we can use periodic boundary conditions in the streamwise x direction given by (2.10).

2.2.2. Plane Jet Flow Formulation

We consider the temporal stability problem for the two-dimensional symmetric plane jet flow (the Bickley jet) which constitutes another example of free shear layer flows. For two-dimensional jet flow there is a similarity solution which gives the laminar velocity profile of the viscous equations of the boundary-layer type (Schlichting, 1979). We will use in this study, a base profile which previously had been subject to linear and temporal

stability analyses in the context of the temporal evolution of two-dimensional infinitesimal disturbances (Betchov and Criminale, 1967; Pozrikidis, 1997). This velocity profile is of the form,

$$U = u = U_0 \, \mathrm{sech}^2(y/b) \tag{2.23}$$

where U_0 is the maximum velocity and b is the profile thickness. The Reynolds number is defined accordingly as,

$$\mathrm{Re} = \frac{U_0 b}{\nu} \tag{2.24}$$

The boundary conditions are periodic boundary conditions in the streamwise direction since we consider the temporal stability problem as in the case of mixing layer. In the cross-stream direction, the boundary conditions on the velocity can be written as,

$$u \to 0 \qquad as \quad y \to \pm\infty \tag{2.25}$$

We also mention that the temporal stability problem formulated with the base profile (2.23), has to be considered as an approximate problem and is not expected to represent the full physics of the real problem although it can reveal qualitatively some interesting features.

3. SPECTRAL METHODS OF SOLUTION

Spectral methods of solution are numerical methods which can be considered as a development of discretization schemes for differential equations known as the method of weighted residuals (MWR). These schemes use trial functions (also known as the expansion or approximating functions) as the basis functions for a truncated series expansion of the solution. To ensure that the differential equation to be solved is satisfied as closely as possible by the truncated series expansion, the residual (the error produced by using the truncated expansion instead of the exact solution) is minimized with respect to a suitable norm. An equivalent requirement is that the residual satisfy a suitable weighted orthogonality condition with respect to each of the test functions.

The choice of the trial functions distinguish spectral methods from other numerical solution methods as finite element or finite difference methods. In spectral methods, the trial functions are infinitely differentiable global functions which are generally tensor products of the eigenfunctions of singular Sturm-Liouville problems. In finite elements and finite difference solution methods, the trial functions are local in character and they are specified in each element into which the problem domain is decomposed.

The choice of test functions distinguish between the commonly used spectral schemes: the Galerkin, collocation and tau versions. Following the historical documentation (Orszag and Israeli, 1974; Canuto et al., 1988), in the Galerkin version (Collatz, 1960; Kantorovich and Krylov, 1964), the test functions are chosen to be the same as the trial functions. They are infinitely smooth functions which individually satisfy the boundary conditions. In the collocation version (Lanczos, 1956; Collatz, 1960), the test functions are translated Dirac delta functions centered at the so-called collocation points. In this approach, the differential equation is required to be satisfied exactly at the collocation points. The spectral tau approach (Lanczos, 1956) is a modification of the Galerkin method that is applicable to problems with non-periodic boundary conditions since in that approach, the test functions are not required to satisfy the boundary conditions, hence, a supplementary set of equations is used to apply the boundary conditions. It can be viewed as a special case of the Petrov-Galerkin method. Although the collocation method, also

known as the pseudospectral approach for the fact that it uses the discrete Fourier transform to evaluate the nonlinear terms in the differential equation, which in turn allows the use of fast Fourier transforms (FFT) which accelerate the discrete transform, seems to be computationally most efficient, it suffers from aliasing errors, not present in the Galerkin and tau techniques (Canuto et al., 1988).

The first unifying mathematical assessment of the theory of spectral methods has been given by Gottlieb and Orszag (1977). Since then, the theory has been extended to cover variable-coefficient and nonlinear problems. Stability and convergence analyses for spectral methods have been conducted on several type of problems (Canuto et al., 1988).

3.1. Classical Galerkin Spectral Solution Method

For the numerical solution of the flow problems described in the previous chapter, we use first the classical Galerkin spectral solution which is also termed as the fully spectral Galerkin technique to distinguish it from the pseudospectral (collocation) method. The fully spectral method, as mentioned above, is free of aliasing errors. As the trial and test functions are the same and they are chosen to satisfy exactly the boundary conditions, this method can also be considered as a semi-analytic method of solution.

The spectral solution method is applied to the streamfunction differential equation (2.5), with the necessary boundary and initial conditions. It has been noted that the streamfunction formulation of the Navier-Stokes equations, compared to other formulations (primitive variable, vorticity-velocity formulations etc.) is well fitted to spectral approximations since the accuracy of spectral methods increases with the regularity of the function (the streamfunction being more regular than velocity) (Maday and Métivet, 1987).

The streamfunction ψ, for both wall-bounded shear flow case (plane Poiseuille flow and oscillatory Poiseuille flow) and free shear layer flow case (mixing layer and plane jet flows) is subjected to periodic boundary conditions in the streamwise x direction. Therefore, it is suitable to decompose it into Fourier functions in the streamwise x direction.

In the cross-stream y direction non-periodic boundary conditions are applied in both cases so that the use of Fourier functions in that direction is not a natural choice. They will converge rather slowly because of the Gibbs phenomenon at the boundaries. We can decompose ψ as follows,

$$\psi = \sum_{k=-N}^{N} \sum_{m=0}^{M} a_{km}(t) \exp(2\pi i k x / L) \Phi_m(y) \tag{3.1}$$

where $a_{km}(t)$ are time dependent complex coefficients and $\Phi_m(y)$ are the trial functions in the cross-stream y direction which will be defined below according to the type of flow problem. The reality of the streamfunction ψ implies a condition on the expansion coefficients $a_{km}(t)$ as,

$$a_{-km}(t) = \overline{a}_{km}(t) \tag{3.2}$$

where the bar denotes the complex conjugate.

In the case of wall-bounded shear flow (plane channel Poiseuille flow and oscillatory plane Poiseuille flow), the trial functions in the cross-stream y direction are formed from Chebyshev polynomials of the first kind defined on the finite interval [-1,1] by,

$$T_m(y) = \cos(m \arccos(y)) \tag{3.3}$$

They can be considered as cosine functions after a change of variable. This transformation enables many mathematical relations as well as theoretical results concerning the Fourier system to be adapted to the Chebyshev system (Appendix A). Chebyshev polynomials of the first kind are orthogonal on the interval [-1,1] with respect to the weight function $w(y)$,

$$w(y) = \frac{1}{\sqrt{1-y^2}} \tag{3.4}$$

Chebyshev polynomials have been extensively used in the numerical approximation of non-periodic boundary value problems and reported to have very good convergence properties (Canuto et al., 1988). Therefore, in the above spectral decomposition (3.1), we form the trial functions $\Phi_m(y)$ for the case of channel flow, from linear combinations of the Chebyshev polynomials to satisfy the no-slip boundary conditions (2.11) on the perturbation streamfunction as (Moser et al., 1983),

$$\Phi_m(y) = \frac{T_{m+2}(y)}{m(m+1)} - \frac{2T_m(y)}{m^2-1} + \frac{T_{m-2}(y)}{m(m-1)} \tag{3.5}$$

where $\Phi_m(y)$ are defined for $m \geq 2$. In this case, the summation on m in the equation (3.1) starts from $m = 2$.

In the case of free shear layer (mixing layer and plane jet flows), the problem domain is the infinite interval. A natural choice is the Hermite functions which are solutions of the corresponding Sturm-Liouville problem defined on the infinite interval. However, in many attempts for the application of Hermite functions to differential equations defined on the infinite interval, slow convergence or even divergence have been reported. The reason is that the exponential convergence with the use of Hermite functions requires the function decay exponentially fast at infinity (Boyd, 1984). In fluid mechanics problems for unbounded flows, generally the infinite flow domain is either truncated (domain truncation) or mapped using mapping functions onto a finite domain and the flow is decomposed using Fourier or Chebyshev expansions (Grosch and Orszag, 1977). However, this mapping renders the differential equation a variable coefficient equation and mapping functions involve a mapping parameter which should be optimized to ensure convergence. Similarly, in domain truncation, the domain size has to be optimized. Hermite functions do not involve any free parameter to be optimized and possess orthogonality properties hence we expect them to be more effective unless the convergence conditions are violated. As it will be discussed in the next chapter, the formulation of the nonlinear stability problem in terms of the perturbation streamfunction enables us the use of Hermite functions since the boundary conditions on the perturbation streamfunction are such that it vanishes exponentially fast at infinity and the above requirement on the exponential convergence for the use of Hermite

functions is fulfilled. Thus, in the case of free shear layer flows, the trial functions in the cross-stream direction are chosen as,

$$\Phi_m(y) = (2^m m!\sqrt{\pi})^{-1/2} \exp(-y^2/2)\, H_m(y) \tag{3.6}$$

where $H_m(y)$ represent Hermite polynomials. It should be noted that the above Hermite functions form an orthonormal set on the infinite interval (Appendix B).

The spectral decomposition (3.1), is then replaced in the streamfunction differential equation (2.5) and the equation is integrated using the orthogonality properties with the corresponding weight functions, on the interval $[0,L]$ in the streamwise x direction, on the intervals [-1,1] and [-∞,∞] in the cross-stream y direction, for wall-bounded shear flow and free shear layer flows respectively, to obtain an ordinary differential equation system for the time evolution of the $a_{km}(t)$ expansion coefficients as,

$$M\frac{d\mathbf{a}}{dt} = N\mathbf{a} + F(\mathbf{a}) \tag{3.7}$$

where M and N are matrices corresponding to the linear terms and the vector $F(\mathbf{a})$ results from the integration of the nonlinear terms. All the above space integrations have been carried out analytically. The properties of the Chebyshev and Hermite polynomials involving their high-order derivatives and their double and triple products which enabled the integration of the linear and nonlinear terms have been summarized in the appendices (Appendix A-C).

The initial conditions for the evolution system (3.7) are generated from the solutions of the Orr-Sommerfeld linear stability equation (2.7). The Orr-Sommerfeld eigenvalue problem is also solved using spectral methods. The eigenfunctions $\phi(y)$ according to the boundary conditions are spectrally decomposed as (Orszag, 1971),

$$\phi_N(y) = \sum_{n=0}^{N} a_{2n} Q_{2n}$$
$$Q_{2n} = T_{2n}(y) - n^2 T_2(y) + (n^2 - 1) T_0(y) \tag{3.8}$$

in the case of wall-bounded shear flow and as,

$$\phi_N(y) = \sum_{n=0}^{N} a_n Q_n$$
$$Q_n = (2^n n! \sqrt{\pi})^{-1/2} \exp(-y^2/2) H_n(y) \tag{3.9}$$

in the case free shear layer.

The eigenfunctions $\phi(y)$ of the Orr-Sommerfeld equation corresponding to the most unstable eigenvalue for a wavenumber α for a certain Reynolds number, are used as initial conditions on the expansion coefficients for the differential system (3.7).

3.2. Nonlinear Galerkin Methods

3.2.1. Introduction

It is well known that many infinite-dimensional nonlinear dissipative evolution equations, which arise frequently in mathematical physics, exhibit finite-dimensional behavior. This is suggested first, as it was mentioned in the introduction, by the universal routes to chaos commonly observed in low dimensional dynamical systems. Evidence to this behavior includes also the fact that the Hausdorff and fractal dimensions of the global attractor (the largest bounded invariant set which attracts all the solutions in the phase space) of these dissipative partial differential equations, are bounded. Following the documentation in Temam (1988), the first study of the global attractor for a flow is known to be performed by Billotti and LaSalle (1971). The finite dimensionality of the global attractor for certain flows was proved by Mallet-Paret (1976) on a Hilbert space, and by Mañé (1981) in the Banach space setting. Explicit bounds on the number of degrees of

freedom and the dimension of attractors of the physical systems such as some reaction-diffusion equations, pattern formation equations (the Kuramoto-Sivashinsky equation related to phase turbulence phenomena in chemistry and combustion and the Cahn-Hilliard equations modeling pattern formation in phase transition phenomena), dissipative wave equations (Sine-Gordon equation) or the complex Ginzburg-Landau equation which governs the finite amplitude evolution of instability waves in a large variety of dissipative systems as well as in hydrodynamic instability theory, can be found in Temam (1988). Navier-Stokes equations for viscous incompressible case, can be written in functional form in an appropriate Hilbert space H as,

$$\begin{aligned} &\mathbf{u}: t \in \Re \rightarrow \mathbf{u}(t) \in H \\ &\frac{d\mathbf{u}}{dt} - \nu A\mathbf{u} + B(\mathbf{u}) = \mathbf{f} \end{aligned} \tag{3.10}$$

where $\mathbf{u}$ is the velocity vector, A is the Stokes operator associated with the boundary conditions, ν is the kinematic viscosity, $B(\mathbf{u})$, a quadratic term related to the inertial term $(\mathbf{u}.\nabla)\mathbf{u}$, represents the nonlinear inertial terms dominated by A and $\mathbf{f}$ represents forcing. The estimates of the finite Hausdorff and fractal dimension of their global attractor can be found in the literature (Foias and Temam, 1979).

3.2.2. Global Attractors and Inertial Manifolds

In this section, we will follow the descriptions and the corresponding notation in Temam (1995). Under suitable hypothesis, the initial-value problem (3.10) with the initial condition,

$$\mathbf{u}(0) = \mathbf{u}_0 \tag{3.11}$$

is well posed, in the sense that for every $\mathbf{u}_0 \in H$, there exists a unique function $\mathbf{u}=\mathbf{u}(t)$ defined, continuous and bounded for $t \geq 0$ such that (3.10) and (3.11) hold. Denoting $S(t)$ for $t \geq 0$, the semi-group of nonlinear operators in H defined by,

$$S(t)\mathbf{u}_0 = \mathbf{u}(t), \qquad \forall t \geq 0 \tag{3.12}$$

and assuming further hypothesis on equation (3.10), it can be shown that there exists a compact connected set $\mathrm{A} \subset H$ which has the following property of invariance under the flow (hence the name of invariant or integral manifold),

$$S(t)\mathrm{A} = \mathrm{A}, \qquad \forall t \geq 0 \tag{3.13}$$

A attracts all the solutions of (3.10) and (3.11) and more generally, for any bounded subset B of H,

$$dist\ (S(t)\mathrm{B}, \mathrm{A}) \to 0 \qquad as\ \ t \to \infty \tag{3.14}$$

This set A, which is unique, is called the global or universal attractor for the equation (3.10) since it describes all the possible dynamics that the given system can produce, in the sense that all the orbits corresponding to different initial data converge to it. It is also the largest (maximal among all bounded attractors) attractor for (3.10).

The global attractor A can be as simple as a point attractor or as complicated as a chaotic attractor of fractal type. Hence, the idea was to imbed the global attractor A into a smooth finite-dimensional manifold M called the inertial manifold. The inertial manifold for the above semi-group $S(t)$ is a Lipschitz manifold of finite-dimension in H such that it is invariant under the flow, i.e.,

$$S(t)\mathrm{M} \subseteq \mathrm{M}, \qquad \forall t \geq 0 \tag{3.15}$$

with the property that it attracts all the solutions of (3.10) at an exponential rate, thus for every $\mathbf{u}_0 \in H$, $S(t)\mathbf{u}_0$ converges to M with the rate,

$$dist(S(t)\mathbf{u}_0, \mathrm{M}) \leq c_1 \exp(-c_2 t) \tag{3.16}$$

where c_1 and c_2 depend boundedly on $|\mathbf{u}_0|$. Since the inertial manifold M attracts all the solutions at an exponential rate, it necessarily contains the global attractor ($A \subset M$). However, there are differences between attractors and inertial manifolds (Temam, 1995):

(a) attractors may be complicated sets, such as fractals, while inertial manifolds are required to be smooth, at least Lipschitz manifolds, in the sense that they are constructed as the graph of a Lipschitz function mapping subspaces of H,

(b) the convergence of orbits to the attractors may be slow, as the negative power of time or even slower, however, the convergence of the orbits to an inertial manifold is required to be exponential. Hence, after a short transient period, the orbits essentially lie on the inertial manifold and most of the dynamics takes place on M.

When an inertial manifold exists, the restriction of the semi-group $S(t)$ to M, defines a finite-dimensional semi-group of operators $\Sigma(t)$ for $t \geq 0$ such that,

$$\begin{aligned} &\Sigma(t) = S(t)\big|_M, \\ &\Sigma(t):\ M \to M, \end{aligned} \tag{3.17}$$

and which fully reproduces the dynamics of the initial equation (or semi-group). The resulting finite-dimensional system is called the inertial system or the inertial form (a finite number of ordinary differential equations).

The existence of inertial manifolds has been established for a variety of partial differential equations modeling physical systems such as the above mentioned Kuramoto-Sivashinsky equation with even-periodic initial data, the complex Ginzburg-Landau, the Cahn-Hilliard, the nonlocal Burgers and several reaction-diffusion equations. Although, the existence of inertial manifolds has been shown for the modified Navier-Stokes equations with enhanced viscosity (the addition of a higher order viscous term) for space dimension n, the rigorous mathematical proof of their existence in the case of two- or three-dimensional full Navier-Stokes equations is an open problem (Temam, 1988).

Recently, the existence of an inertial system (inertial form) for Navier-Stokes equations in space dimension two with space periodic boundary conditions, has been established (Kwak, 1992). The proof consists of the imbedding of the Navier-Stokes equations, through the so-called Kwak transform, into a reaction-diffusion system for which an inertial manifold and an inertial system exists. It has been shown that the embedded system (a finite-dimensional differential system) is also an inertial form for two-dimensional Navier-Stokes equations. In another work (Temam and Wang, 1993), the existence of a finite-dimensional dynamical system (inertial form) which produces the same dynamics as the Navier-Stokes equations around a sphere (flow of a thin layer of incompressible fluid around a sphere) has been proved. Furthermore, an upper bound on the dimension of the differential system (inertial manifold) has been derived and expressed in terms of Grashof numbers.

3.2.3. Approximate Inertial Manifolds and the Nonlinear Galerkin Methods

The first example of an approximate inertial manifold for the Navier-Stokes equations, as mentioned in the previous section, is the modified Navier-Stokes equations with enhanced viscosity (addition of a higher order viscosity term) in space dimension n, which takes the form,

$$\frac{\partial \mathbf{u}}{\partial t} + \varepsilon(-\Delta)^r \mathbf{u} - \nu\Delta\,\mathbf{u} + (\mathbf{u}.\nabla)\mathbf{u} + \nabla p = \mathbf{f} \tag{3.18}$$

$$\nabla.\mathbf{u} = 0 \tag{3.19}$$

where $r > 1$ (an integer) and ε is a strictly positive number. This system can be shown to have an inertial manifold. For values of ε close to zero, this constitutes an approximate inertial manifold for Navier-Stokes equations (Temam, 1988).

A more useful concept of approximate inertial manifolds for two-dimensional Navier-Stokes equations, has been considered in (Foias et al., 1988a). These are finite-dimensional manifolds attracting all orbits in a thin neighborhood in a finite time and constituting a substitute for exact inertial manifolds in situations where the existence of the

latter ones is an open problem. The existence of approximate inertial manifolds for Navier-Stokes equations has been established and methodologies for their construction have been developed. These construction methods, in the context of spectral and pseudospectral methods, are known as the Nonlinear Galerkin Methods and in the context of finite differences, as the Incremental Unknown Methods. Approximate inertial manifolds are constructed by the simplification of the graph of the nonlinear function mapping subspaces of H which correspond to the separation of large and small scales of the flow, as will be seen in the next section.

3.2.4. Construction of the Approximate Inertial Manifolds via Nonlinear Galerkin Methods for the Flow Problems

In this section, we consider the nonlinear dissipative evolution equation of the form (3.10) corresponding to the Navier-Stokes equations of motion (in primitive variables) in functional form. Equivalently, we could consider the streamfunction formulation (2.5) which can easily be considered in the same form, with the biharmonic viscous term represented by the linear operator A and other linear and nonlinear terms by $B(\mathbf{u})$ and $\mathbf{f}$. The spectral decomposition (3.1) leads to the projection of the evolution equation to a subspace of the Hilbert space H, spanned by the trial functions used in the decomposition (i.e. Fourier and Chebyshev or Fourier and Hermite functions).

If one denotes that projection $P=P_m$ and $\mathbf{u}_m = P_m\mathbf{u}$, then the classical Galerkin spectral method corresponds to the solution of,

$$\frac{d\mathbf{u}_m}{dt} - \nu A\mathbf{u}_m + PB(\mathbf{u}) = P\mathbf{f} \tag{3.20}$$

Another projection $Q = Q_m=I-P_m$ can be defined for the subspace spanned by the rest of the trial functions not included in the decomposition (3.1), together with,

$$\mathbf{u} = \mathbf{y} + \mathbf{z}, \qquad \mathbf{y} = P\mathbf{u}, \quad \mathbf{z} = Q\mathbf{u} \tag{3.21}$$

then, projecting the evolution equation respectively in both subspaces, one can obtain the following coupled system of equations (Foias et al., 1988b),

$$\frac{d\mathbf{y}}{dt} - \nu A\mathbf{y} + PB(\mathbf{y}+\mathbf{z}) = P\mathbf{f} \tag{3.22a}$$

$$\frac{d\mathbf{z}}{dt} - \nu A\mathbf{z} + QB(\mathbf{y}+\mathbf{z}) = Q\mathbf{f} \tag{3.22b}$$

The inertial manifold can be defined as,

$$\begin{aligned} \Phi:\ & PH \rightarrow QH \\ & \mathbf{z} = \Phi(\mathbf{y}) \end{aligned} \tag{3.23}$$

Physically, this equation can be considered as an interaction law between small and large scales of motion in fluid flow, **y** representing the large scales (low frequencies in the spectral decomposition) and **z** representing the small scales (high frequencies in the spectral decomposition). This interaction can bring a correction in the evolution of large scales of motion (3.22a), which in the absence of it (**z** = 0), reduces to the classical Galerkin decomposition.

As it is not possible to write this interaction law (3.23) explicitly, methodologies to approximate it, have been developed. These methodologies are based on the simplification of the interaction law by the consideration of the order of magnitude of the terms in the large and small scale evolution equations (3.22a-b). After a short transient period, it can be shown that, for sufficiently large m, the order of magnitude of **z** is much smaller than that of **y** which is of the same order of **u**, regardless of the initial condition on **z**. This implies that, for the nonlinear terms which consist of quadratic nonlinearities, small scale-small scale interactions are much smaller than large scale-small scale interactions and those are both much smaller than large scale-large scale interactions. Hence, in a first approximation, $QB(\mathbf{y}+\mathbf{z})$ is comparable to $QB(\mathbf{y})$. Furthermore, the relaxation time for the large scale evolution (3.22a), is much smaller than that for small scale evolution (3.22b) so that it is reasonable to consider that the small scale evolution is quasi-static and this fact

permits to neglect *dz/dt* term in the evolution equation (3.22b), to give the simplest approximate inertial manifold as (Foias et al., 1988b),

$$\begin{aligned} \Phi_0: \quad & PH \rightarrow QH \\ & \mathbf{z} = \Phi_0(\mathbf{y}) = -(\nu A)^{-1}(Q\mathbf{f} - QB(\mathbf{y})) \end{aligned} \tag{3.24}$$

Similarly, another approximate inertial manifold can be defined through the equation (Titi, 1988),

$$-\nu A\mathbf{z} + QB(\mathbf{y}+\mathbf{z}) = Q\mathbf{f} \tag{3.25}$$

in which the small scale interactions are not neglected. An infinite sequence of approximate inertial manifolds is defined in the literature giving better and better approximation to the exact inertial manifold (Devulder and Marion, 1992).

Another approximation, known as the Euler-Galerkin algorithm (Foias et al., 1988c), does not neglect *dz/dt* term and integrates the small scale evolution equation (3.22b) using the implicit Euler time integration scheme, τ being the time step and $\mathbf{z}$ initially zero,

$$\mathbf{z}^{n+1} - \tau\nu A\mathbf{z}^{n+1} + \tau QB(\mathbf{y}+\mathbf{z}^{n+1}) = \tau Q\mathbf{f} \tag{3.26}$$

Then the inertial manifold, in a first approximation, can be given as,

$$\Phi(\mathbf{y}) = \tau(I - \tau\nu A)^{-1}(Q\mathbf{f} - QB(\mathbf{y})) \tag{3.27}$$

As it is mentioned in the above, it is possible to construct sequences of approximate inertial manifolds giving better convergence to the exact inertial manifold. However, these sequences are obviously of increasing complexity in the sense that they require much more numerical iterations for each level in this hierarchy. It should be noted that these new integration algorithms have to be considered in terms of efficiency as well as convergence.

3.2.5. Theoretical and Numerical Aspects of the Nonlinear Galerkin Methods

The theory of inertial manifolds has special significance in the numerical computation of solutions of the underlying partial differential equation. The reduction of an infinite-dimensional problem to a finite-dimensional one is a fundamental cause of error in any numerical computation. In the case where the partial differential equation has an inertial form, then the reduction to the finite-dimensional problem is exact. Therefore, approximation schemes based on the theory of inertial manifolds hold the promise for significant increases in computational efficiency (Sell, 1993).

It can be proved that, under reasonable conditions, every approximate inertial manifold for a given equation is an actual inertial manifold of an approximate equation (Sell, 1993). The stability and convergence properties of the nonlinear Galerkin methods have been investigated both mathematically and numerically in the context of two-dimensional Navier-Stokes equations, mostly for homogeneous flows (space periodic boundary conditions in both directions) (Jauberteau et al. 1990; Jolly, 1993; Debussche and Dubois, 1994).

It is well known that large scale scientific computing, in the context of fluid systems, requires the utilization of large number of spatial variables and the integration of evolution equations on large intervals of time. In direct numerical simulations with spectral methods, it can be observed that the modes corresponding to small wavelengths carry a very few per cent of the total kinetic energy. This fact is also recognized by conventional turbulence theory in the sense that the high frequencies, by the effect of the viscosity, attain a statistical equilibrium much faster than the low frequencies. Computationally, the nonlinear Galerkin methods use this fact of the separation of scales and model their interaction making direct use of the deterministic Navier-Stokes equations of motion. It has been advocated that, in large scale computing, the magnitudes ratio of small to large scales being so small, there is a stiffness built into the discrete system and this stiffness problem should be addressed directly and that the components of the motion should be decomposed into arrays of different orders of magnitude to be treated differently (Temam, 1993).

These methods can also be generalized into the multilevel numerical methods for the numerical simulation of turbulence (Temam, 1996). Their effectiveness are justified by the aspects of their enhanced convergence properties with respect to the classical numerical schemes, by the savings in computation time due to the decrease in the number of operations and the increase in the maximum allowable time step for the stability of the scheme and finally by the filtering role of the utilization of approximate inertial manifolds which act as nonlinear filters for the numerical scheme.

Nonlinear Galerkin methods have also been subject to numerical experiments with spectral decompositions using Chebyshev and Legendre polynomials in the cases of one-dimensional Poisson and the one-dimensional Helmholtz equations. Improvements in terms of convergence and stability of the new numerical algorithm with respect to the classical Galerkin method have been noted (Shen and Temam, 1995).

4. RESULTS AND DISCUSSION

In this chapter, we will present the results of the numerical simulations concerning the solutions of the nonlinear stability problem for two-dimensional wall-bounded and free shear flows as formulated in the previous chapters. The main fourth-order scalar streamfunction partial differential equation (2.5) together with the appropriate boundary conditions has been integrated using the classical Galerkin and the nonlinear Galerkin fully spectral methods. For this purpose, computer programs in FORTRAN language have been written and used.

Initial conditions for the problems have been generated from the eigenfunctions of the Orr-Sommerfeld linear stability equation (2.7) corresponding to the most unstable eigenvalue for a given Reynolds number. In the solution of this eigenvalue problem, we made use of the MATHEMATICA FOR UNIX symbolic computer program. MATHEMATICA has also been used in the testing of the above mentioned FORTRAN programs in the case of low number of modes. Both MATHEMATICA and FORTRAN programs have been run on a Digital Alphastation 200.

The time integration of the finite-dimensional ordinary differential equations system resulting from the spectral methods, has been performed by using the fourth order explicit Runge-Kutta time integration scheme, for the testing and comparisons of the methods. For further numerical simulations in high Reynolds numbers, to detect the bifurcations of solutions, a less costly second order accurate Crank-Nicholson Adams-Bashforth mixed scheme has been used. Linear terms in the equation, have been integrated in time using the implicit Crank-Nicholson time integration scheme and the nonlinear terms have been integrated using the explicit Adams-Bashforth time integration scheme.

In the first section (4.1), we present the tests and numerical comparisons of the classical and nonlinear Galerkin methods parametrically for both plane Poiseuille and temporally growing mixing layer flow cases. In the next section (4.2), we present numerically and parametrically the bifurcations leading to turbulence for plane Poiseille, oscillatory Poiseuille, temporally growing mixing layer and plane jet flows.

4.1. Classical versus Nonlinear Galerkin Methods

4.1.1. Wall-Bounded Shear Flow Case

4.1.1.1. Stability Tests. It is well known that in plane Poiseuille flow, all infinitesimal and finite perturbations are damped when Reynolds number is below 500-600. The stability tests for the numerical schemes have been conducted by the consideration of the damping of an arbitrary initial perturbation satisfying the continuity, and of the development of the parabolic velocity profile in laminar regime for the plane Poiseuille flow. Accordingly, the streamfunction which gives the initial velocity distribution is chosen to be (Moin and Kim, 1980),

$$\psi_0(x,y) = C(y - \frac{y^9}{9}) - \frac{\varepsilon L}{4\pi}(1+\cos\pi y)\cos(4\pi x / L) \qquad (4.1)$$

where C=0.75 and ε =0.075. Reynolds number is taken to be 100, i. e. laminar regime where all finite disturbances are expected to die out, and the wavenumber α =0.5.

The classical Galerkin solution which uses the first 5 Fourier and the first 10 Chebyshev modes is accepted as the reference solution (SGM1). The classical Galerkin solution using 3 Fourier and 4 Chebyshev modes together with the nonlinear Galerkin algorithms which bring corrections to it with respect to the reference solution, making use of the formulation (3.24) (NGM1) and the Euler-Galerkin formulation (3.27) (NGM2) are presented. The initial perturbation is damped, as expected in the laminar regime. The development of the parabolic velocity profile given for SGM1 in Fig. 4.1 and for NGM1 in Fig. 4.2, demonstrates the stability of the numerical algorithms.

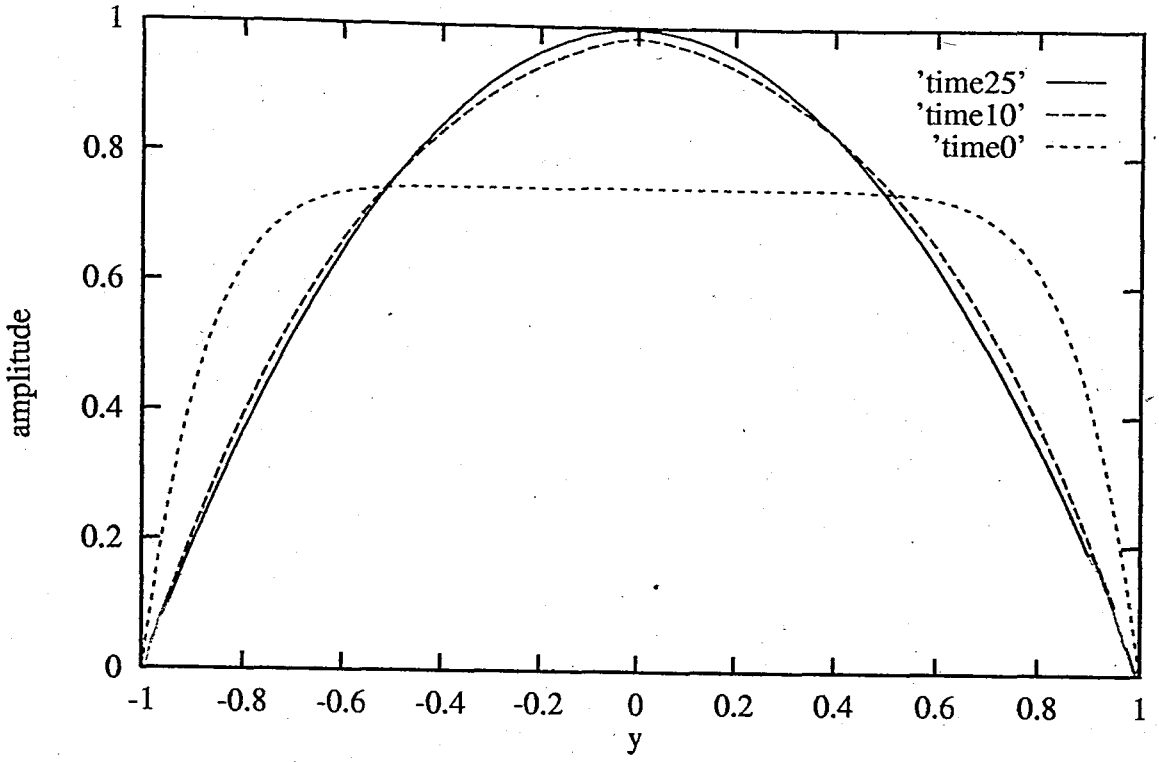

FIGURE 4.1. The development of the parabolic velocity profile for plane channel flow with classical Galerkin method (SGM) ($x = \pi/2$, $t = 0$-25)

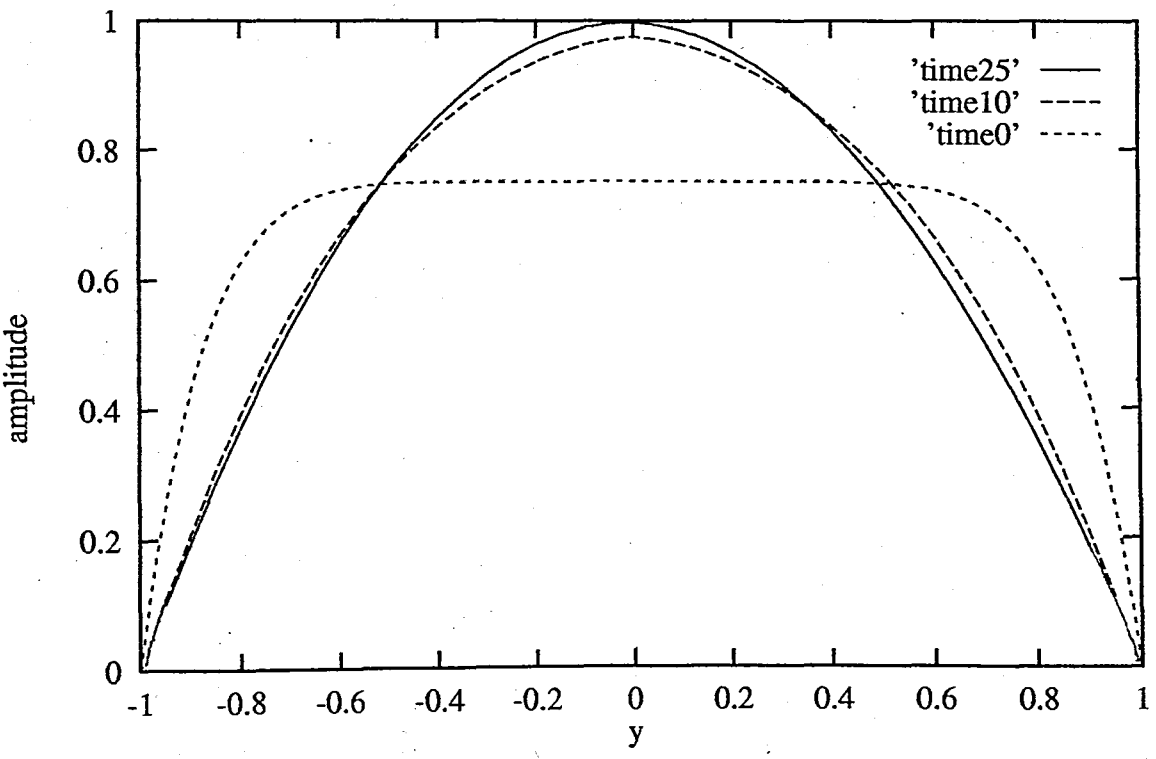

FIGURE 4.2. The development of the parabolic velocity profile for plane channel flow with nonlinear Galerkin method (NGM1) ($x = \pi/2$, $t = 0$-25)

In Fig. 4.3 and Fig. 4.4, the time evolution of some low Fourier-Chebyshev modes are presented. These low modes are observed to be corrected by the use of the nonlinear Galerkin methods with respect to the reference Galerkin solution. In Fig. 4.5 a high Fourier mode and in Fig. 4.6 a high Chebyshev mode, not present in the low-mode classical Galerkin solution (SGM2) are presented. As these high modes are not in the low-mode spectral decomposition (SGM2), their values are zero. The nonlinear Galerkin algorithms using the same number of modes as low-mode Galerkin solution (SGM2) estimate the values of these high modes through the approximate inertial manifolds (3.24) and (3.27), i. e. through the law of the interaction between the small and large scales of motion. As expected, the Euler-Galerkin algorithm (NGM2) which does not neglect the *dz/dt* term gives better results compared to the algorithm (NGM1) which neglects it.

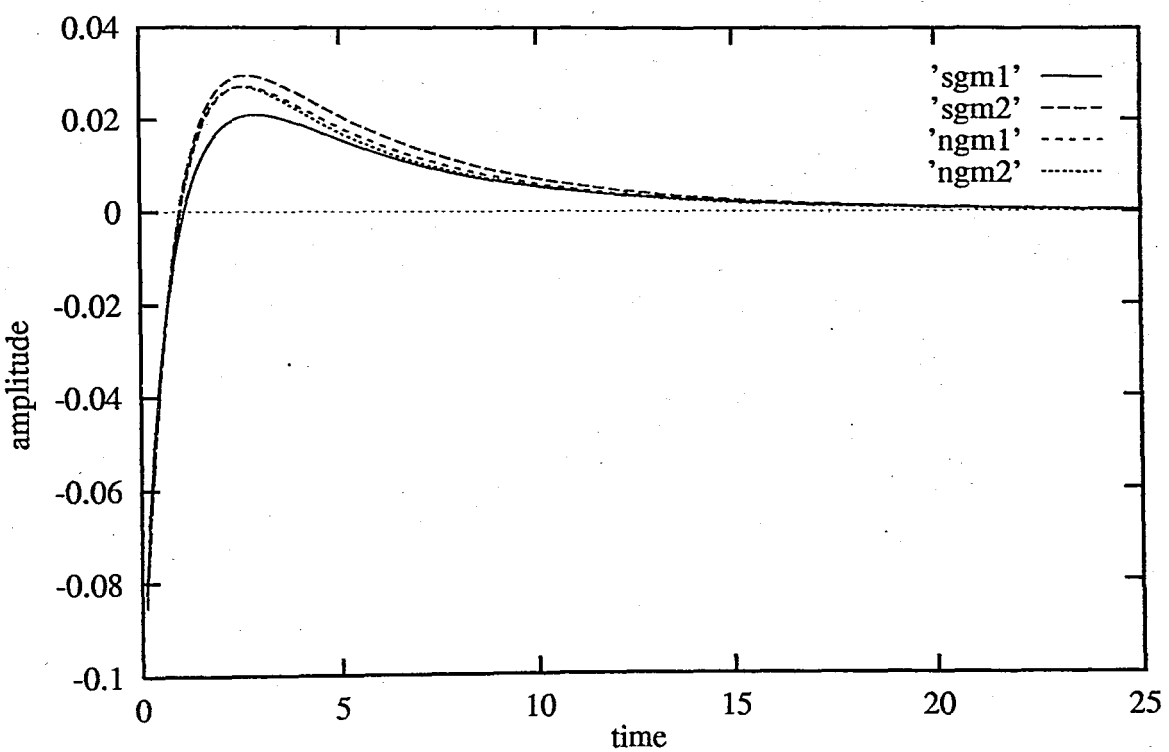

FIGURE 4.3. Time evolution of the real part of the coefficient $a_{0,5}$ for plane channel flow at Re=100, $\alpha = 0.5$

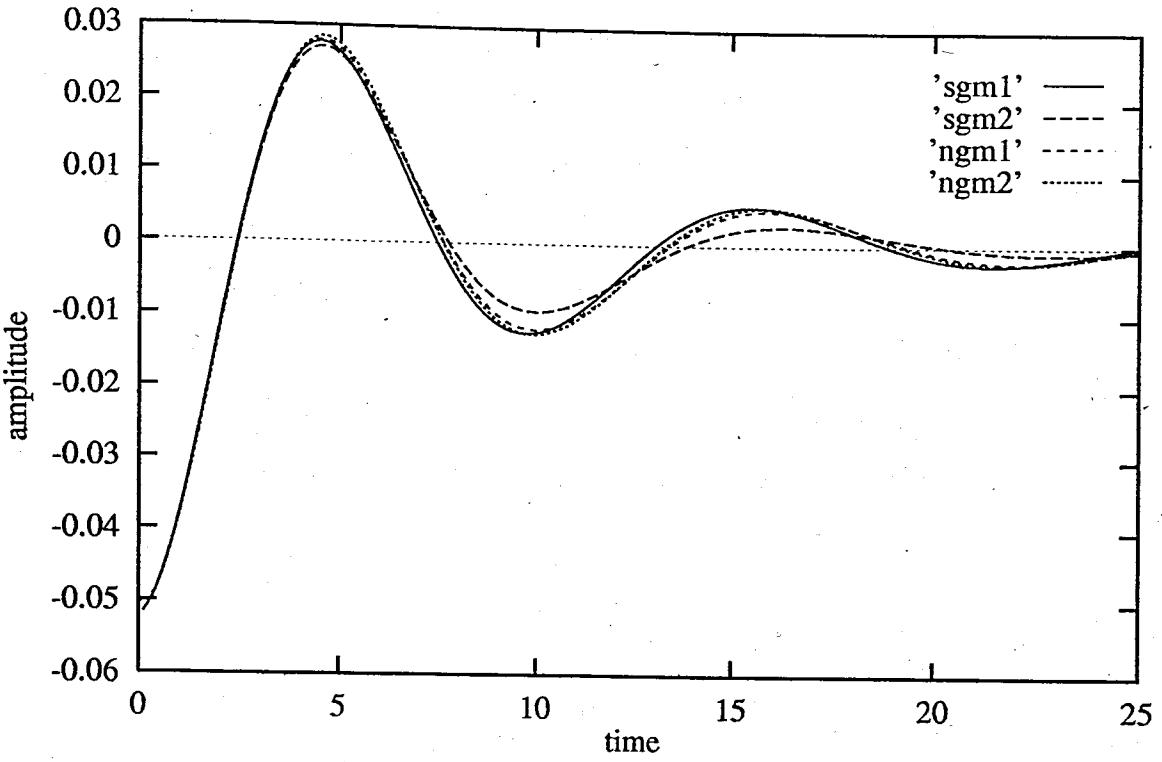

FIGURE 4.4. Time evolution of the real part of the coefficient $a_{-2,2}$ for plane channel flow at Re=100, $\alpha = 0.5$

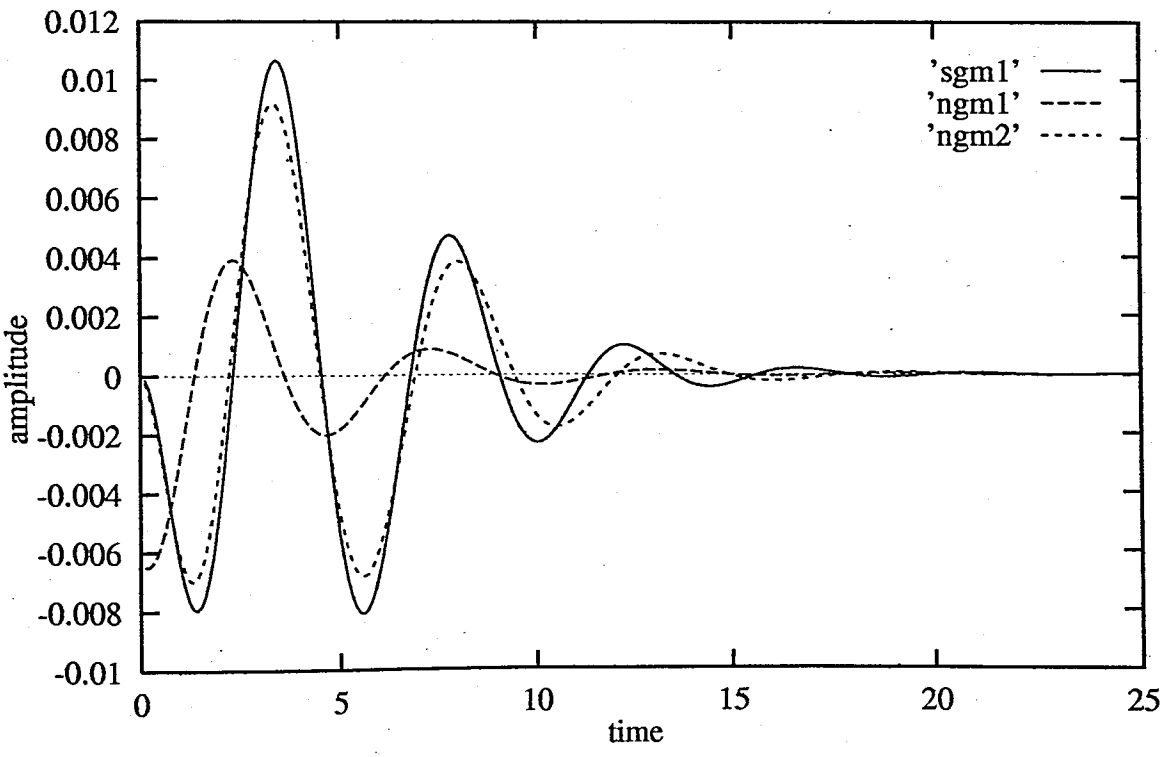

FIGURE 4.5. Time evolution of the real part of the coefficient $a_{-4,3}$ for plane channel flow at Re=100, $\alpha = 0.5$

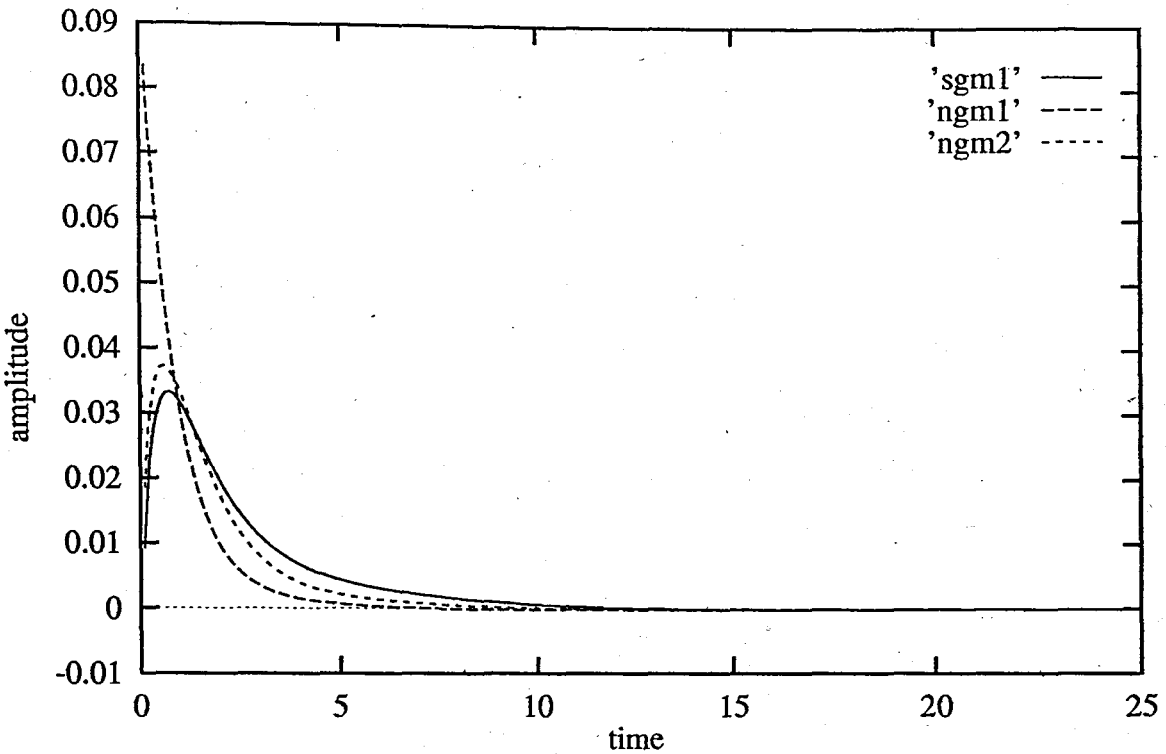

FIGURE 4.6. Time evolution of the real part of the coefficient $a_{0,7}$ for plane channel flow at Re=100, $\alpha = 0.5$

4.1.1.2. Comparisons with the Linear Stability Theory. Linear stability theory using the Orr-Sommerfeld stability equation, estimates the limit of stability for two-dimensional infinitesimal perturbations as Re=5772.22 for the wavenumber α =1.02. The nonlinear theory estimates a Reynolds number around Re=2700 for two-dimensional finite perturbations. The inclusion of three-dimensional infinitesimal perturbations through secondary instability mechanism lowers this Reynolds number around Re=1000 in parallel with the experiments (Orszag and Kells, 1980).

A second test for the numerical algorithms and developed computer programs, is the comparison between the linear and nonlinear theories for an infinitesimal initial perturbation (of the order 10^{-6}) at Re=1500, which is in the limits of the linear theory.

For Re=1500 and the wavenumber α =1, the eigenvalues of the Orr-Sommerfeld equations have been calculated with the MATHEMATICA program and eigenvectors

corresponding to the most unstable eigenvalue (c = 0.326299-i 0.028205) have been generated and used as the initial conditions in the main FORTRAN programs. The reference solution (SGM1) uses 9 Fourier, 16 Chebyshev modes. The low-mode Galerkin (SGM2) and the corresponding nonlinear Galerkin algorithms (NGM1 and NGM2) use 5 Fourier, 10 Chebyshev modes.

In Fig. 4.7 the time evolution of a low Fourier-Chebyshev mode is shown to be corrected with respect to the reference solution (SGM1). In Fig. 4.8 the evolution of a high Fourier-Chebyshev mode is shown to be estimated through the nonlinear Galerkin algorithms. In Table 4.1 the amplitude reduction of the initial perturbation at t =10 is presented for the methods in comparison with the reduction given by the linear theory for this perturbation which is in the limits of its applicability (Atalık and Tezel, 1998).

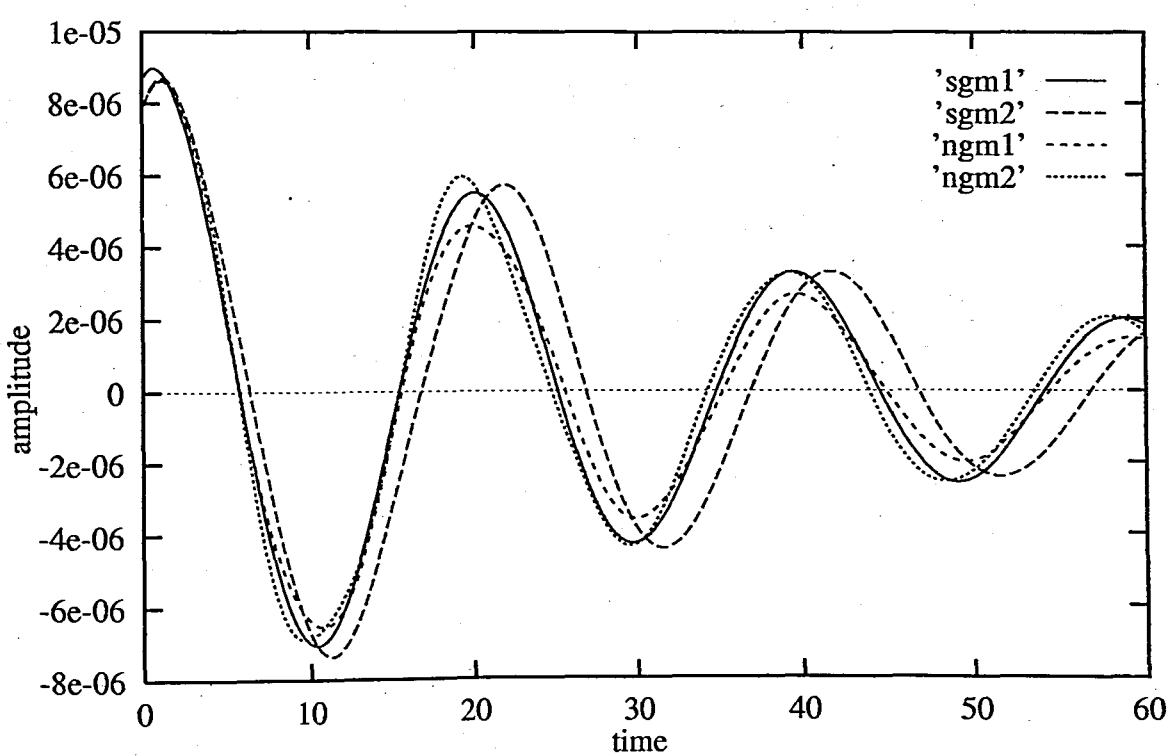

FIGURE 4.7. Time evolution of the real part of the coefficient $a_{1,6}$ for plane channel flow at Re=1500, $\alpha = 1$

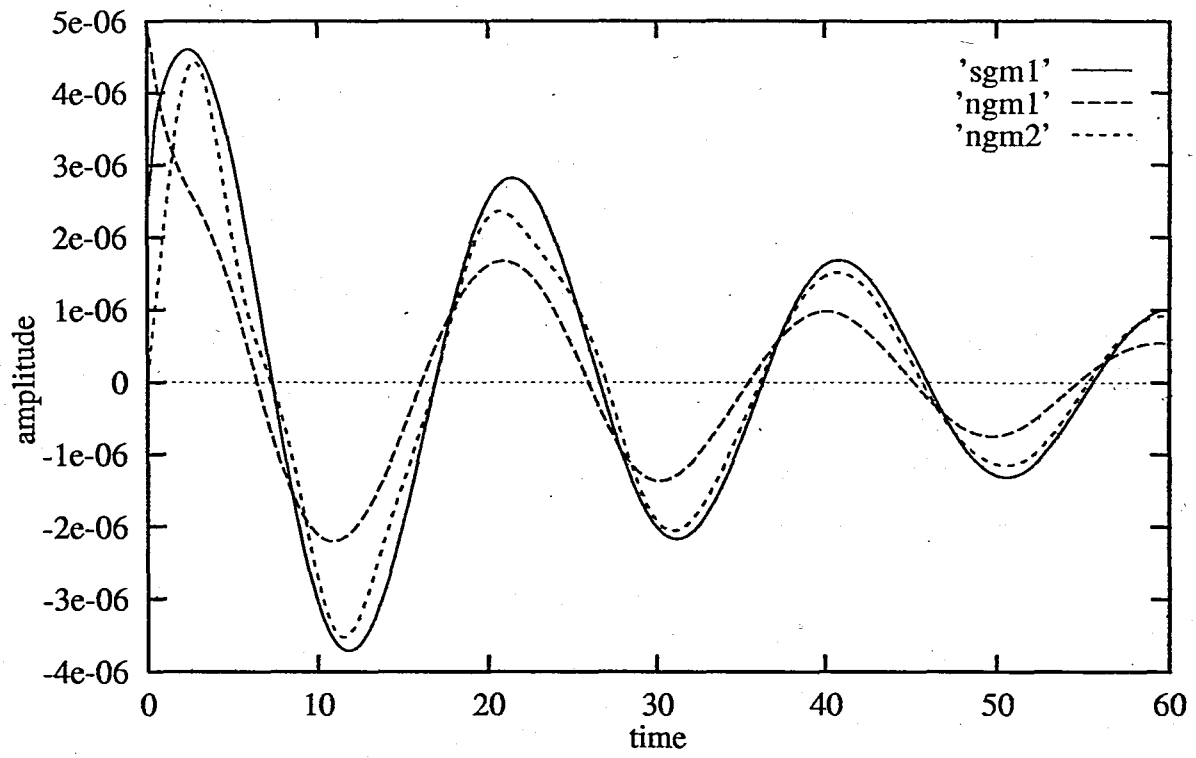

FIGURE 4.8. Time evolution of the real part of the coefficient $a_{1,12}$ for plane channel flow at Re=1500, $\alpha = 1$

TABLE 4.1. Comparison of the amplitude reductions of the initial perturbation for plane channel flow at Re=1500, α=1 and t=10

	amplitude reduction
linear theory	0.7542
SGM1	0.7385
SGM2	0.7225
NGM1	0.7316
NGM2	0.7376

4.1.1.3. Transition Regime. It is known that finite two-dimensional disturbances are no more damped but saturate into finite amplitude waves at Reynolds numbers near Re=2700 for plane channel flow based on constant-flux and near Re=2900 for channel flow based on constant-pressure formulations around wavenumbers α =1. These waves arise from a first Hopf bifurcation at these critical Reynolds numbers and correspond to periodic solutions or attractors (the so-called Tollmien-Schlichting waves) in the phase space of the Navier-Stokes equations of motion for plane channel flow.

The most critical eigenvalue of the Orr-Sommerfeld linear stability equation for Re=2935, α =1.3231 is calculated to be c = 0.328984-i 0.0137505. The corresponding eigenvectors are used as an initial condition with a finite perturbation of the order 10^{-3}. The reference Galerkin solution (SGM1) uses 9 Fourier and 18 Chebyshev modes. The low-mode Galerkin solution (SGM2) and the nonlinear Galerkin solution (NGM1) use 5 Fourier and 14 Chebyshev modes. The Euler-Galerkin (NGM2) results are found to be very close to the NGM1 results for this case and they are not presented. In Fig. 4.9 the time evolution of a low Fourier-Chebyshev mode is presented and the correction brought by the nonlinear Galerkin algorithm to the low-mode Galerkin solution is observed. The amplitude and phase errors of the low-mode Galerkin solution are corrected by the nonlinear Galerkin algorithm in comparison to the reference solution. In Fig. 4.10 the time evolution of a high Fourier-Chebyshev mode is presented. The small scale reference solution is approximated through the use of the inertial manifold from the large scales of motion.

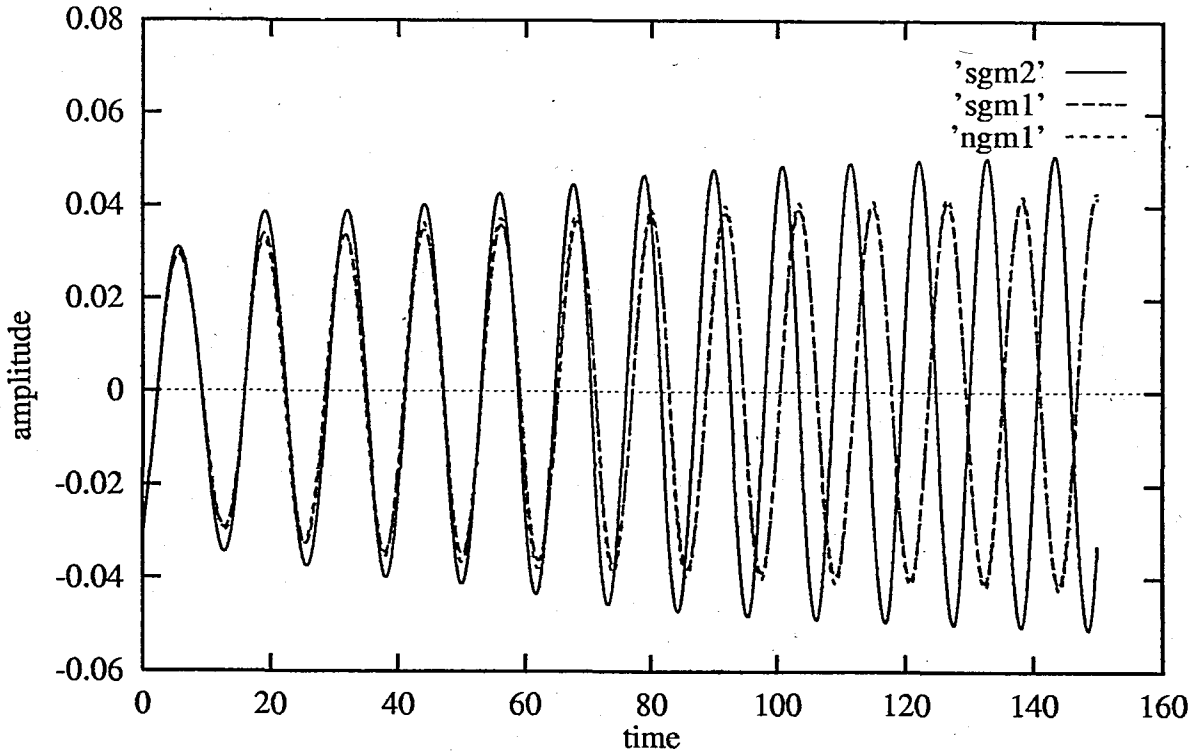

FIGURE 4.9. Time evolution of the real part of the coefficient $a_{1,8}$ for plane channel flow at Re=2935, α =1.3231

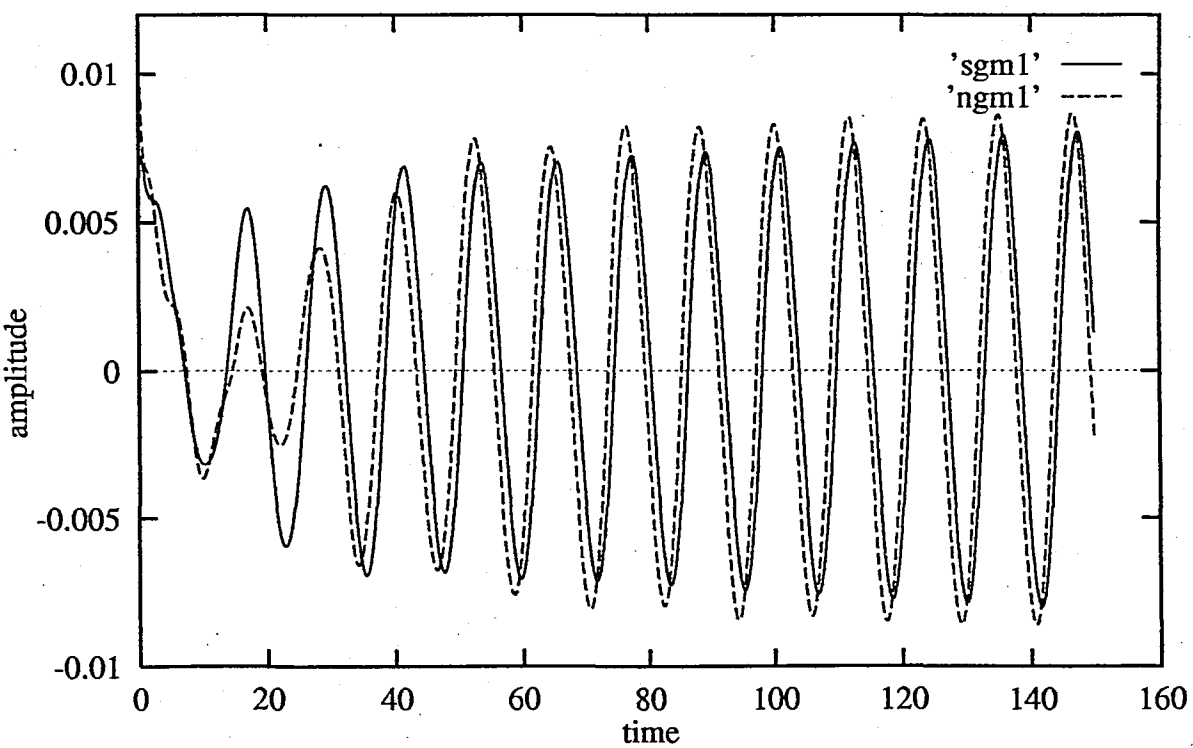

FIGURE 4.10. Time evolution of the real part of the coefficient $a_{1,16}$ for plane channel flow at Re=2935, α = 1.3231

In Fig. 4.11, the velocity profiles for $t = 150$ at $x = \pi / 2$, are presented. As there are phase differences between the low-mode Galerkin solution (SGM1) and the reference solution (SGM2), the corresponding velocity profiles are inverse of each other. The nonlinear Galerkin algorithm (NGM1) corrects these differences (Atalık and Tezel, 1998).

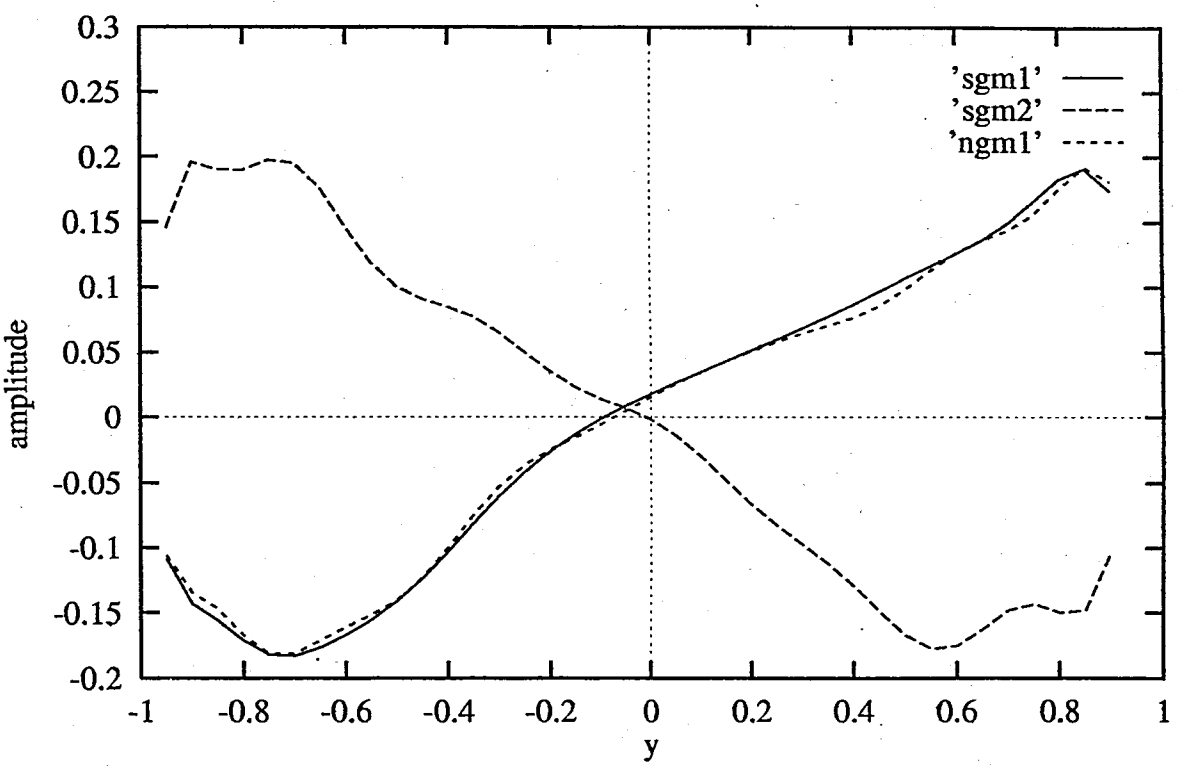

FIGURE 4.11. u velocity profiles at $x=\pi/2$, $t=150$ for plane channel flow at Re=2935, $\alpha = 1.3231$

4.1.2. Free Shear Layer Flow Case

4.1.2.1. Tests on Hermite Functions Use. As we mentioned in the Section 3.1, the use of Hermite functions with spectral methods in flow problems for unbounded domain is not common, although their natural domain of orthogonality is the infinite interval. In some cases slow convergence and even divergence have been reported. The reason is given to be that exponential convergence is achieved with the use of Hermite functions if the function to be expanded decays exponentially fast at the infinity (Boyd, 1984). In general, for problems in unbounded domains the question of which basis to use seems not to be settled yet. The usual method for dealing with the infinite interval is to truncate the interval $[-\infty,\infty]$ to $[-L, L]$ and then use Fourier series. This method is known as the domain truncation (Grosch and Orszag, 1977). Alternatively, the infinite interval can be mapped into a finite interval using an algebraic mapping which is also associated with the use of orthogonal rational functions such as the Higgins and Christov functions (Higgins, 1977; Christov, 1982) or rational Chebyshev functions (Boyd, 1990), a trigonometric mapping such as the cotangent mapping (Cain et al., 1983) or a hyperbolic mapping function such as the 'sinh-mapping' (Weideman and Cloot, 1994) which involve all a free mapping parameter and then Fourier series or Chebyshev functions can be used in the spectral decomposition. However, in domain truncation the optimum domain size and in mapping techniques, the optimum value of the mapping parameter is to be determined to ensure convergence. Although some theory exists such as the method of steepest descent for simple cases for estimating these optimal parameters, these formulas are difficult to use and they require some a priori knowledge of the function to be approximated (Boyd, 1982; 1984). When solving equations, the properties of the function are changing with time and even if the optimal parameter corresponding to the initial condition can be found theoretically, it may soon become non-optimal resulting in a significant decrease in accuracy. An interesting conclusion was that the optimal parameter associated with mapping techniques, is not only a function of the singularities and asymptotic behavior of the solution but also depends upon the number of the expansion terms or functions (Chebyshev or Fourier) kept in the decomposition (Boyd, 1982; 1984). In other words, the optimal parameter for the expansion with ten Chebyshev polynomials may be much different than the best choice for forty Chebyshev polynomials. Hence, the optimalization can be conducted only through numerical tests.

We prefer here to use Hermite functions which seem to be the natural choice for the problems defined on the infinite interval, which however have been avoided due to the solution's asymptotic behavior at the infinity and the related boundary conditions. Hermite functions do not involve any free parameter to be adjusted and they possess orthogonality properties on the infinite interval so that we can expect them to be more effective than the above mentioned methods, if the above convergence criterion is satisfied. For the nonlinear stability problem formulated in terms of the perturbation streamfunction (2.5), the boundary conditions are of the exponentially fast vanishing type at the infinity. Thus, the exponential convergence criterion for the use of Hermite functions is fulfilled as the numerical tests carried on the solution of the linear stability Orr-Sommerfeld equation demonstrate (Table 4.2) (Atalık and Tezel, 1999).

TABLE 4.2. Growth rates of the Orr-Sommerfeld eigenfunctions of the most rapidly growing mode for the temporally growing mixing layer at Re=100

	x wavenumber α		
M	0.25	0.50	0.75
15	0.557	0.338	0.131
20	0.567	0.337	0.134
25	0.580	0.340	0.135
31	0.585	0.341	0.137
35	0.595	0.342	0.136
40	0.596	0.342	0.137

4.1.2.2. Transition Regime. Tests on the classical and nonlinear Galerkin spectral methods for the temporally growing mixing layer have been carried out for the Reynolds number Re=100 with initial conditions generated from the eigenfunctions of the corresponding Orr-Sommerfeld equation for the wavenumber α =0.25, with a perturbation of the order of 10^{-3}. The reference solution (SGM1) uses 8 Fourier and 18 Hermite modes. The low-mode Galerkin (SGM2) and the nonlinear Galerkin algorithms (NGM1 and NGM2) use 4 Fourier and 14 Hermite modes. Two-dimensional finite perturbations are observed to saturate into a vortical state while the associated dynamical system's solutions converge to a fixed point attractor. In Fig. 4.12 and Fig. 4.13 the time evolution of low Fourier-Hermite modes, in

Fig. 4.14 the time evolution of a high Fourier-Hermite mode are plotted. Similar observations (as in the case of channel flow) on the convergence of the nonlinear Galerkin algorithms can be done. The low Fourier-Hermite modes are corrected by the use of these algorithms and high Fourier-Hermite mode, zero in the case of the low-mode Galerkin (SGM2) is estimated through the approximate inertial manifold. Although in the mathematical development of the inertial manifold theory, only bounded or space periodic flows have been treated due to the lack of compactness theorems in the unbounded flow case (Temam, 1995), in this study the mixing layer case which has been subject to the application of classical spectral methods in the literature is also considered from a purely computational point of view.

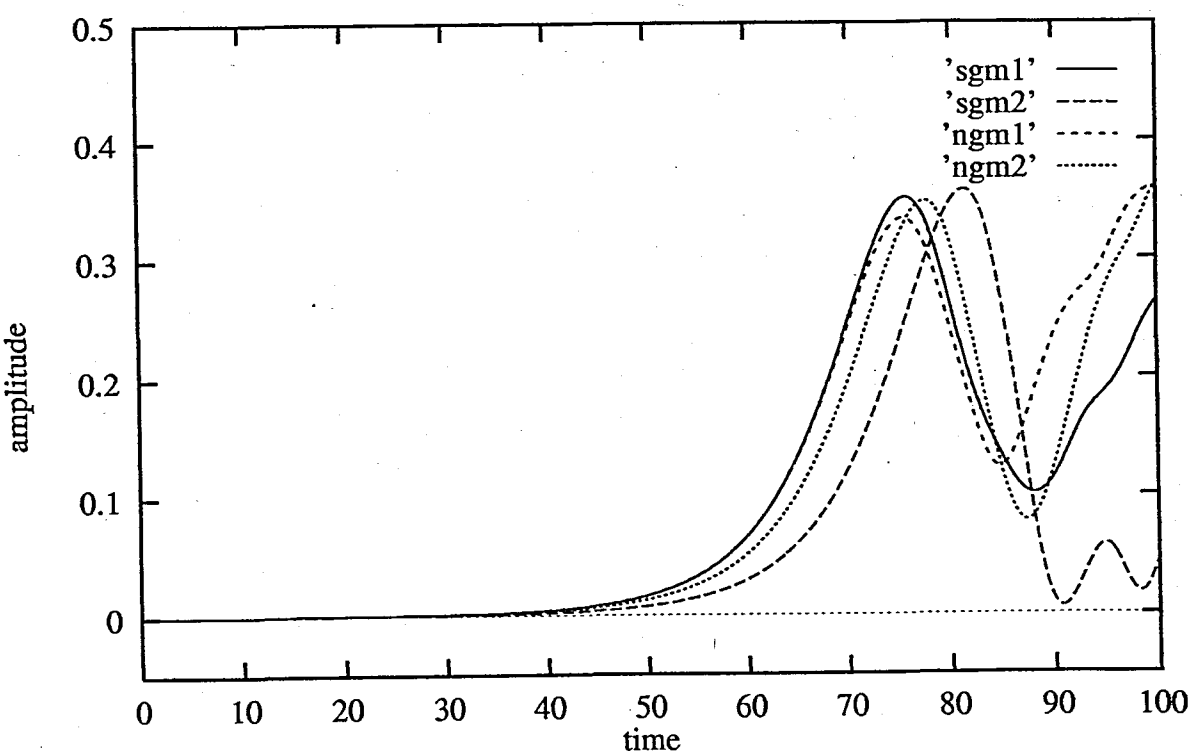

FIGURE 4.12. Time evolution of the real part of the coefficient $a_{1,1}$ at Re=100, $\alpha = 0.25$ for the temporally growing mixing layer

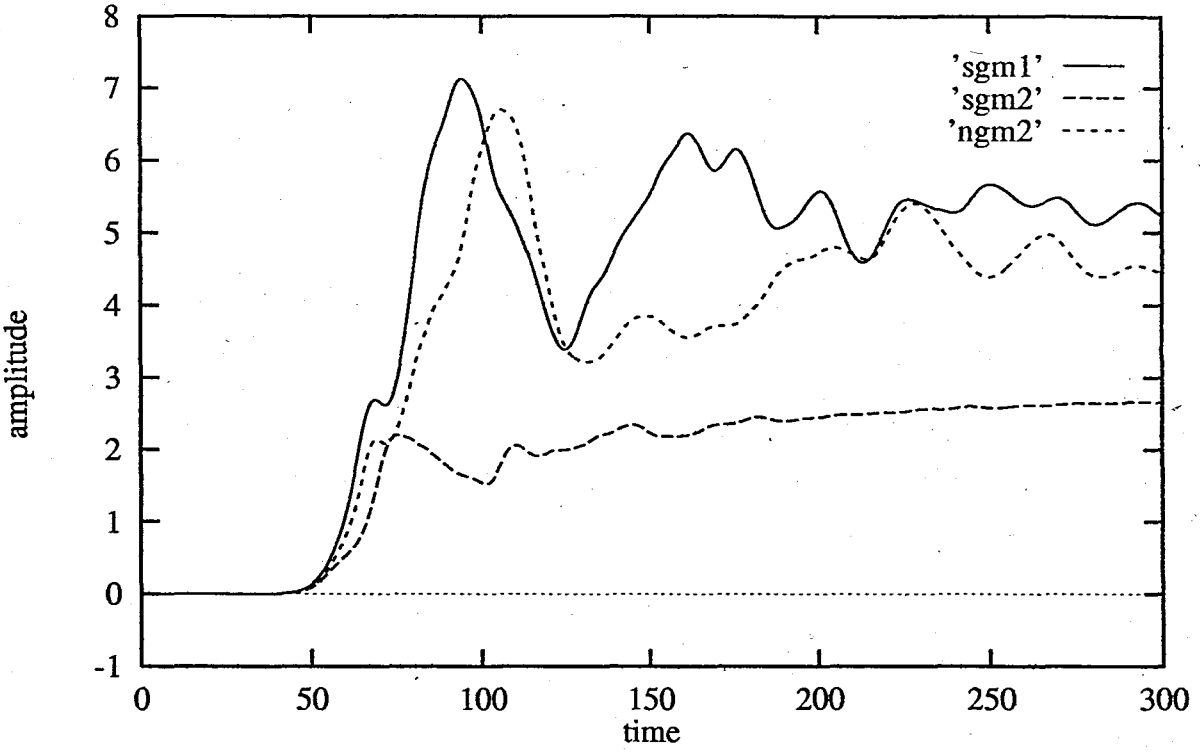

FIGURE 4.13. Time evolution of the real part of the coefficient $a_{0,1}$ at Re=100, $\alpha = 0.25$ for the temporally growing mixing layer

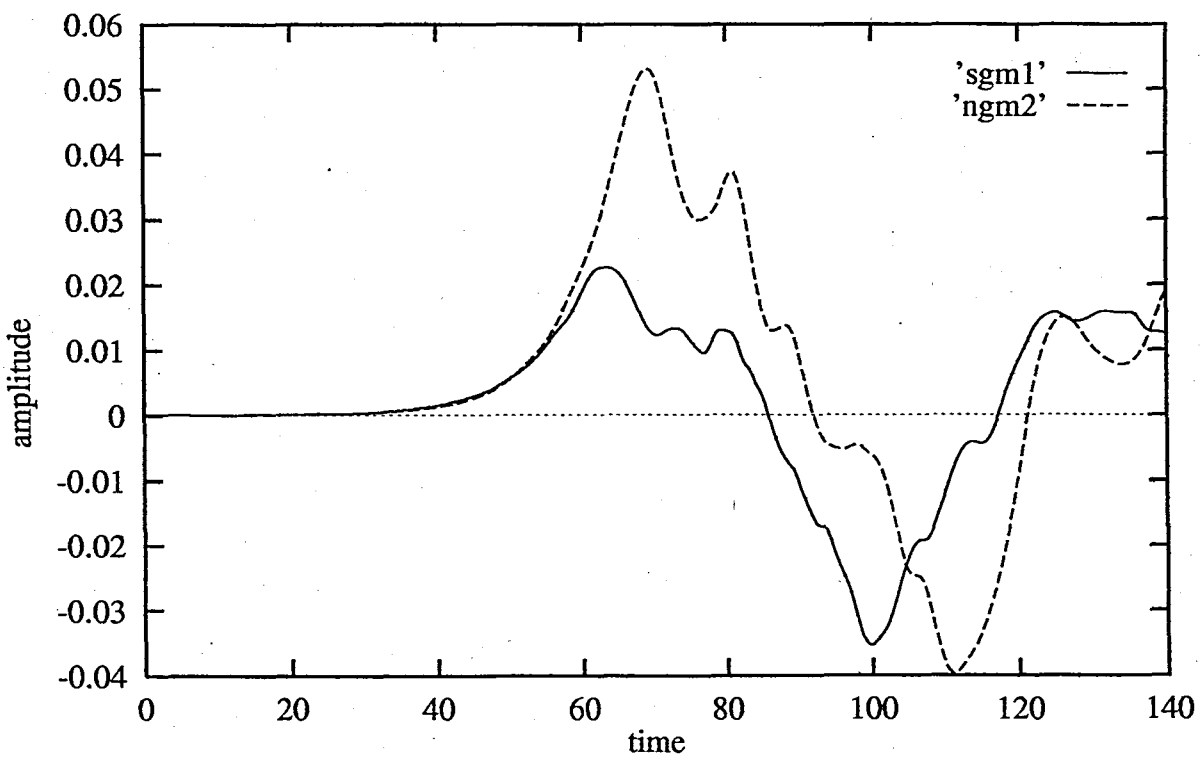

FIGURE 4.14. Time evolution of the real part of the coefficient $a_{-6,0}$ at Re=100, $\alpha = 0.25$ for the temporally growing mixing layer

4.1.3. Convergence and Efficiency of the Nonlinear Galerkin Methods

As it has been shown in the previous sections, the nonlinear Galerkin algorithms have better convergence properties with respect to the classical Galerkin schemes. However, to challenge the classical Galerkin method, these algorithms have to be investigated also upon their efficiency. As nonlinear Galerkin algorithms work with less number of modes for comparable accuracy with respect to the classical Galerkin method, the number of operations per time step in the time integration of the differential system will be less. This decrease in the number of operations is especially important in the treatment of the nonlinear terms for each time step. For the above plane channel and temporally growing mixing layer tests an efficiency comparison in terms of the number of time steps per computation time between the methods is presented in Table 4.3. As it can be observed there is no big difference between the two nonlinear Galerkin algorithms, but they are approximately two times more efficient with respect to the classical Galerkin scheme for comparable accuracy.

TABLE 4.3. Efficiency test in terms of the number of time steps per computation minute of the algorithms for different flow cases

	SGM	NGM1	NGM2
Plane channel Re=100, α=0.5	1100	2000	1970
Plane channel Re=1500, α=1	110	220	210
Plane channel Re=2935, α=1.3231	83	155	145
Mixing layer Re=100, α=0.25	200	390	375

Another point is the maximum allowable time step concern. As it is well known, the maximum allowable time step for the stability of the numerical scheme decreases when the dynamical system dimension increases. It has been noted, in the case of homogeneous flows, that the stability condition with the use of nonlinear Galerkin algorithms is based on the number of large scale modes rather than the total number of modes (large scales plus small scales) (Jauberteau et al., 1990; Temam, 1995). Hence one can use larger time steps with nonlinear Galerkin algorithms with respect to the classical Galerkin scheme for comparable accuracy. This constitutes another aspect of numerical efficiency. For the wall-

bounded shear flow case, analysed in this work, we compared using the same time step, the number of steps at which the solution blows up due to the accumulation of numerical errors, for all the methods, in the case of plane channel flow (Table 4.4). As it can be seen, with the nonlinear Galerkin algorithms, the solution blows up at later times. With the use of the Euler-Galerkin algorithm, the numerical instability causes the blow-up of the solution approximately three times later than the classical Galerkin scheme.

TABLE 4.4. Efficiency test in terms of the maximum allowable time step for plane channel flow at Re=6500, α=1.3231

	SGM	NGM1	NGM2
Blow-up time step	650	1600	1950

Based on the numerical simulations conducted in this work, we can expect an overall efficiency of six or seven, in terms of the decrease in the number of operations and the increase in the maximum allowable time step, for the nonlinear Galerkin algorithms with respect to the classical Galerkin scheme for comparable accuracy. This increase in the efficiency is significant in the context of the direct numerical simulations of the Navier-Stokes equations.

4.2. Parametrical Investigation of the Transition to Turbulence in Plane Shear Flows

Two-dimensional turbulence has been subject to many studies in the literature, although a full turbulence study requires the consideration of three-dimensional effects and hence the study of the three-dimensional Navier-Stokes equations. There are indications that some physical mechanisms such as vortex tilting and vortex stretching, which are absent in two-dimensional case play important roles in the laminar to turbulent transition and in many shear flows this transition is mediated by three-dimensional secondary instabilities of two-dimensional nonlinear disturbances (Orszag and Patera, 1983). However, two-dimensional disordered or chaotic motion is known to be associated with the large scale motion of some turbulent flows even after the small scales become fully turbulent and three-dimensional (Roshko, 1976). This implies the existence of two-dimensional attractors with time scales comparable to those of three-dimensional structures so that both types of motion can coexist in the final flow. Therefore, it is interesting to study those two-dimensional structures to determine their possible influence in the first appearance of disorder in the flow.

4.2.1. Wall-Bounded Plane Shear Flows

4.2.1.1. Plane Channel (Poiseuille) Flow. It is known that two-dimensional finite disturbances saturate into a periodic motion around Re=2800-2900 for plane channel Poiseuille flow (Orszag and Kells, 1980). In Fig. 4.15, the streamlines and in Fig. 4.16 the vorticity lines corresponding to the flow case Re=2935, $\alpha = 1.3231$ at $t = 150$ are plotted. It is observed that the straight horizontal streamlines in the laminar flow regime begin to gain a wavy structure under the influence of the saturated perturbation. A similar wavy structure is also observed for the vorticity lines together with the formation of the vortices near the walls. With this periodic (Hopf) bifurcation, the symmetry of the laminar solution with respect to the boundary conditions is observed to be broken.

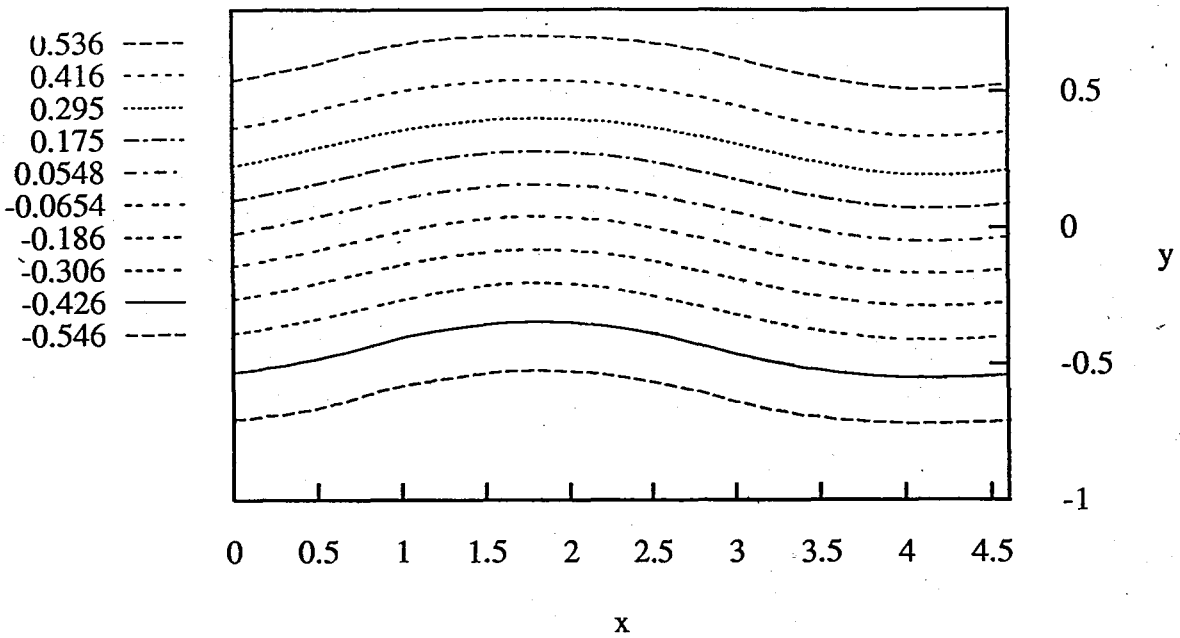

FIGURE 4.15. Streamlines for plane channel flow at t=150 for Re=2935, $\alpha = 1.3231$

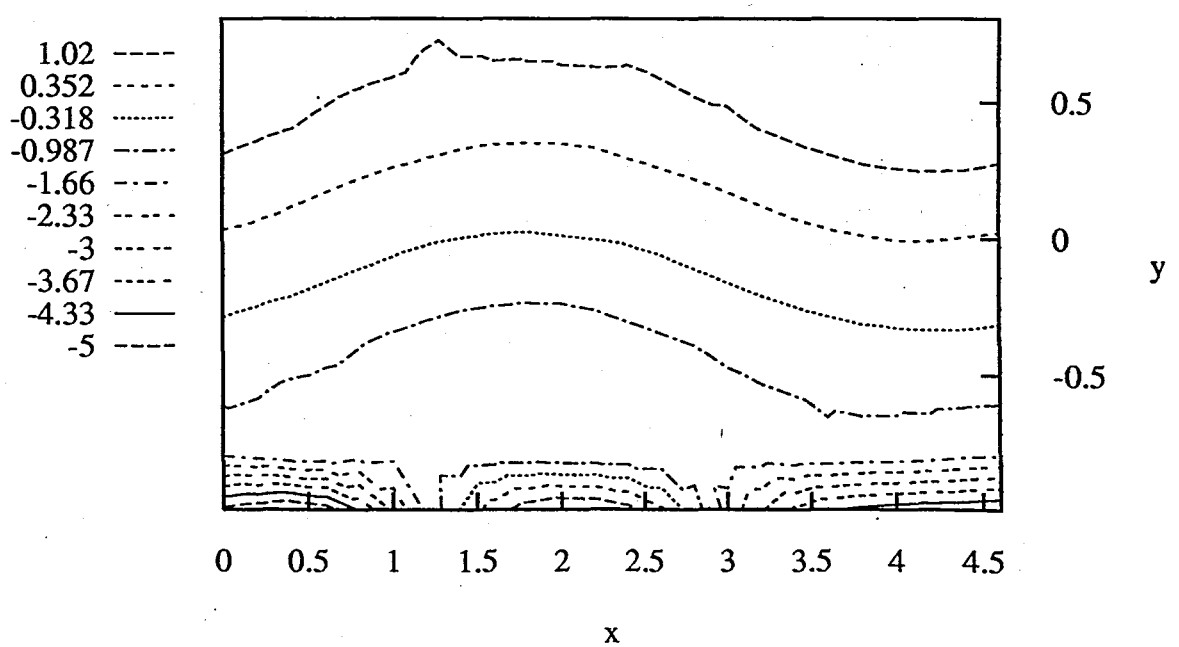

FIGURE 4.16. Vorticity lines for plane channel flow at t=150 for Re=2935, $\alpha = 1.3231$

We continue to increase the Reynolds number for the same disturbance wavenumber ($\alpha = 1.3231$) and with a perturbation of the order 10^{-3} using 8 Fourier modes in the streamwise direction and 24 Chebyshev modes in the cross-stream direction. To follow the bifurcations, instead of monitoring the time evolution of a particular mode, we choose the time evolution of the vorticity at the lower wall which is formed using the information from all of the modes so that it gives a measure for the system behavior. We also perform long-time integrations to capture the solution attractor in the phase space arising after a transient period. At Re=5200, we find a second periodic (Hopf) bifurcation and the formation of two-periodic motion (periodic with two incommensurate frequencies). We also observe, based on the time evolution of the vorticity at the lower wall, an intermittent behavior with periodic jumps to a stochastic state (Fig. 4.17). Vorticity lines are also presented in Fig. 4.18.

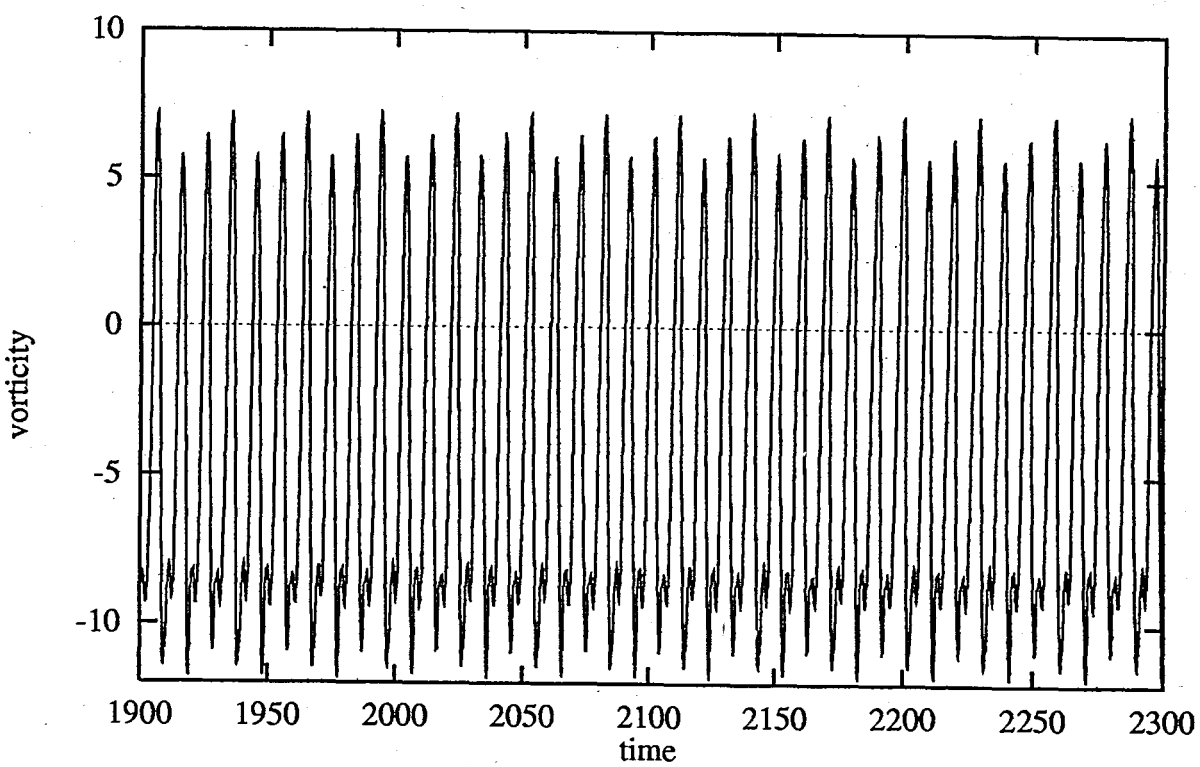

FIGURE 4.17. Time evolution of the vorticity at the lower wall for plane channel flow at Re=5200, $\alpha = 1.3231$

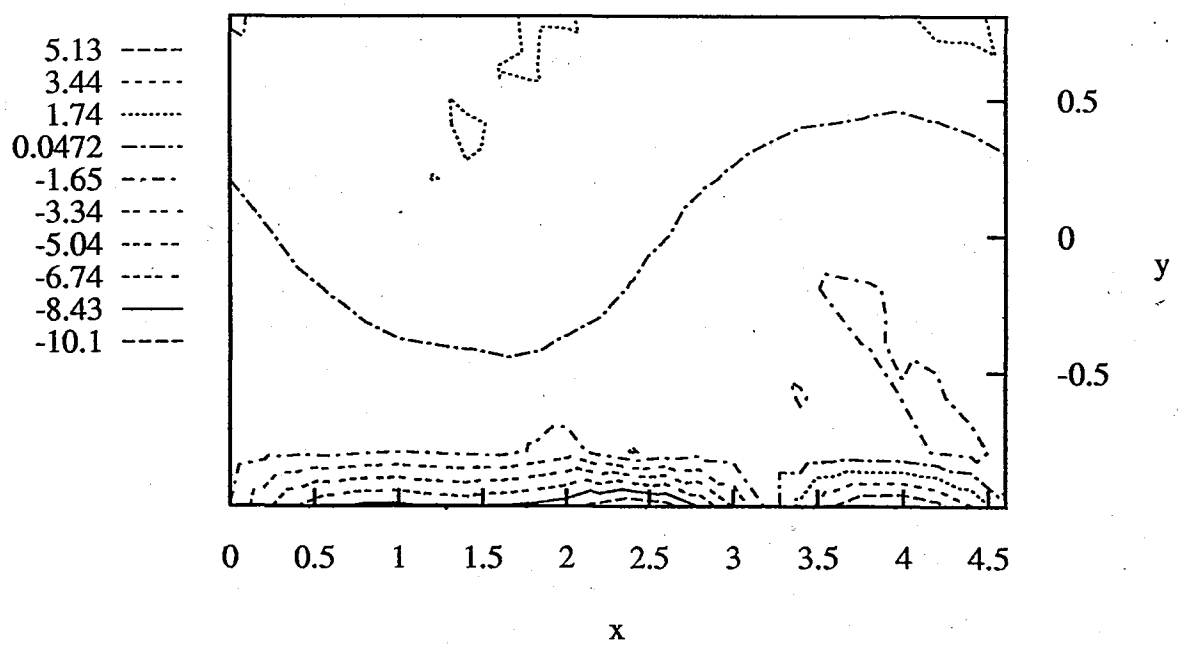

FIGURE 4.18. Vorticity lines for plane channel flow at Re=5200, $\alpha = 1.3231$, t=2300

At Re=8000 and Re=9000 with the same disturbance wavenumber (α = 1.3231), we observe the settlement of a three-periodic motion in the time evolution of the vorticity at the lower wall. The intermittency effects are also present in the system behavior (Fig 4.19 and Fig. 4.20). At Re=10000, the instabilities set in the three-periodic motion which signifies the onset of chaos (Fig. 4.21). For those simulations, 31 Chebyshev modes have been used in the cross-stream direction together with 4 Fourier modes in the streamwise direction corrected with 8 Fourier modes through the use of Euler-Galerkin nonlinear Galerkin algorithm. The evolution of the flow dynamics is also monitored through some streamlines and vorticity lines at different Reynolds numbers in Fig. 4.22-24.

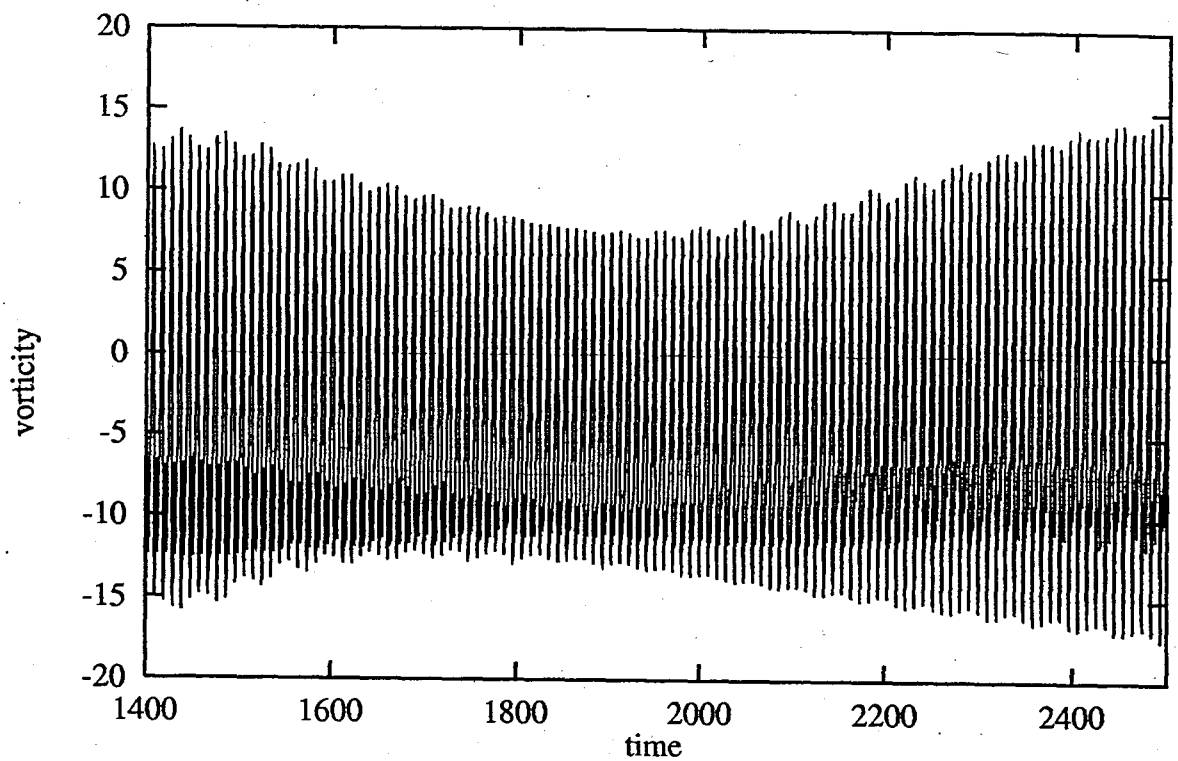

FIGURE 4.19. Time evolution of the vorticity at the lower wall for plane channel flow at Re=8000, $\alpha = 1.3231$

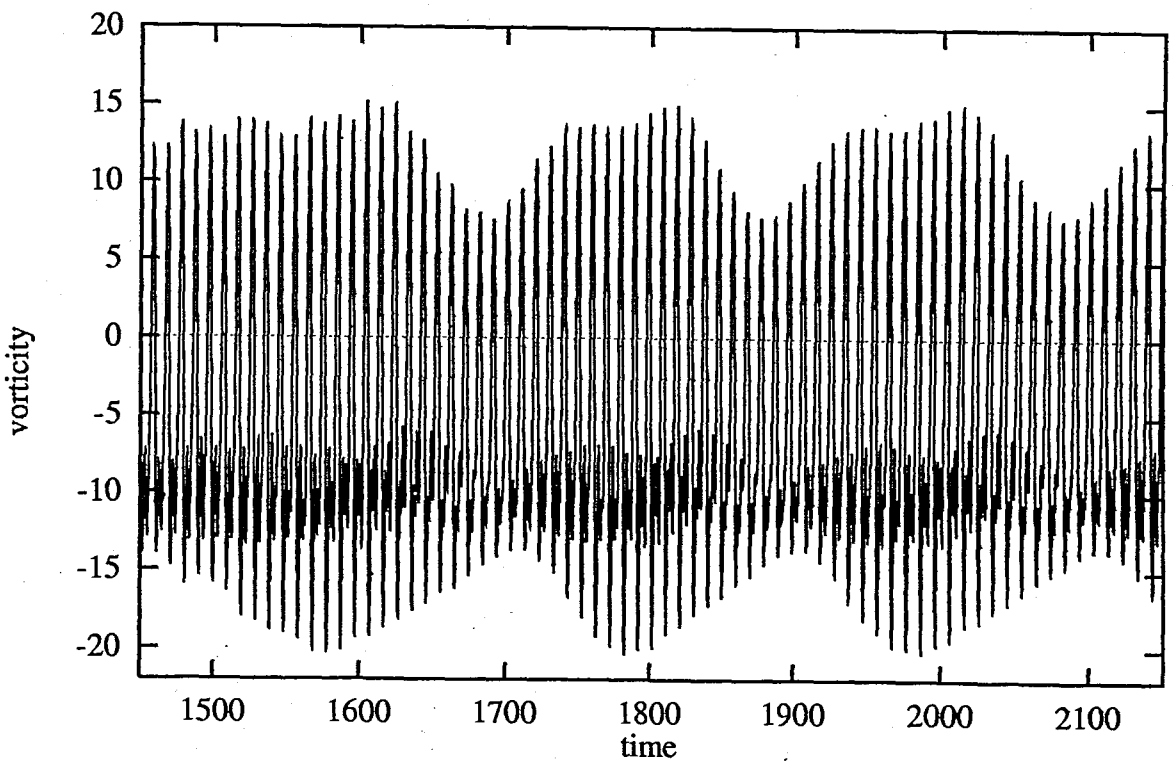

FIGURE 4.20. Time evolution of the vorticity at the lower wall for plane channel flow at Re=9000, $\alpha = 1.3231$

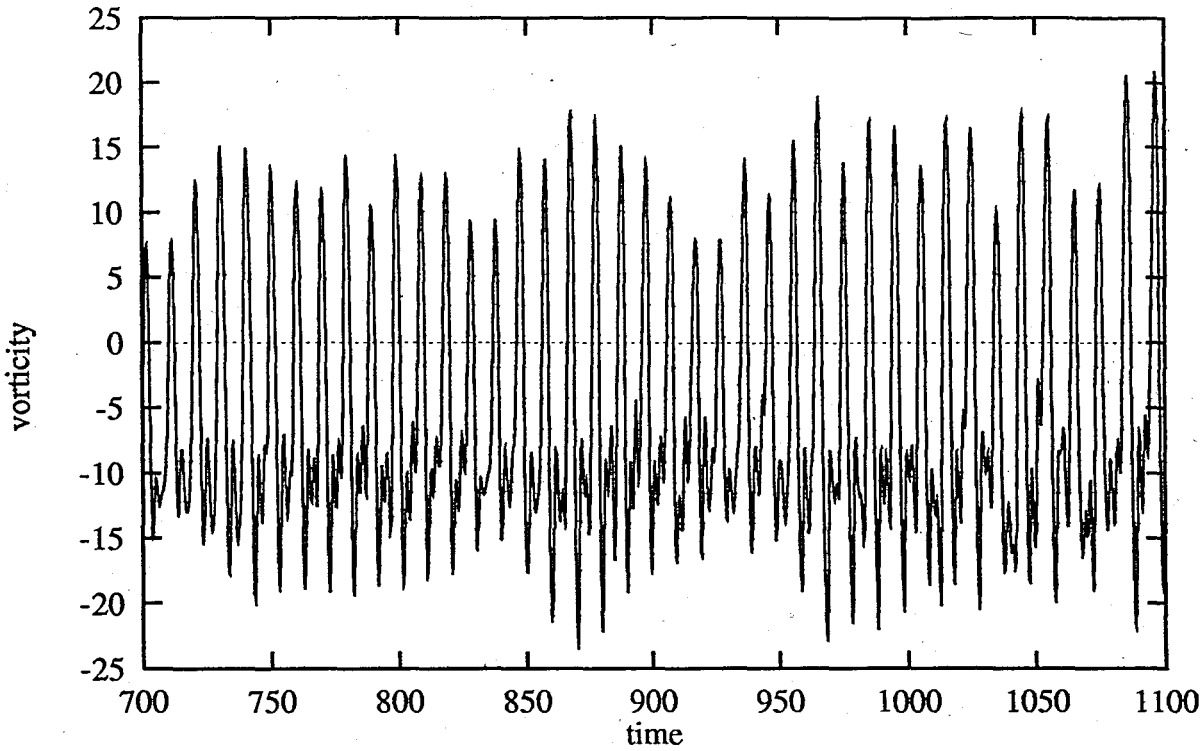

FIGURE 4.21. Time evolution of the vorticity at the lower wall for plane channel flow at Re=10000, $\alpha = 1.3231$

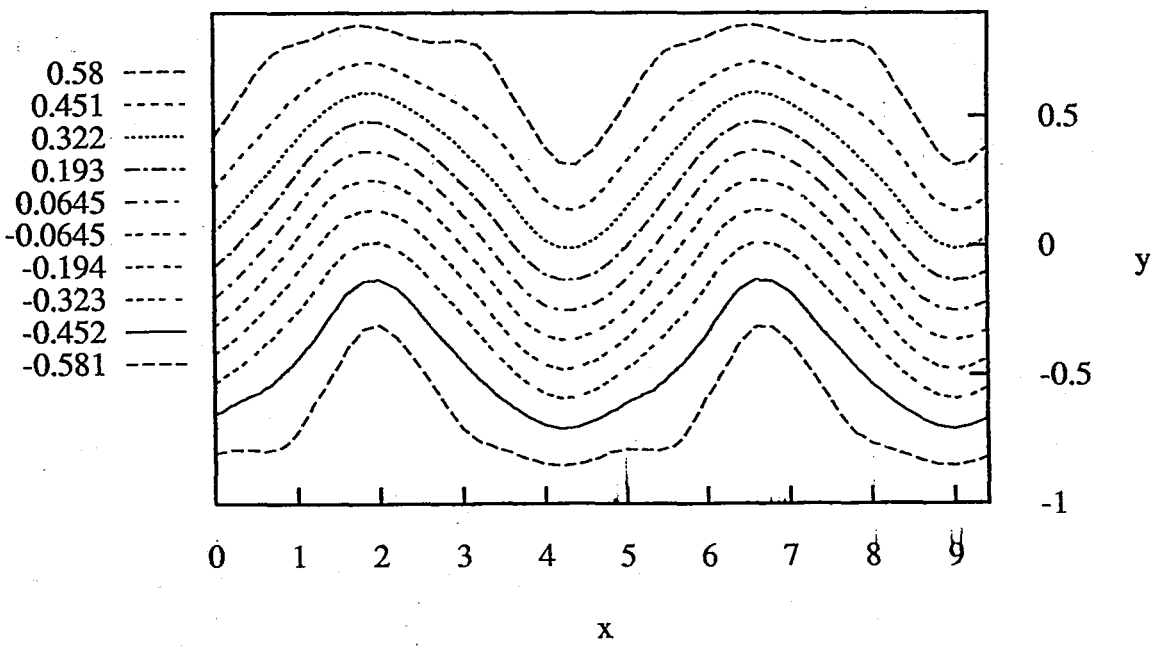

FIGURE 4.22. Streamlines for plane channel flow at Re=8000, $\alpha = 1.3231$, t=2500

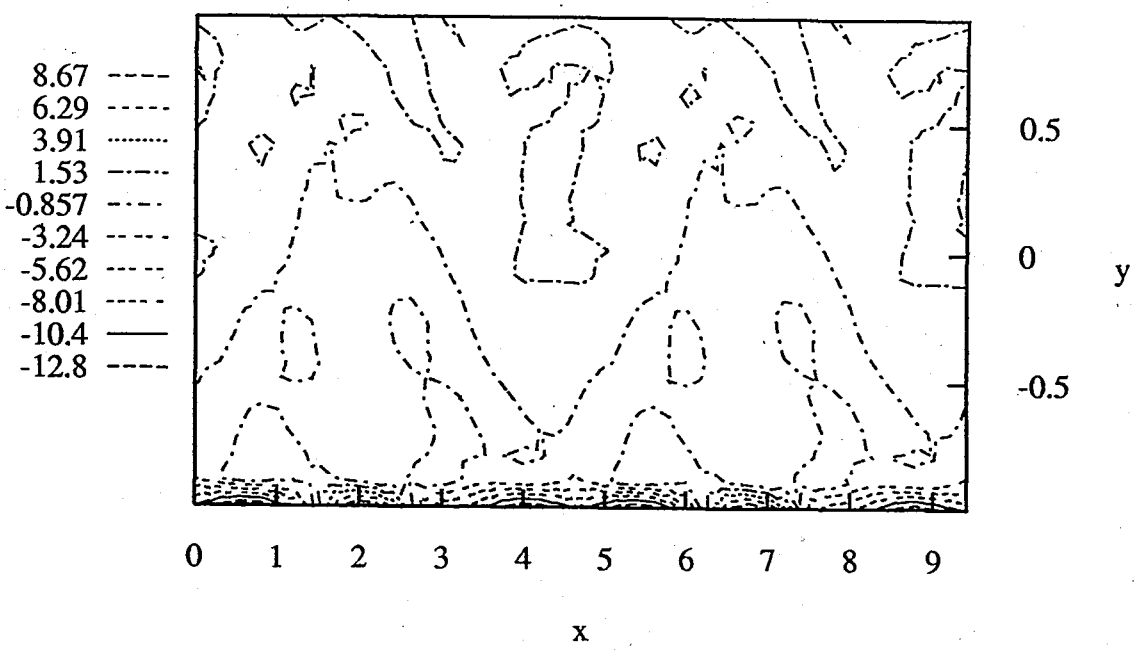

FIGURE 4.23. Vorticity lines for plane channel flow at Re=8000, $\alpha = 1.3231$, t=2500

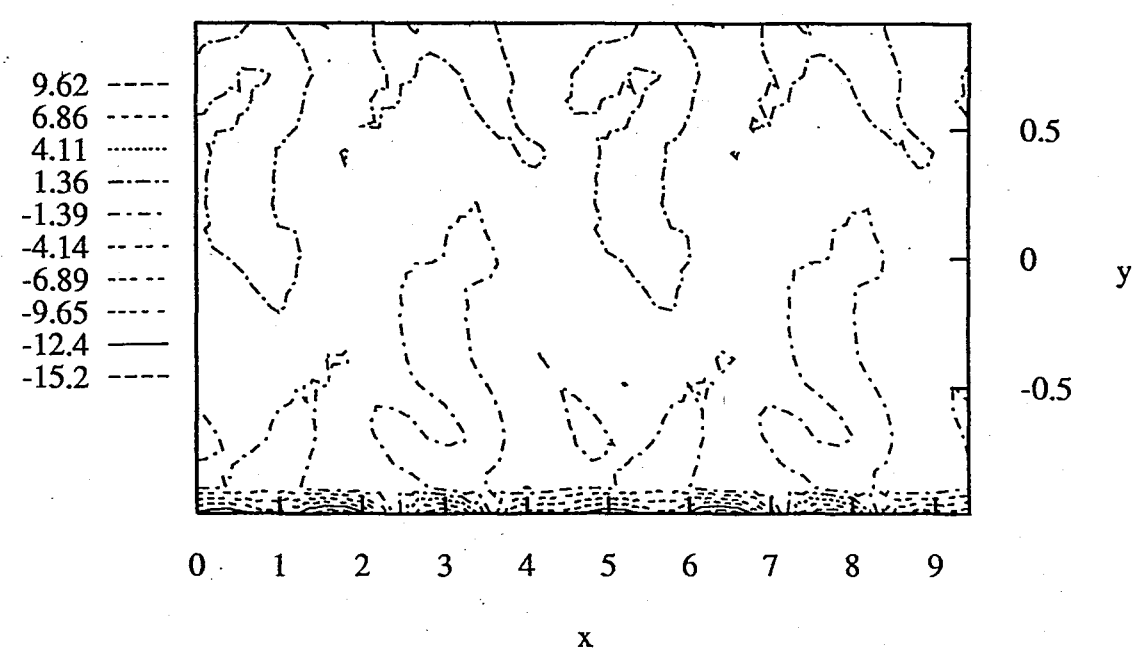

FIGURE 4.24. Vorticity lines for plane channel flow at Re=10000, $\alpha = 1.3231$, t=1100

To investigate the system behavior for lower disturbance wavenumbers, similar numerical computations have been conducted at α = 0.5. Disturbances decayed even at Reynolds numbers as high as 5000, using an initial perturbation of the order of 10^{-3}, which was the case in the previous simulations at α = 1.3231. Initial perturbation had to be increased to the order of 10^{-2} for the formation of periodic solutions at Re=5000. The qualitative behavior in the transition has been found to be similar to the previous simulations.

4.2.1.2. Oscillating Poiseuille flow. The bifurcation parameters for this problem are chosen to be the Reynolds number Re and the ratio of the amplitude of the oscillatory to steady velocity, Δ. The disturbance wavenumber is fixed at α = 1.3231 and the ratio of the channel half-width to Stokes layer thickness at β =16.1. The initial perturbation is of the order of 10^{-3}. The Reynolds number is changed up to Re=5000. For Δ, two values are investigated as Δ=0.1 and Δ=0.4. In the numerical simulations, 19 Chebyshev modes are used in the cross-stream direction together with 8 Fourier modes in the streamwise direction. Up to Re=2900, we observe decay of disturbances for both values of Δ. From Re=2900 to Re=5000, we observe quasi-periodic behavior for Δ=0.1 (Fig. 4.25). However, for Δ=0.4 we observe decay of finite perturbations up to Re=5000. At Re=5000, for Δ=0.4 wave packets form (Fig. 4.26). At higher Reynolds numbers, we notice the arising of instabilites. We also present some streamlines and vorticity lines to highlight the plane channel flow dynamics under the effect of flux oscillations (Fig. 4.27-30).

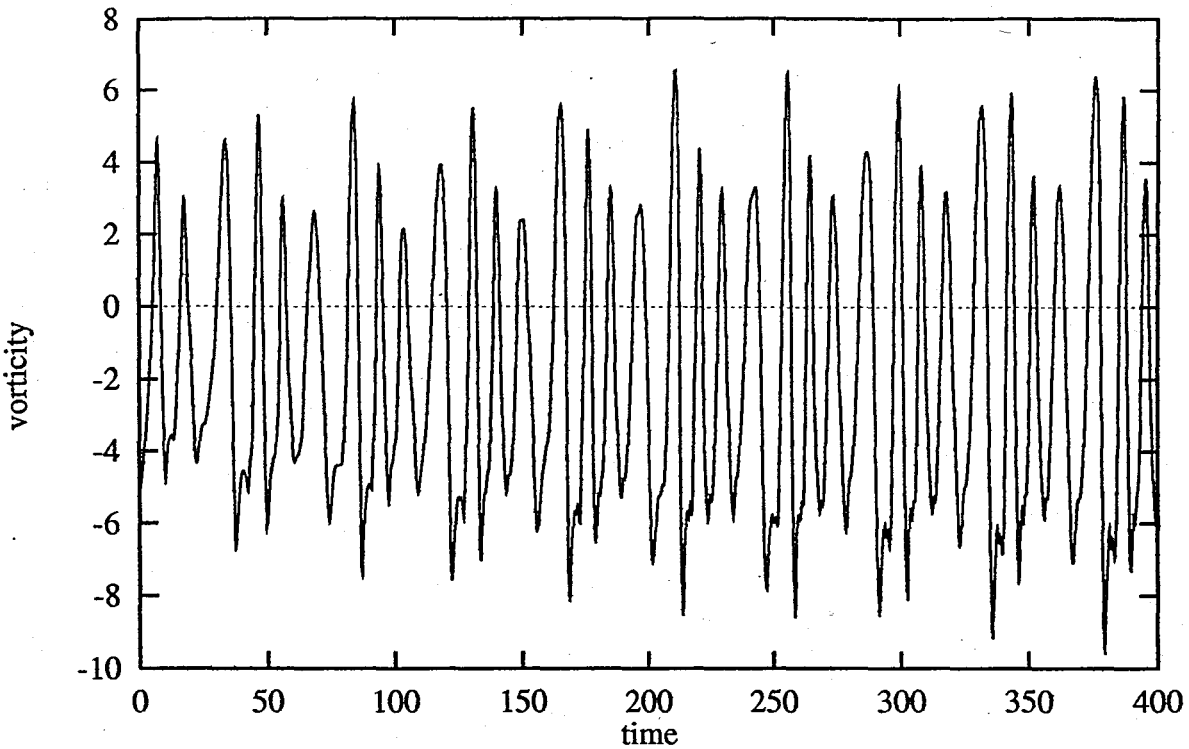

FIGURE 4.25. Time evolution of the vorticity at the lower wall for oscillating Poiseuille flow at Re=3500, $\alpha = 1.3231$, Δ=0.1, β=16.1

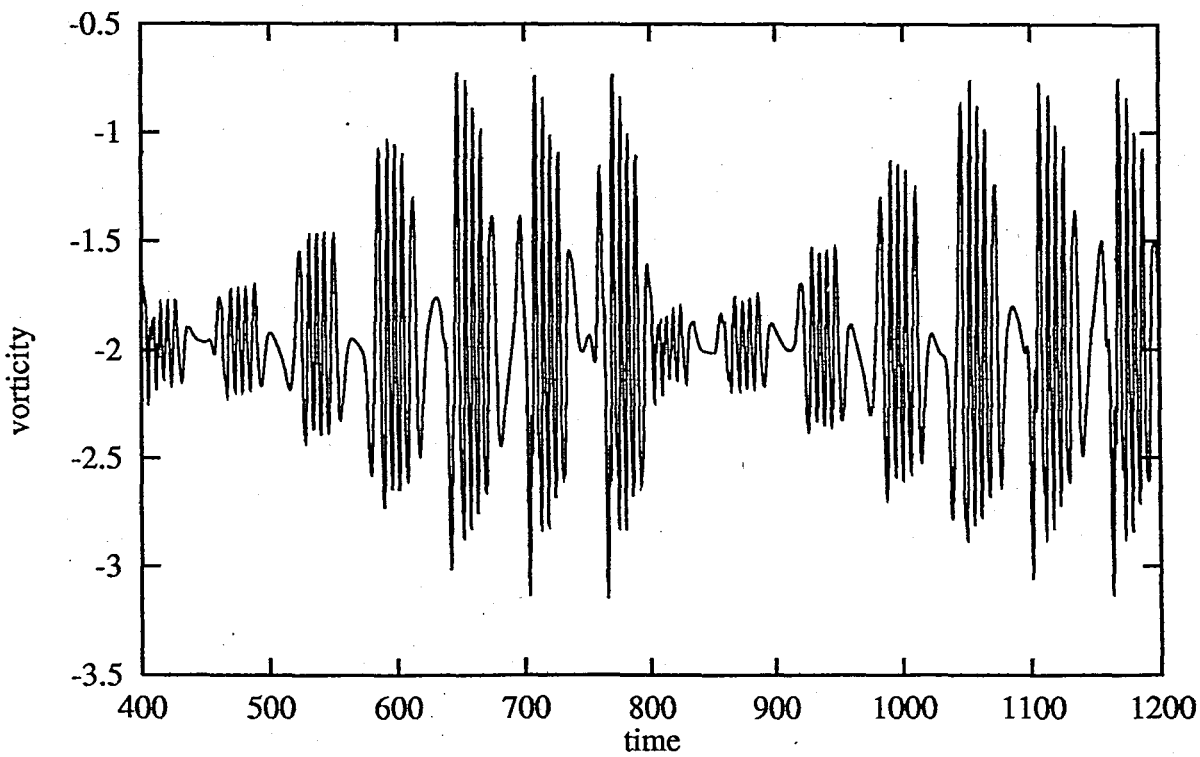

FIGURE 4.26. Time evolution of the vorticity at the lower wall for oscillating Poiseuille flow at Re=5000, $\alpha = 1.3231$, Δ=0.4, β=16.1

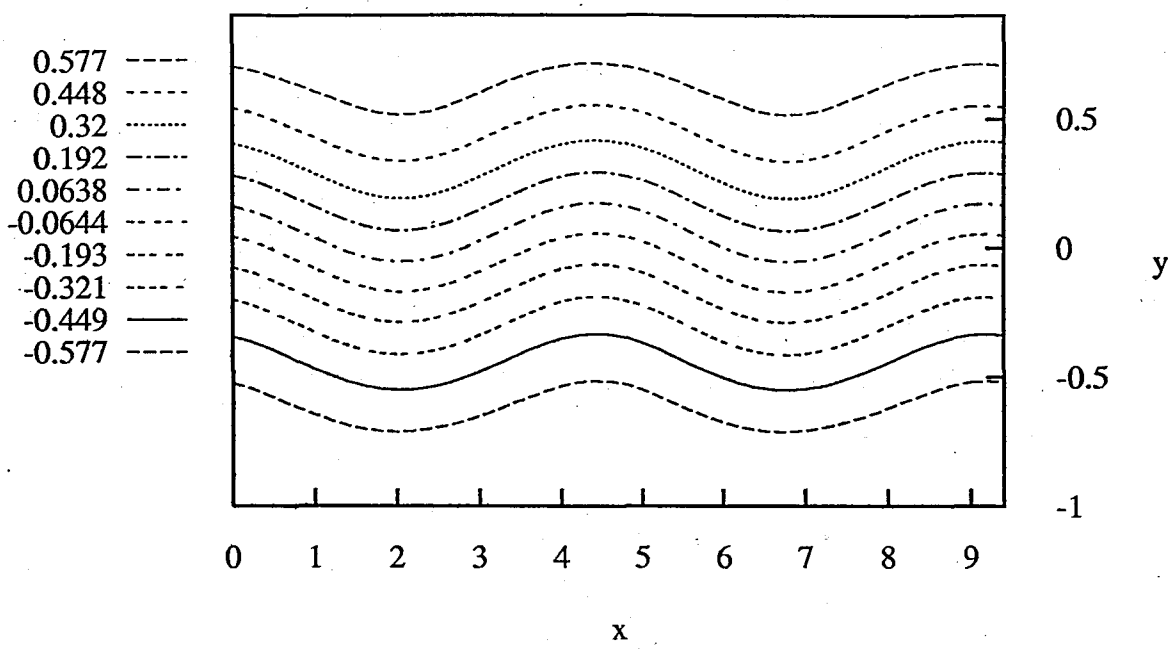

FIGURE 4.27. Streamlines for oscillating Poiseuille flow at Re=3500, $\alpha = 1.3231$, Δ=0.1, β=16.1, t=400

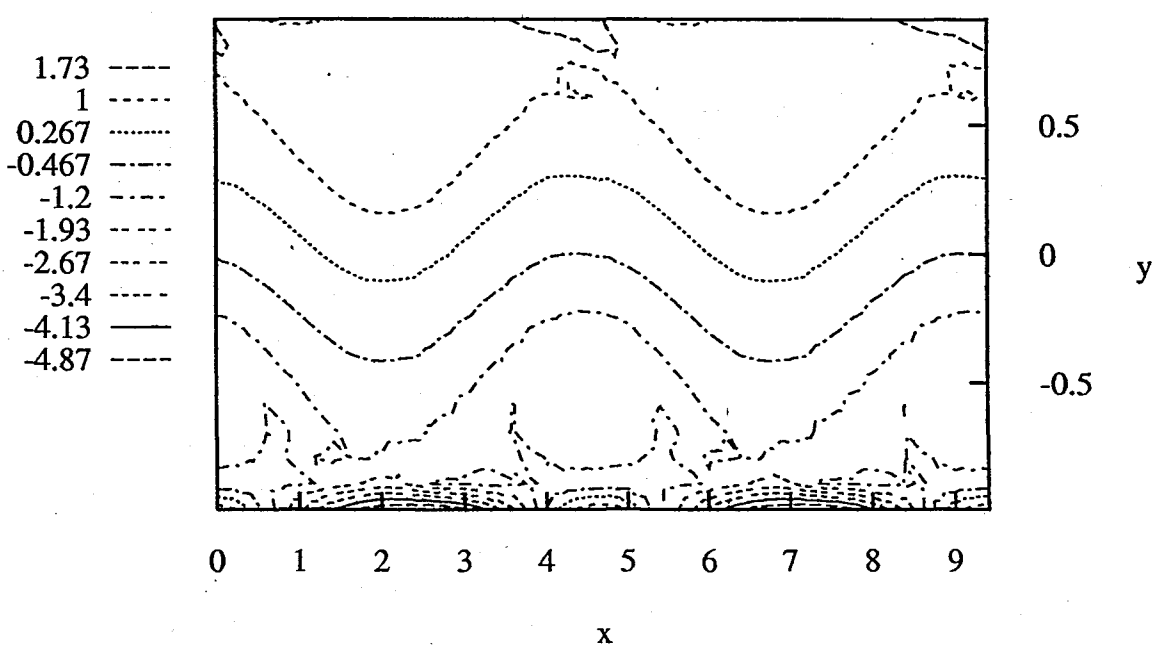

FIGURE 4.28. Vorticity lines for oscillating Poiseuille flow at Re=3500, $\alpha = 1.3231$, Δ=0.1, β=16.1, t=400

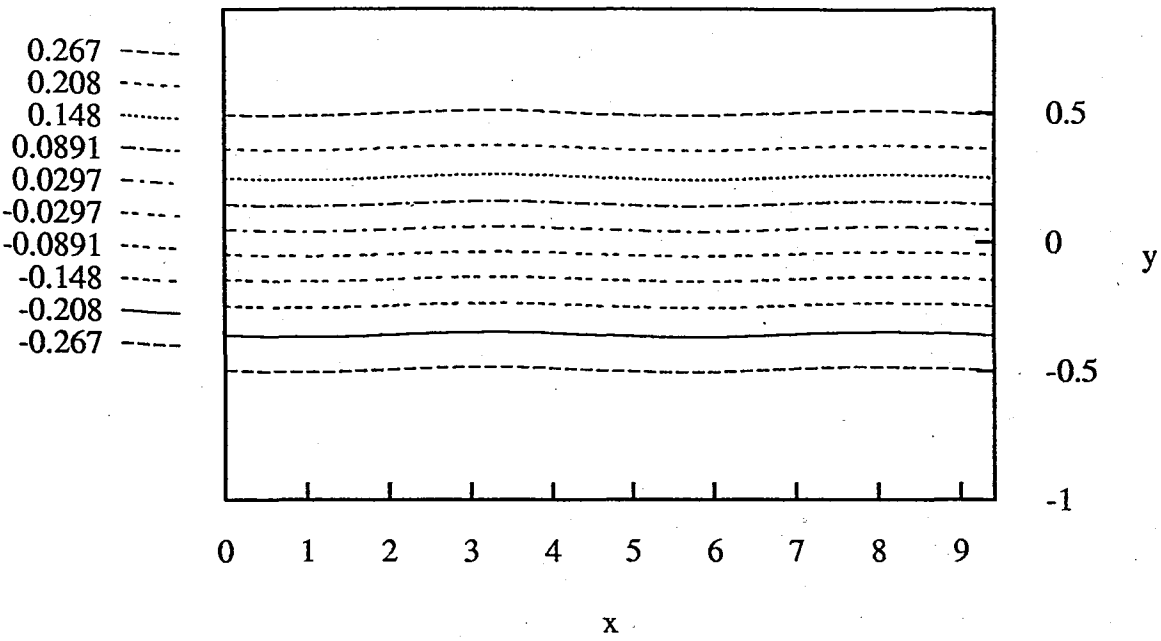

FIGURE 4.29. Streamlines for oscillating Poiseuille flow at Re=5000, $\alpha = 1.3231$, Δ=0.4, β=16.1, t=1200

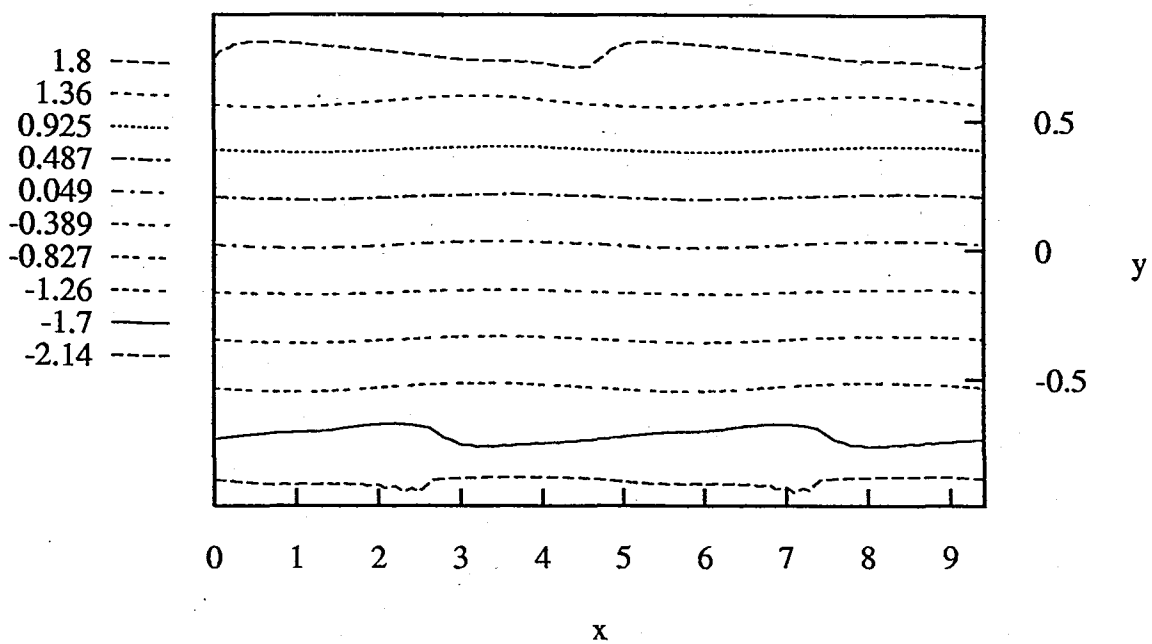

FIGURE 4.30. Vorticity lines for oscillating Poiseuille flow at Re=5000, $\alpha = 1.3231$, Δ=0.4, β=16.1, t=1200

4.2.2. Free Shear Layer Flows

Free shear flows differ from wall-bounded flows in that they are subject to inviscid instabilities since they typically have inflectional mean velocity profiles (Metcalfe et al., 1987). Experimental work for these flows, demonstrated the importance of two-dimensional dynamical mechanisms, especially through transition regime. While three-dimensional small scales of motion are observed, they do not necessarily destroy two-dimensional structures. Furthermore, it has been reported that the long time evolution of finite amplitude three-dimensional perturbations is to a large extent dictated by the evolution of the underlying two-dimensional flow (Meiburg et al., 1995).

4.2.2.1. Temporally Growing Mixing Layer. As we mentioned in Section 4.1.2.2, two-dimensional finite perturbations are observed to saturate into vortical state and hence the solutions of the dynamical system are attracted by a fixed-point attractor for Re=100 and α = 0.25. Increasing the Reynolds number or the disturbance wavenumber did not very much change the picture. In Fig. 4.31 we present the time evolution of the vorticity close to the centerline for Re=400, $\alpha = 0.75$. In Fig. 4.32, the streamlines at the early period of the time evolution and in Fig. 4.33, the streamlines at late times of the evolution are shown. In Fig. 4.34, the vorticity lines corresponding to that case show clearly the formation of the vortices. In the simulations, 18 Hermite modes in the cross-stream direction and 8 Fourier modes in the streamwise direction were used.

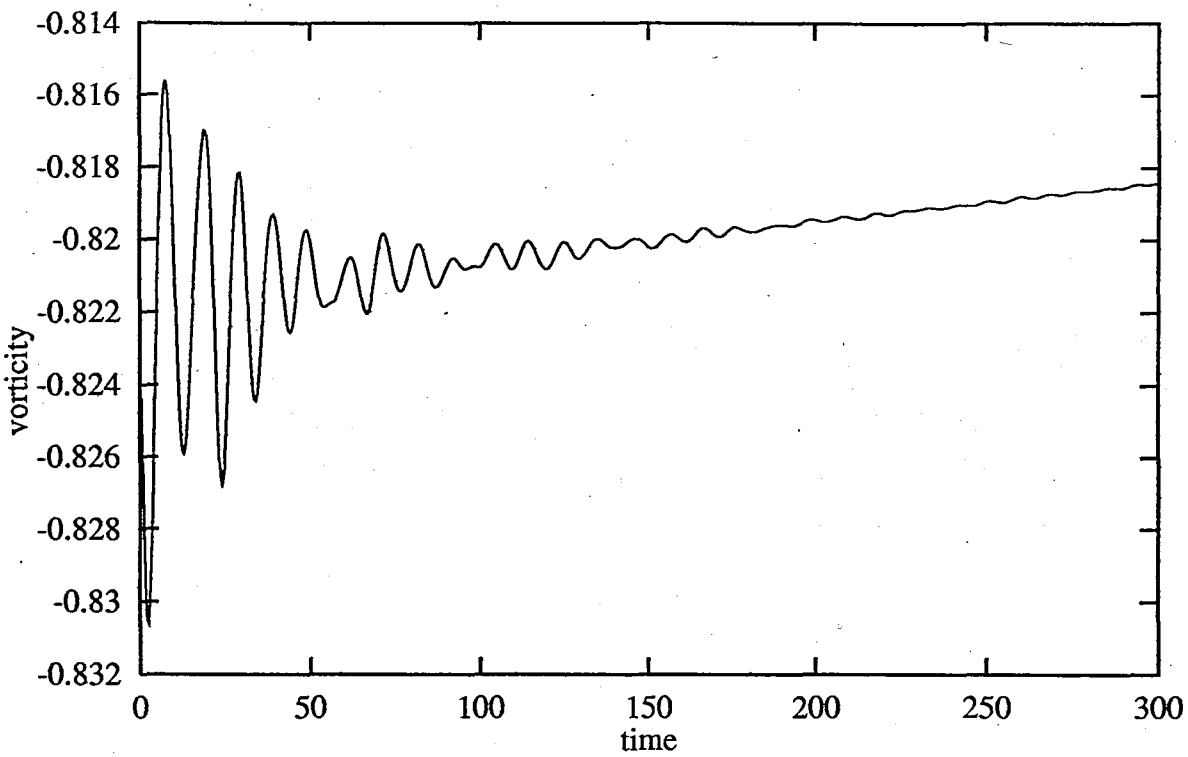

FIGURE 4.31. Time evolution of the vorticity at $x=L/2$, $y=0.5$ for temporally growing mixing layer at Re=400, $\alpha = 0.75$

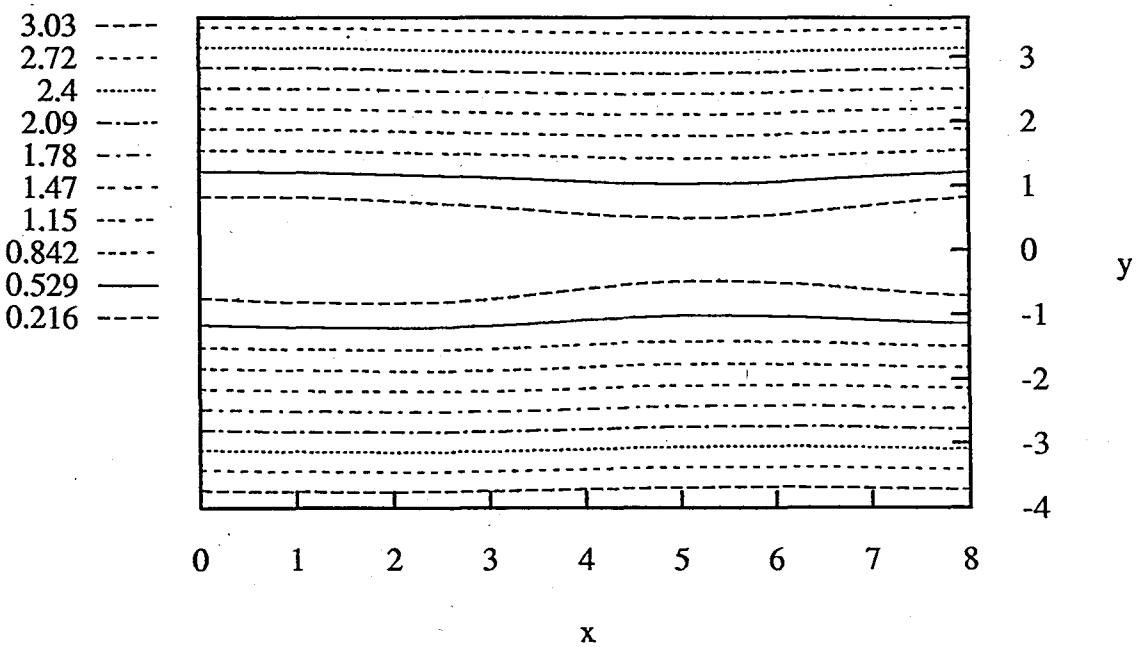

FIGURE 4.32. Streamlines for temporally growing mixing layer at Re=400, $\alpha = 0.75$, t=20

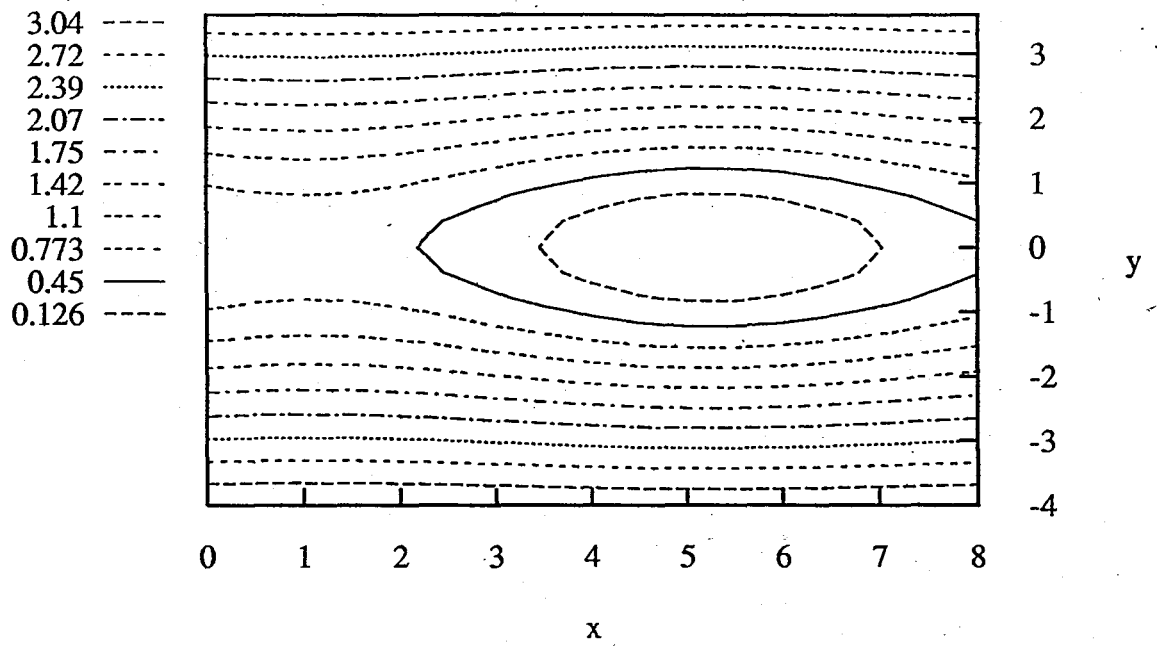

FIGURE 4.33. Streamlines for temporally growing mixing layer at Re=400, $\alpha = 0.75$, t=300

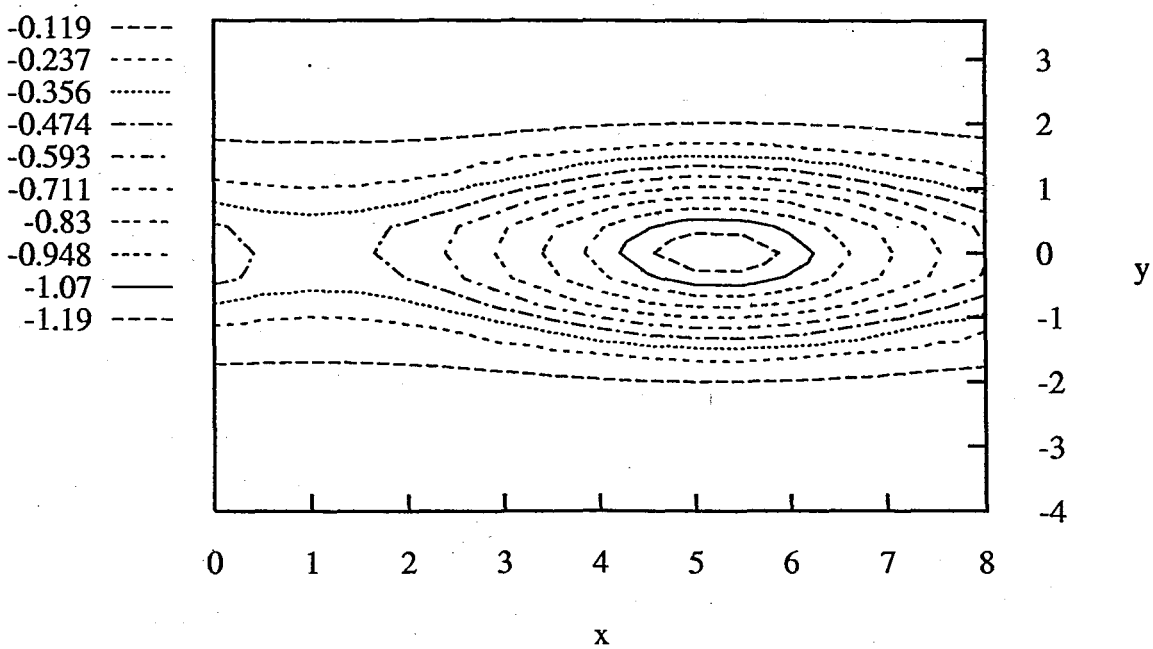

FIGURE 4.34. Vorticity lines for temporally growing mixing layer at Re=400, $\alpha = 0.75$, t=300

It is known that mixing layers perturbed with disturbances of different frequencies can exhibit different dynamical behavior such as vortex pairing which is found to be controlled by the presence of subharmonic modes of the fundamental frequency of instabilities in the mixing layer (Ho and Huang, 1982). Therefore, to investigate new bifurcations of the dynamical system concerning the nonlinear temporal stability of the mixing layer, we introduce subharmonic excitations. To accommodate both the fundamental mode, with x-wavenumber α and its subharmonic, with x-wavenumber $(1/2)\alpha$, the assumed periodicity length is $4\pi / \alpha$. The periodic boundary condition in the streamwise direction can be written as,

$$\psi(x,y,t) = \psi(x+\frac{4\pi}{\alpha},y,t) \tag{4.2}$$

The initial perturbation is of the form,

$$\psi(x,y,0) = A_{10}\phi_{10}(y)\cos(\alpha(x+\theta)) + A_{1/2,0}\phi_{1/2,0}(y)\cos(\alpha/2) \tag{4.3}$$

where θ is the phase shift between the fundamental and subharmonic modes and ϕ corresponds to the most unstable eigenfunctions of the Orr-Sommerfeld linear stability equation.

We present in Fig. 4.35, the time evolution of the vorticity close to the centerline for Re=83, α =0.4446, A_{10} = 0.2, $A_{1/2,0}$ = 0.1 and $\theta/\alpha = \pi/2$. We observe the settlement of some quasi-periodic behavior. In Fig. 4.36, the streamlines and in Fig. 4.37, the vorticity lines for the same flow at t = 1500 are presented. If we further increase the Reynolds number, we find that the instabilities set in and drive the flow to a chaotic state. We present in Fig. 4.38, the time evolution of the vorticity close to the centerline for Re=150 and in Fig. 4.39 for Re=400, other parameter values being the same as the previous case. In Fig. 4.40, we present the vorticity lines for the case where Re=400 at t=1000. In the simulations, 18 Hermite modes in the cross-stream direction and 8 Fourier modes in the streamwise direction were used.

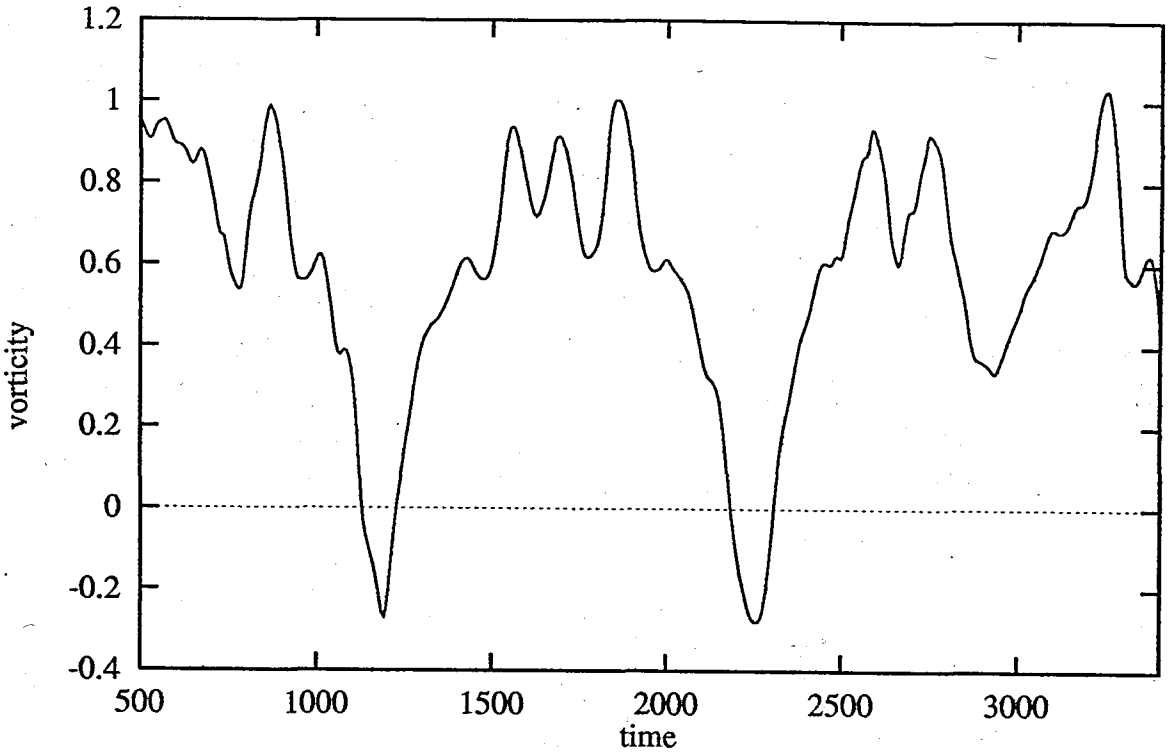

FIGURE 4.35. Time evolution of the vorticity at $x=L/2$, $y=0.5$ for temporally growing mixing layer with subharmonic excitation at Re=83, $\alpha = 0.4446$, $A_{10} = 0.2$, $A_{1/2,0} = 0.1$, $\theta/\alpha = \pi/2$

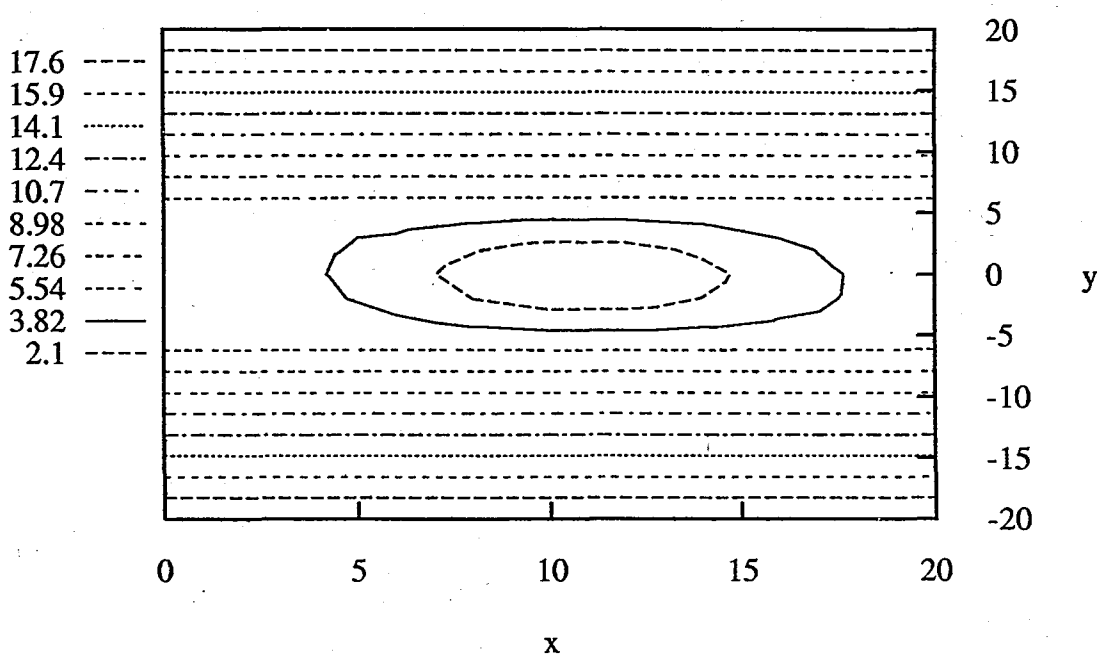

FIGURE 4.36. Streamlines for temporally growing mixing layer with subharmonic excitation at Re=83, $\alpha = 0.4446$, $A_{10} = 0.2$, $A_{1/2,0} = 0.1$, $\theta/\alpha = \pi/2$, t=1500

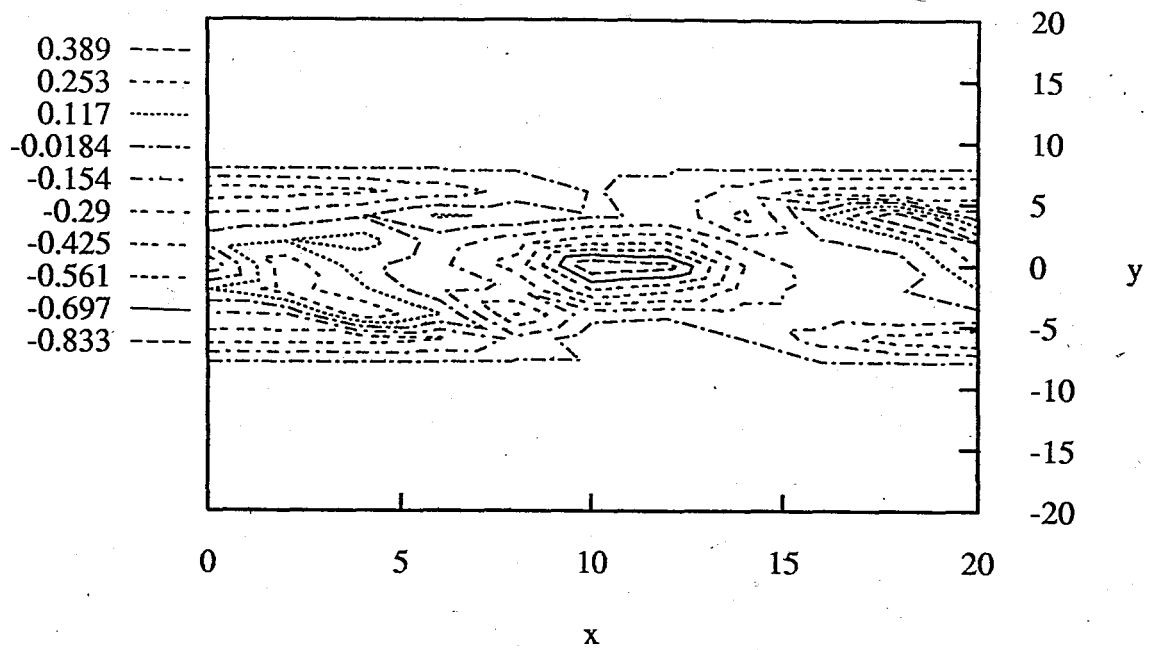

FIGURE 4.37. Vorticity lines for temporally growing mixing layer with subharmonic excitation at Re=83, $\alpha = 0.4446$, $A_{10} = 0.2$, $A_{1/2,0} = 0.1$, $\theta/\alpha = \pi/2$, t=1500

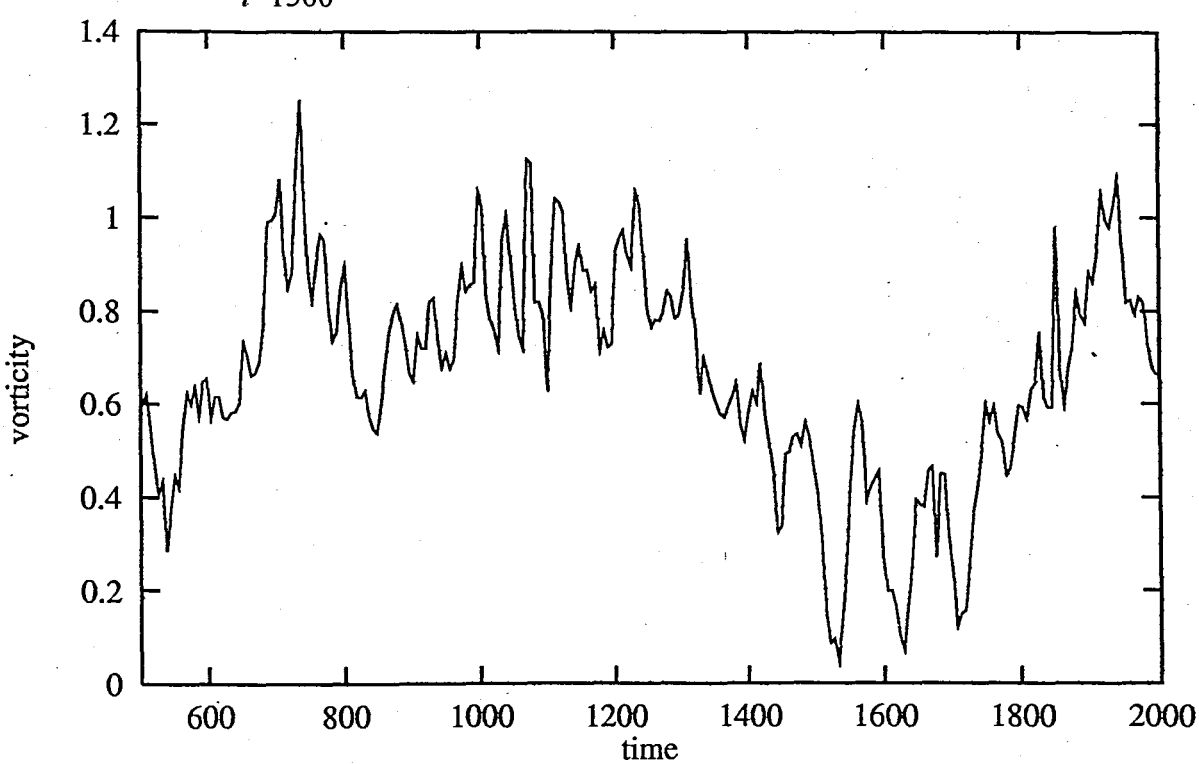

FIGURE 4.38. Time evolution of the vorticity at x=L/2, y=0.5 for temporally growing mixing layer with subharmonic excitation at Re=150, $\alpha = 0.4446$, $A_{10} = 0.2$, $A_{1/2,0} = 0.1$, $\theta/\alpha = \pi/2$

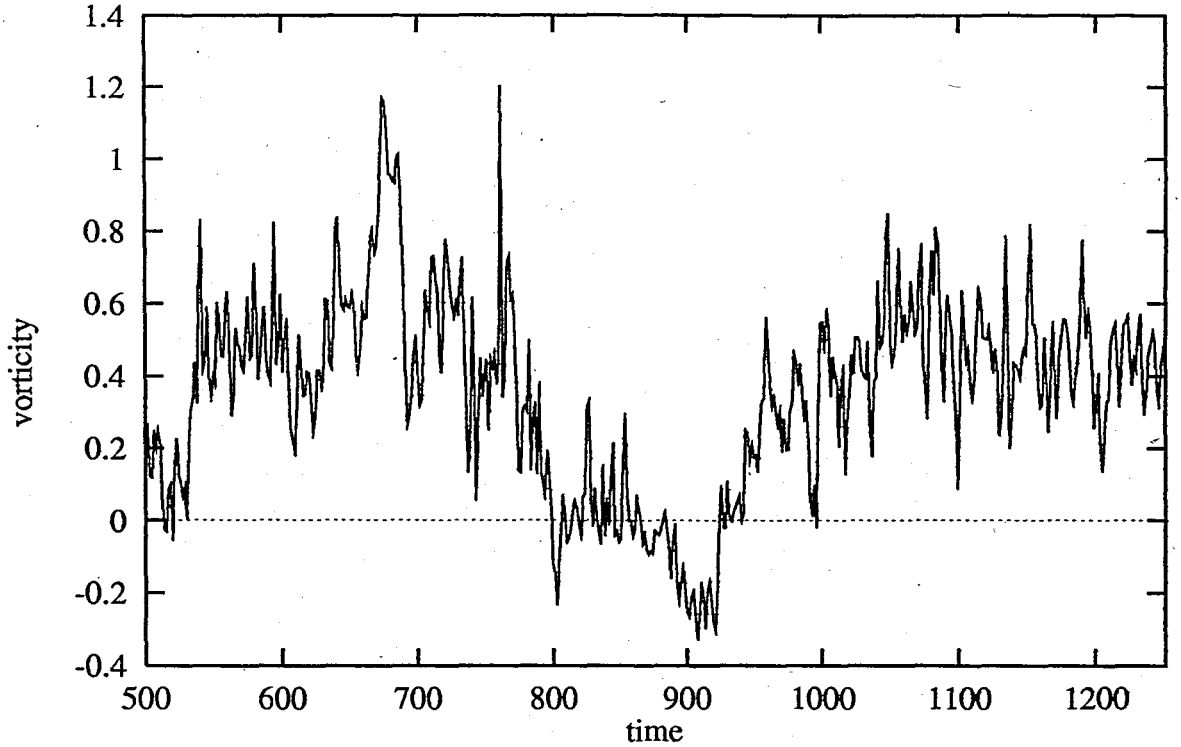

FIGURE 4.39. Time evolution of the vorticity at $x=L/2$, $y=0.5$ for temporally growing mixing layer with subharmonic excitation at Re=400, $\alpha = 0.4446$, $A_{10} = 0.2$, $A_{1/2,0} = 0.1$, $\theta/\alpha = \pi/2$

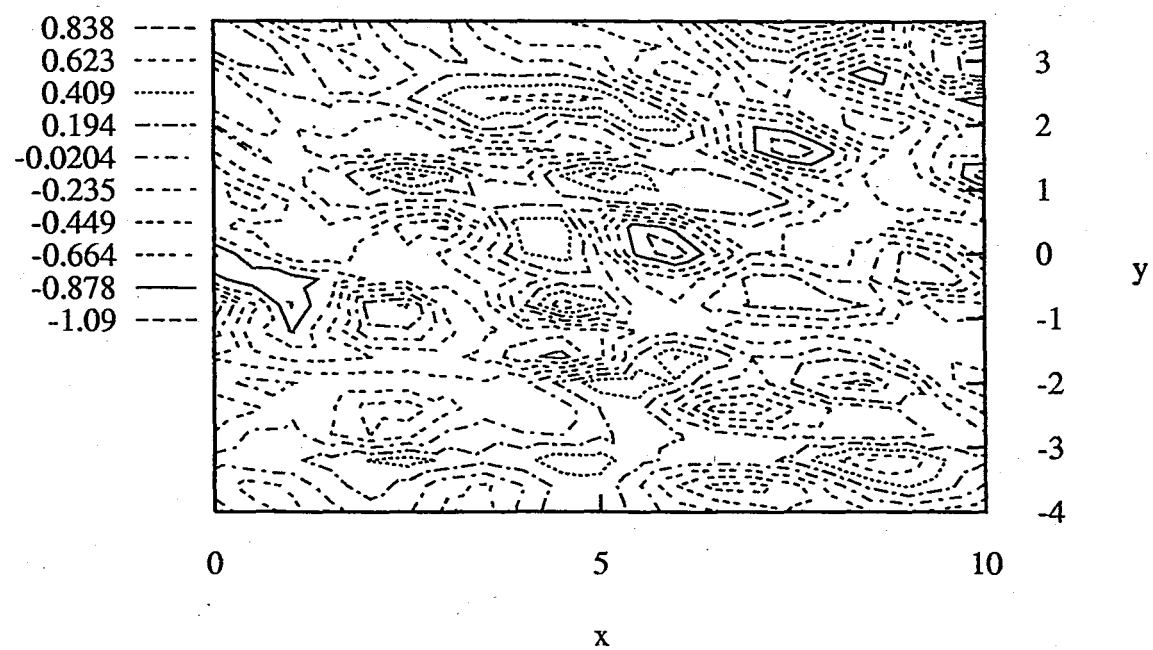

FIGURE 4.40. Vorticity lines for temporally growing mixing layer with subharmonic excitation at Re=400, $\alpha = 0.4446$, $A_{10} = 0.2$, $A_{1/2,0} = 0.1$, $\theta/\alpha = \pi/2$, t=1500

4.2.2.2. Plane Jet Flow. The temporal stability of the plane jet flow is investigated following again the evolution of two-dimensional finite perturbations. Periodic solutions can be observed in Fig. 4.41 where the time evolution of the vorticity close to the centerline is plotted for Re=100, α = 0.8. Quasi-periodic solutions of increasing complexity can be observed in Fig. 4.42 and Fig. 4.43 for Re=100, α = 0.25 and Re=200, α =0.25, respectively. The instabilities set in Fig. 4.44 describing the case where Re=500 and α = 0.25. The streamlines and the vorticity lines corresponding to the above cases are presented in Fig. 4.45-50. The effects of subharmonic excitation are also investigated as in the case of the temporally growing mixing layer. Although similar bifurcation behavior is observed in terms of the time evolution of the vorticity close to the centerline, except the earlier settling of instabilities in the periodic and quasi-periodic solutions, the streamlines and the vorticity lines present different dynamics in Fig. 4.51 and Fig. 4.52. We observe elongated vortices as well as vortex pairing in Fig. 4.52. In the simulations, 18 Hermite modes in the cross-stream direction and 8 Fourier modes in the streamwise direction were used.

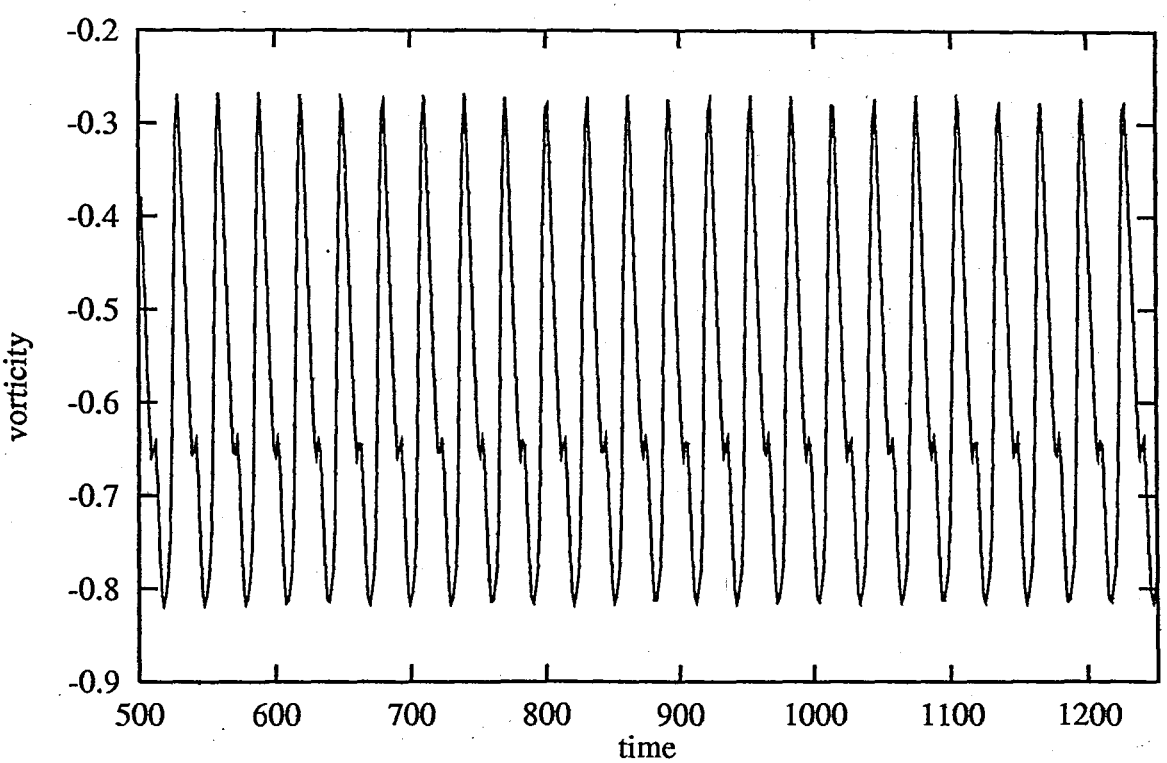

FIGURE 4.41. Time evolution of the vorticity at $x=L/2$, $y=0.5$ for plane jet flow at Re=100, $\alpha = 0.8$

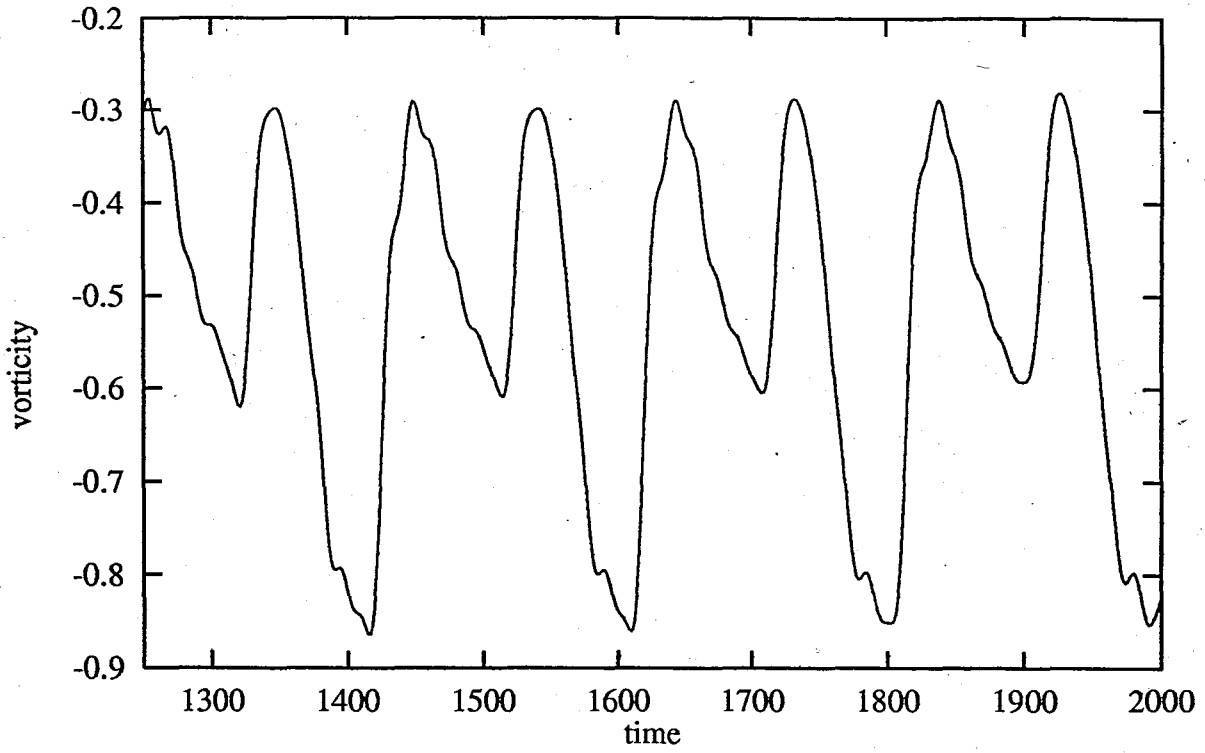

FIGURE 4.42. Time evolution of the vorticity at $x=L/2$, $y=0.5$ for plane jet flow at Re=100, $\alpha = 0.25$

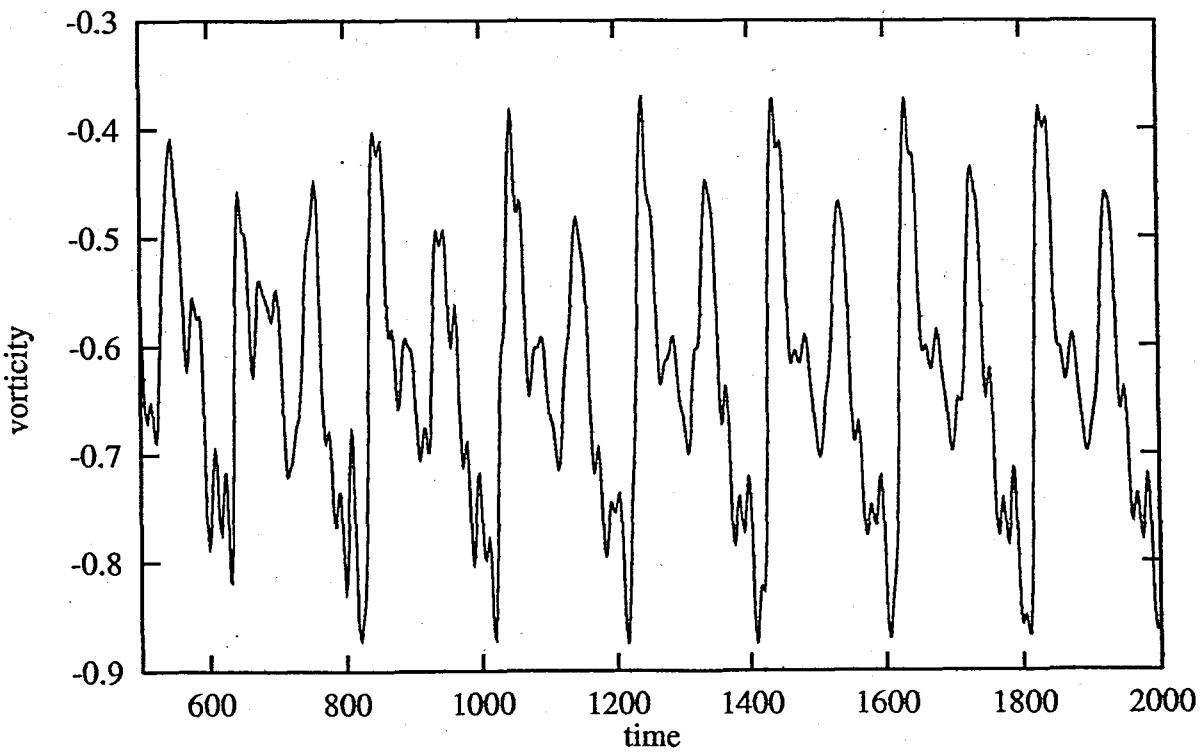

FIGURE 4.43. Time evolution of the vorticity at $x=L/2$, $y=0.5$ for plane jet flow at Re=200, $\alpha = 0.25$

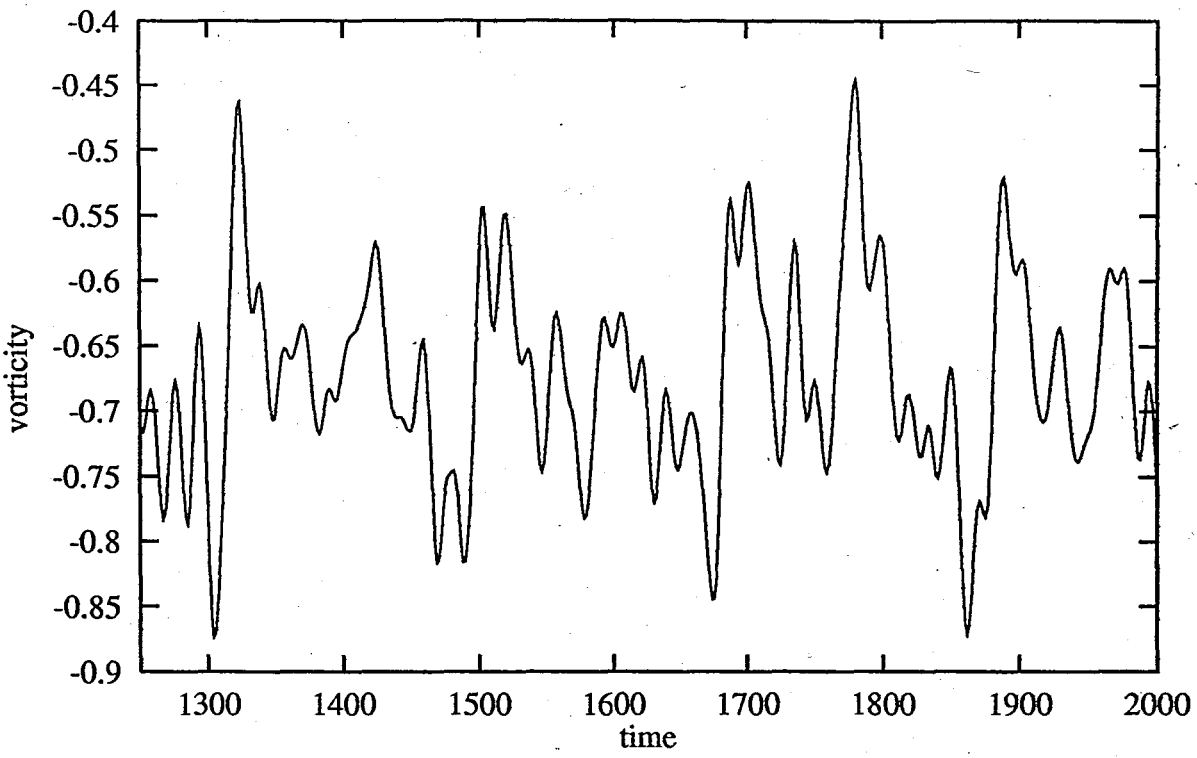

FIGURE 4.44. Time evolution of the vorticity at $x=L/2$, $y=0.5$ for plane jet flow at Re=500, $\alpha = 0.25$

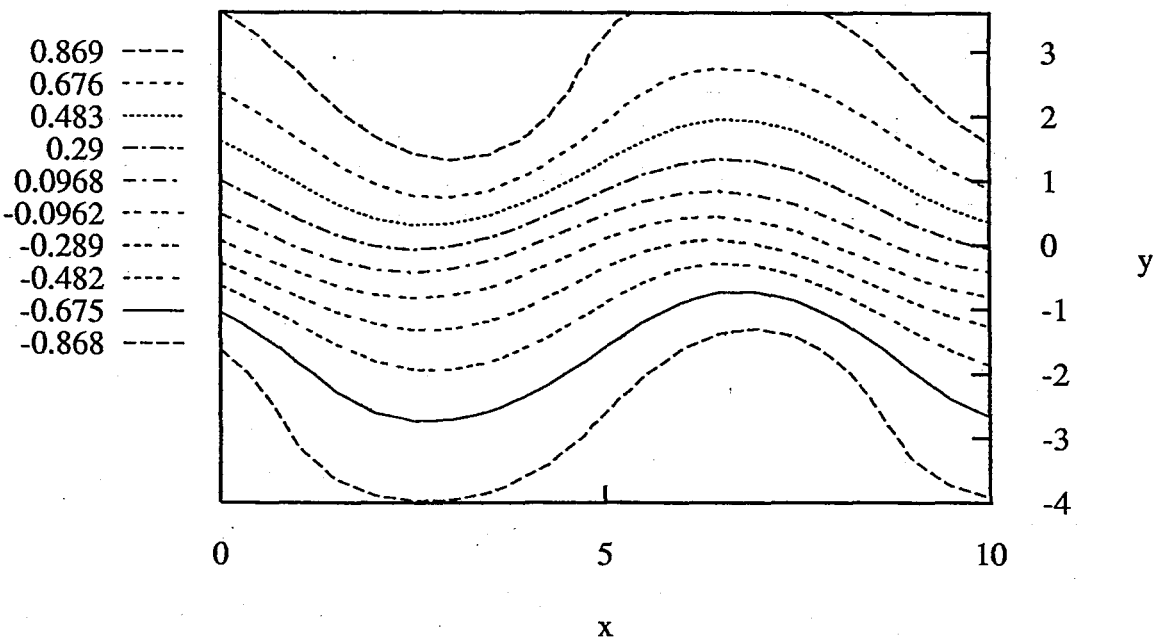

FIGURE 4.45. Streamlines for plane jet flow at Re=100, $\alpha = 0.8$, t=1250

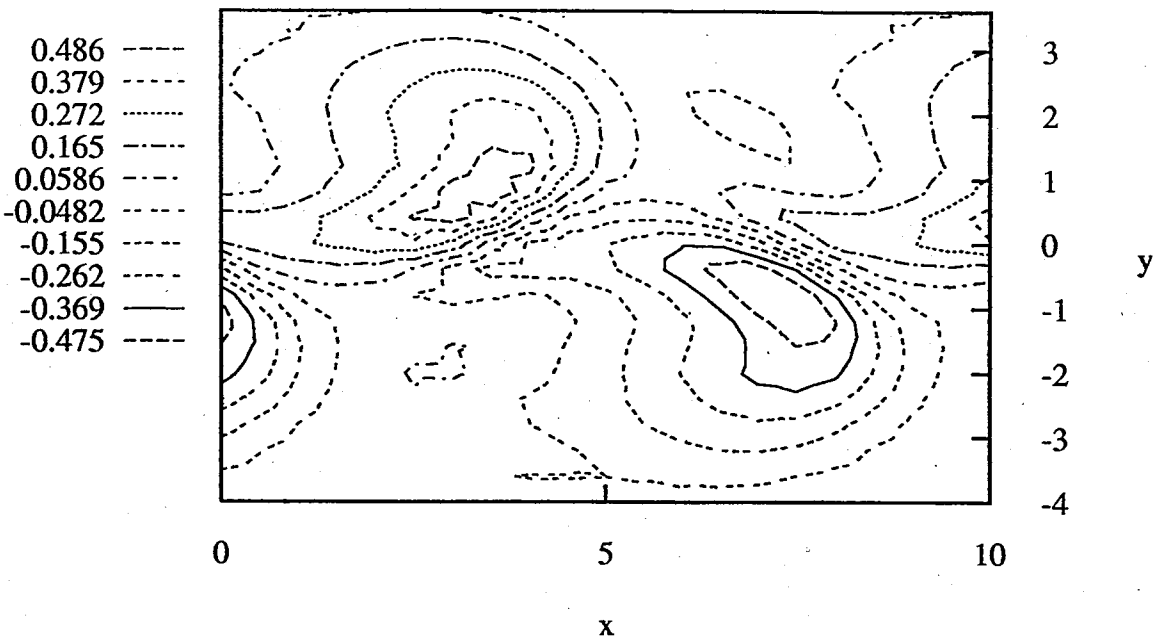

FIGURE 4.46. Vorticity lines for plane jet flow at Re=100, $\alpha = 0.8$, t=1250

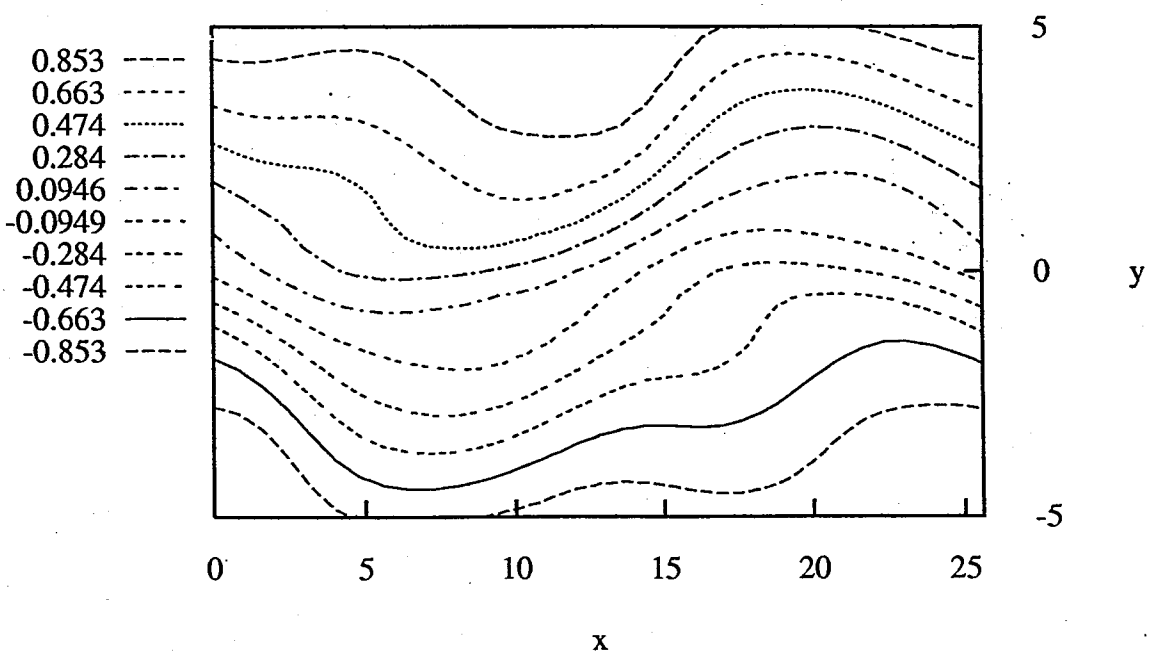

FIGURE 4.47. Streamlines for plane jet flow at Re=100, $\alpha = 0.25$, t=2000

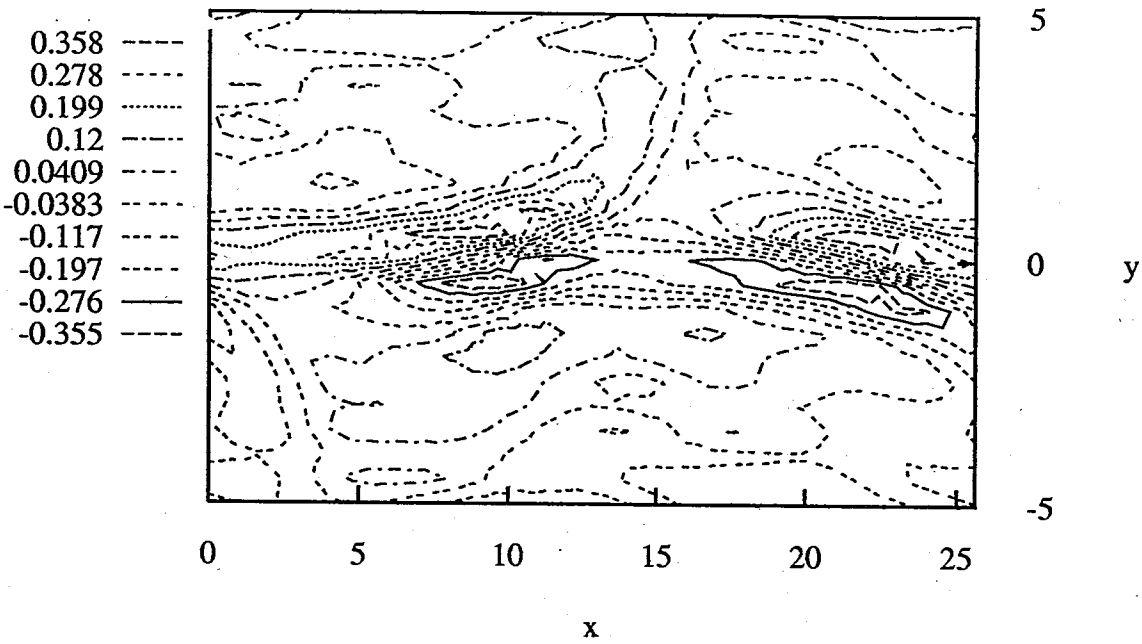

FIGURE 4.48. Vorticity lines for plane jet flow at Re=100, $\alpha = 0.25$, t=2000

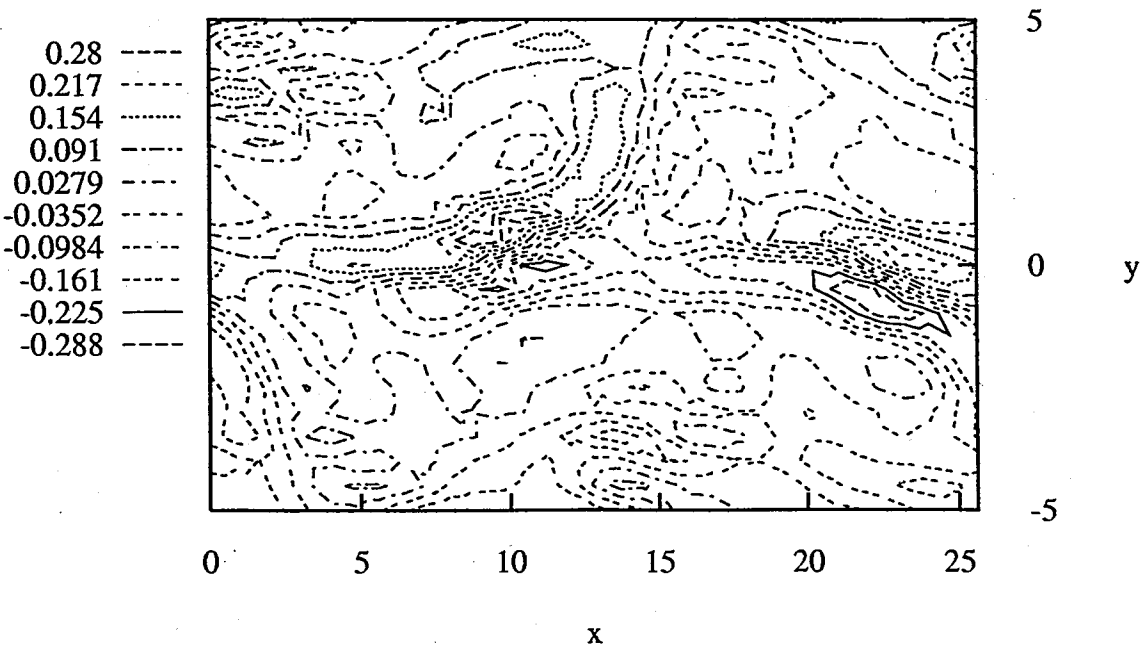

FIGURE 4.49. Vorticity lines for plane jet flow at Re=200, $\alpha = 0.25$, t=2000

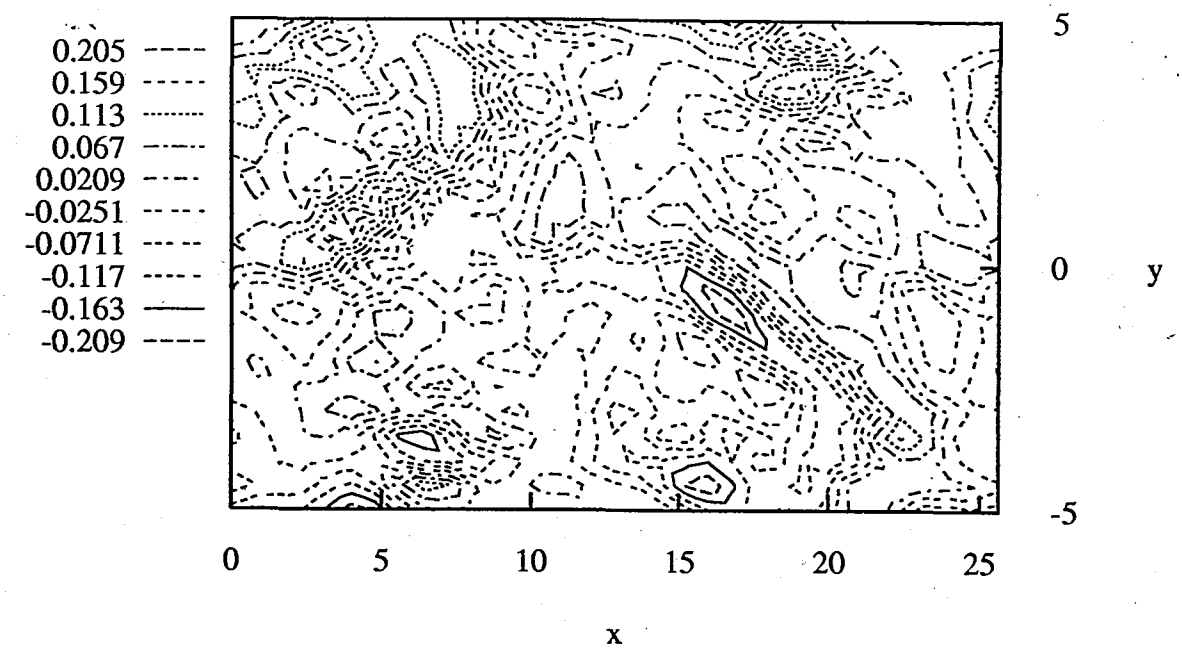

FIGURE 4.50. Vorticity lines for plane jet flow at Re=500, $\alpha = 0.25$, t=2000

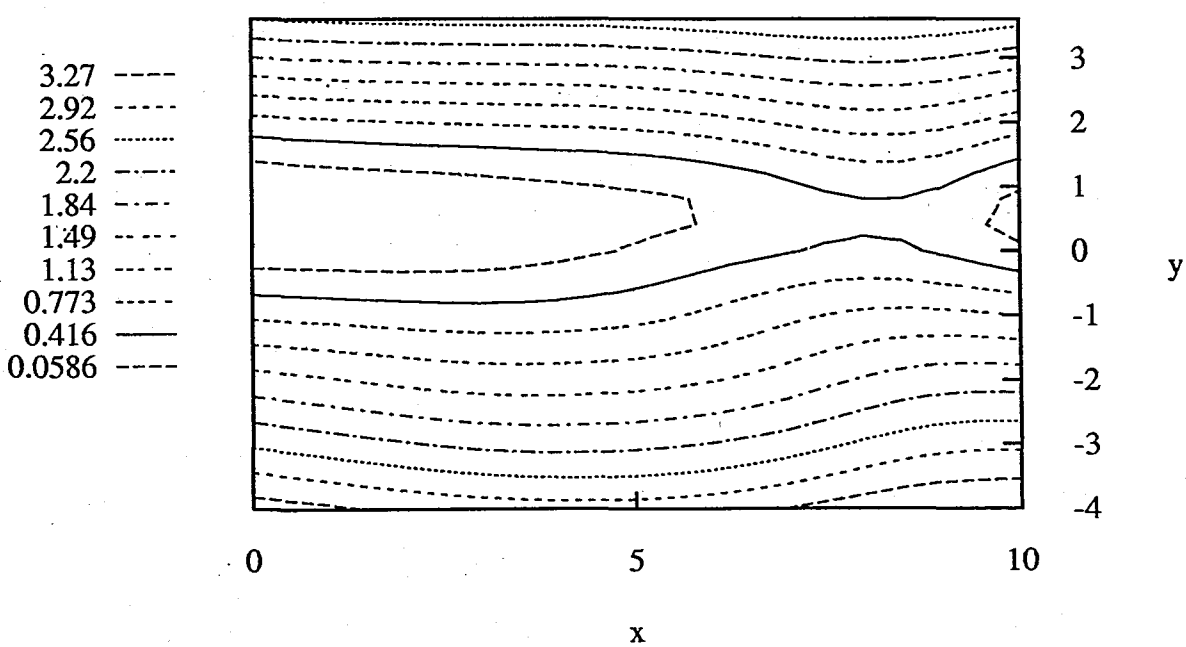

FIGURE 4.51. Streamlines for plane jet flow with subharmonic excitation at Re=100, $\alpha = 0.8$, $A_{10} = 0.2$, $A_{1/2,0} = 0.1$, $\theta/\alpha = \pi/2$, t=1500

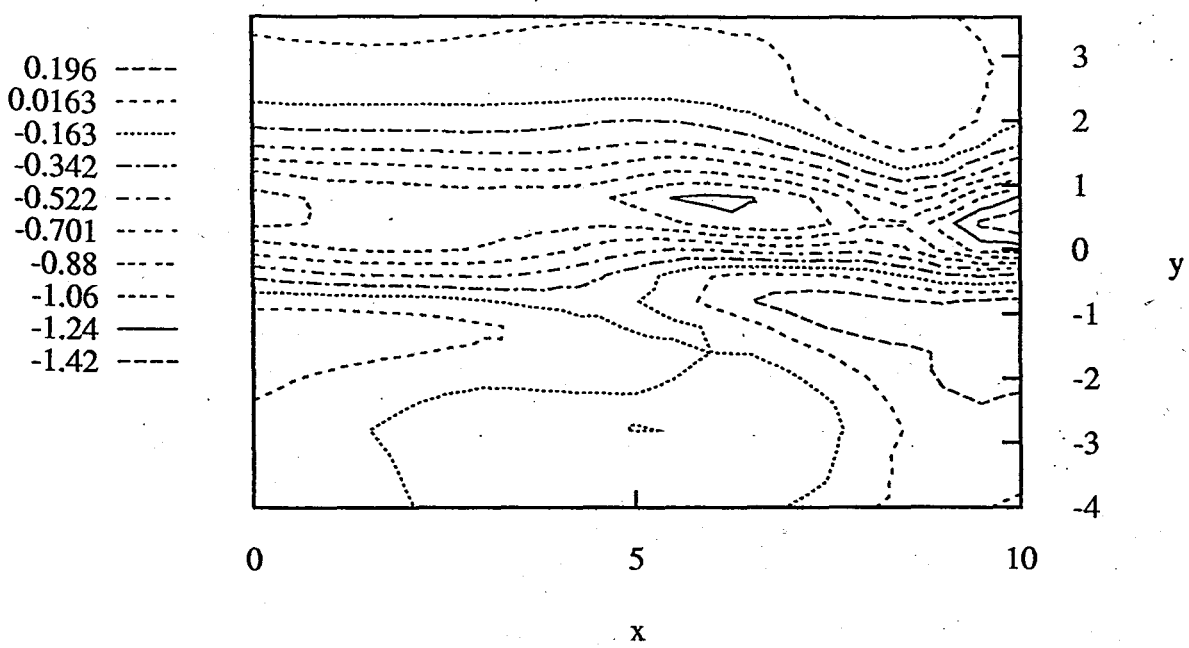

FIGURE 4.52. Vorticity lines for plane jet flow with subharmonic excitation at Re=100, $\alpha = 0.8$, $A_{10} = 0.2$, $A_{1/2,0} = 0.1$, $\theta/\alpha = \pi/2$, t=1500

5. CONCLUSION

As it was mentioned in the introduction, the deterministic approach to fluid problems is one of the main interest topics in the research community nowadays. The full quantitative as well as qualitative aspects of the Navier-Stokes system of equations governing fluid motion, need to be revealed with the aid of the increase in computing power. Although traditional methods, such as the statistical ones, are still in use with new insight to the flow problems, on the numerical side, large eddy and direct numerical simulations which investigate the full solutions of the Navier-Stokes system are of current research areas. The theory of dynamical systems which deals with the qualitative properties of differential systems, seems to be a useful approach to interpret the results of the numerical simulations, as well as it constitutes a reliable guide to investigate parametrically the structure of the phase space associated with the dynamical system. The reduction in the number of degrees of freedom is of crucial importance in systems such as Navier-Stokes, where, due to the increase of Reynolds number with the settling of the turbulent regime, this number can reach very high values and invalidate all numerical approaches even with today's high level computing power. Dynamical systems theory also brings some hope of such a reduction by the introduction of mathematical objects such as the inertial manifolds in the phase space.

In this study, we performed a numerical and parametrical investigation of the solutions of two-dimensional Navier-Stokes equations for the transition to turbulence regime in the case of wall-bounded and free shear layer flows, making use of the spectral methods of solution. At first, we conducted numerical convergence and efficiency tests of new spectral algorithms, called Nonlinear Galerkin Methods, introduced in the context of dynamical systems theory to construct approximate inertial manifolds of dissipative evolution equations such as the Navier-Stokes equations of fluid motion. Early mathematical and numerical results concerning Nonlinear Galerkin Methods mainly consisted of studies of homogeneous flows with periodic boundary conditions in all directions. In this work, we performed their tests in the case of wall-bounded shear flow where there exists one nonhomogeneous direction and in the case of free shear layer flow where the flow domain is unbounded in one direction. We observed that these methods

bring significant improvements with respect to the classical Galerkin spectral method in terms of convergence and efficiency. These results are promising in the context of direct numerical simulations of the Navier-Stokes equations of motion. However, before concluding on the use of these new methods in turbulence study, it should be noted that their tests have to be conducted with more complex flows, in terms of geometry and dimension and in much higher Reynolds numbers where turbulence is fully developed, spatially and temporally, thus necessitating the numerical study of dynamical systems with much more degrees of freedom.

In parallel, we performed tests on the use of Hermite functions in spectral methods of solution for unbounded flow problems where the spectral basis according to which the spectral decomposition has to be made is still an open problem. With the nonlinear stability problem formulation in terms of the perturbation streamfunction which fulfills the convergence criterion for the use of Hermite functions, these functions are found to be much more effective compared to the alternative methods of domain truncation or mapping techniques which necessitate the numerical adjustment of free mapping parameters to ensure convergence.

The parametrical investigation of the transition to turbulence for wall-bounded and free shear layer flows has been conducted using both the classical and nonlinear Galerkin spectral methods where it needs, based on the nonlinear temporal stability problem, following the evolution of finite two-dimensional perturbations to the main flow. Spectral methods used in the study are fully spectral in the sense that they are free of aliasing errors which occur in pseudo-spectral methods. The bifurcations from fixed-point solutions to periodic and quasi-periodic solutions as well as to chaotic solutions have been detected in the range of bifurcation parameters according to which the numerical simulations have been performed. Transition to chaos has been observed to occur after two or three Hopf bifurcations, which seems to be in accordance with the Newhouse-Ruelle-Takens scenario of the transition to turbulence.

In the case of plane Poiseuille flow, a first Hopf bifurcation occurs around Re=2900 for α = 1.3231 with the formation of finite-amplitude waves. For the same

wavenumber, a second Hopf bifurcation has been detected around Re=5200 with the formation of two-periodic motion. We also observe an intermittent behavior in the time evolution of the vorticity with periodic jumps to a stochastic state. Around Re=8000, a three-periodic motion settles. If the Reynolds number is further increased, instabilities set in and drive the flow to a chaotic state. For a lower wavenumber ($\alpha = 0.5$) initial perturbation had to be increased one order of magnitude to detect a first Hopf bifurcation around Re=5000. The qualitative behavior has been observed to be similar to the previous case. In the case of oscillating Poiseuille flow, the effect of oscillations on the nonlinear stability of plane Poiseuille flow has been investigated for two different values of the ratio of the amplitude of the oscillatory to steady velocity, increasing the Reynolds number up to 5000. Up to Re=2900, all finite disturbances decayed for both cases. For Δ=0.1, from Re=2900 to Re=5000, quasi-periodic behavior appeared and settled. For Δ=0.4, however, all finite disturbances decayed up to Re=5000. At Re=5000, we observed the formation of quasi-periodic dynamics. For higher Reynolds numbers, the arising of instabilities has been noted.

In the case of temporally growing mixing layer, in the absence of subharmonic excitation, we observed the convergence of the solution to a fixed-point attractor which corresponds to a vortical state of the flow. In the presence of subharmonic excitations, we observed the settlement of some quasi-periodic behavior beginning from Re=83. For high values of the Reynolds number (Re=400), chaotic behavior appeared. The deformation of vortices and vortex pairing can be observed in vorticity lines figures. In the case of plane jet flow, in the absence of subharmonic excitation, periodic and quasi-periodic solutions can be observed around Re=100. The instabilities set in for higher Reynolds numbers. In the presence of subharmonic excitations, although the dynamic behavior of the vorticity is similar to the previous case, the elongation of vortices and vortex pairing can be observed in vorticity lines figures.

It should be noted that the study is based on the temporal stability problem which investigates the temporal evolution of finite two-dimensional disturbances. The spatial stability problem which needs the imposition of inflow and outflow boundary conditions in the streamwise direction, can offer new aspects in the transition to turbulence. On the other hand, the problem cases consist of plane shear flows. Although, as it was mentioned in

Chapter 4, the study of two-dimensional mechanisms and solutions are worth of interest in the transition to turbulence studies, it is known that three-dimensionality offers new mechanisms in the transition process where three-dimensional infinitesimal disturbances can cause sudden transition to turbulence, thus can change the above picture of the transition to turbulence.

We hope that this study contributes to the investigation of the solution space of Navier-Stokes equations of motion as well as to the testing of new spectral algorithms which seem to be promising in turbulence study.

APPENDIX A. CHEBYSHEV POLYNOMIALS

In this appendix, we give the definition and some useful properties of Chebyshev polynomials of the first kind. The properties related to their derivatives and their product enable the exact integrations we need in the fully spectral decomposition.

Chebyshev polynomials of the first kind $T_k(x)$ are the eigenfunctions of the following singular Sturm-Liouville problem in the interval [-1,1],

$$\frac{d}{dx}(\sqrt{1-x^2}\frac{dT_k(x)}{dx})+\frac{k^2}{\sqrt{1-x^2}}T_k(x)=0 \qquad (A.1)$$

They are related to trigonometric functions with,

$$T_k(x)=\cos(k\arccos(x)) \qquad (A.2)$$

Thus, the Chebyshev polynomials are cosine functions after a change of variable. The transformation $x = \cos\theta$ enables many mathematical relations as well as theoretical results concerning the Fourier system to be adapted to the Chebyshev system. They can be generated through the Rodriguez formula (Canuto et al., 1988),

$$T_k(x)=\frac{(-1)^k x^k k!}{(2k)!}\sqrt{1-x^2}\frac{d^k}{dx^k}((1-x^2)^{k-(1/2)}) \qquad (A.3)$$

as $T_0(x)=1$, $T_1(x)=x$, $T_2(x)=2x^2-1$ etc. Hence, the Chebyshev polynomials can be expanded in power series as,

$$T_k(x)=\frac{k}{2}\sum_{l=0}^{[k/2]}(-1)^k\frac{(k-l-1)!}{l!(k-2l)!}(2x)^{k-2l} \qquad (A.4)$$

where $[v]$ denotes the largest integer less than or equal to v. Some of their useful properties can be summarized as (Snyder, 1966);

(a) they satisfy the following recurrence relation;

$$T_{k+1}(x) - 2xT_k(x) + T_{k-1}(x) = 0 \tag{A.5}$$

(b) their first derivatives satisfy the following recurrence relation;

$$2T_k(x) = \frac{1}{k+1}T'_{k+1}(x) - \frac{1}{k-1}T'_{k-1}(x) \qquad k \geq 1 \tag{A.6}$$

(c) they and their first derivatives are bounded in the interval [-1,1] , such that;

$$\left|T_k(x)\right| \leq 1 \qquad \textit{and} \qquad \left|T'_k(x)\right| \leq k^2 \tag{A.7}$$

(d) at the boundaries, they and their first derivatives satisfy;

$$T_k(\pm 1) = (\pm 1)^k \qquad \textit{and} \qquad T'_k(\pm 1) = (\pm 1)^k k^2 \tag{A.8}$$

(e) they satisfy the following orthogonality relation;

$$\int_{-1}^{1} T_n(x)T_m(x)w(x)dx = c_n\delta_{mn} \qquad \textit{with} \qquad c_n = \begin{cases} c_0 = \pi \\ c_n = \pi/2, \; n \neq 0 \end{cases} \tag{A.9}$$

where δ_{mn} is the Kronecker delta symbol and where the weight function $w(x)$ is,

$$w(x) = 1/\sqrt{1-x^2} \tag{A.10}$$

(f) their product satisfy;

$$T_n(x)T_m(x) = \frac{1}{2}(T_{n+m}(x) + T_{n-m}(x))$$
$$x^r T_n(x) = \frac{1}{2^r}\sum_{i=0}^{r}\frac{r!}{i!(r-i)!}T_{n-r+2i}(x) \qquad \text{(A.11)}$$

In fully spectral methods, it is important to be able to write the derivatives of the trial functions in terms of the same trial functions to use the orthogonality properties. It is possible to develop expressions for the derivatives of the Chebyshev polynomials in terms of them. Since we need derivatives up to order four, we can write them as follows: We consider the function u expanded in terms of Chebyshev polynomials,

$$u(x) = \sum_{k=0}^{\infty}\hat{u}_k T_k(x) \qquad \text{(A.12)}$$

The first derivative of u can then be written as a consequence of (A.6) (Canuto et al., 1988),

$$u'(x) = \sum_{m=0}^{\infty}\hat{u}_m^{(1)}T_m \qquad where \qquad \hat{u}_m^{(1)} = \frac{2}{c_m}\sum_{\substack{p=m+1 \\ p+m\ odd}}^{\infty} p\hat{u}_p \qquad \text{(A.13)}$$

Generalizing the relation (A.6), the second derivative of u can be written as (Canuto et al., 1988),

$$u''(x) = \sum_{m=0}^{\infty}\hat{u}_m^{(2)}T_m \qquad where \qquad \hat{u}_m^{(2)} = \frac{1}{c_m}\sum_{\substack{p=m+2 \\ p+m\ even}}^{\infty} p(p^2-m^2)\hat{u}_p \qquad \text{(A.14)}$$

The forth derivative of u can be written as (Orszag, 1971),

$$u^{iv}(x) = \sum_{m=0}^{\infty} \hat{u}_m^{(4)} T_m \qquad where$$
$$\hat{u}_m^{(4)} = \frac{1}{24 c_m} \sum_{\substack{p=m+4 \\ p+m\ even}}^{\infty} p(p^2(p^2-4)^2 - 3m^2p^4 + 3m^4p^2 - m^2(m^2-4)^2)\hat{u}_p \tag{A.15}$$

In order to handle the nonlinear terms which involve quadratic nonlinearities, it is also important to be able to express the product of two functions each expanded in Chebyshev series as one Chebyshev series. If we consider the two functions,

$$v(x) = \sum_{n=0}^{\infty} a_n T_n(x) \qquad and \qquad w(x) = \sum_{n=0}^{\infty} b_n T_n(x) \tag{A.16}$$

Then, we can write their product as (Orszag, 1971),

$$v(x)w(x) = \frac{1}{2} \sum_{n=0}^{\infty} e_n T_n(x) \tag{A.17}$$

where,

$$e_n = \frac{1}{c_n} \sum_{m=-\infty}^{\infty} \bar{a}_{n-m} \bar{b}_m \qquad with \qquad \bar{a}_{n-m} = c_{|n-m|} a_{|n-m|}\ ,\ \bar{b}_m = c_{|m|} b_{|m|} \tag{A.18}$$

APPENDIX B. HERMITE POLYNOMIALS AND FUNCTIONS

In this appendix, we give the definitions and some useful properties of Hermite polynomials and Hermite functions.

Hermite polynomials $H_k(x)$ are the eigenfunctions of the following singular Sturm-Liouville problem defined in the interval [-∞,∞],

$$\frac{d^2H_k(x)}{dx^2} - 2x\frac{dH_k(x)}{dx} + 2kH_k(x) = 0 \tag{B.1}$$

They can be generated through the Rodriguez formula,

$$H_k(x) = (-1)^k \exp(x^2)\frac{d^k}{dx^k}(\exp(-x^2)) \tag{B.2}$$

as $H_0(x) = 1$, $H_1(x) = 2x$, $H_2(x) = 4x^2-2$ etc. Hence, the Hermite polynomials can be expanded in power series as,

$$H_k(x) = \sum_{n=0}^{[k/2]} \frac{(-1)^n k!}{n!(k-2n)!}(2x)^{k-2n} \tag{B.3}$$

where $[\nu]$ denotes the largest integer less than or equal to ν.

Some of their useful properties can be summarized as (Lebedev, 1965);

(a) they satisfy the following recurrence relation;

$$H_{k+1}(x) - 2xH_k(x) + 2kH_{k-1}(x) = 0, \qquad k = 1, 2, \ldots \tag{B.4}$$

hence we can write,

$$H_1(x)H_k(x) = H_{k+1}(x) + 2kH_{k-1}(x) \tag{B.5}$$

(b) at zero, they satisfy;

$$H_{2k}(0) = (-1)^k \frac{(2k)!}{k!}, \qquad H_{2k+1}(0) = 0 \tag{B.6}$$

(c) they have the following weighted orthogonality relation;

$$\int_{-\infty}^{\infty} H_m(x)H_n(x)w(x)dx = \begin{cases} 0 & if\ m \neq n \\ 2^n n!\sqrt{\pi} & if\ m = n \end{cases} \tag{B.7}$$

where the weight function $w(x)$ is,

$$w(x) = \exp(-x^2) \tag{B.8}$$

(d) their product satisfy;

$$H_p(x)H_q(x) = p!q! \sum_{n=0}^{\min(p,q)} \frac{2^n H_{p+q-2n}(x)}{n!(p-n)!(q-n)!} \qquad p,q = 0,1,2,... \tag{B.9}$$

(e) their derivatives can be obtained in terms of them with the following recurrence relation;

$$H_n'(x) = 2nH_{n-1}(x) \qquad n = 1,2,... \tag{B.10}$$

We can define an orthonormal set of functions on [-∞,∞] $u_n(x)$, called the Hermite functions as,

$$u_n(x) = (2^n n!\sqrt{\pi})^{-1/2} \exp(-x^2/2) H_n(x) \tag{B.11}$$

Thus they satisfy,

$$\int_{-\infty}^{\infty} u_n(x)u_m(x)dx = \delta_{mn} \tag{B.12}$$

Using (B.10), we can easily develop formulas to express derivatives of Hermite functions up to order four, in terms of them,

$$u_n' = A_n(-\frac{1}{2A_{n+1}}u_{n+1} + \frac{n}{A_{n-1}}u_{n-1}) \tag{B.13}$$

$$u_n'' = A_n(\frac{1}{4A_{n+2}}u_{n+2} - \frac{(n+(1/2))}{A_n}u_n + \frac{n(n-1)}{A_{n-2}}u_{n-2}) \tag{B.14}$$

$$u_n''' = A_n(-\frac{1}{8A_{n+3}}u_{n+3} + \frac{3(n+1)}{4A_{n+1}}u_{n+1} - \frac{3n^2}{2A_{n-1}}u_{n-1} + \frac{n(n-1)(n-2)}{A_{n-3}}u_{n-3} \tag{B.15}$$

$$\begin{aligned} u_n^{iv} = A_n(\frac{1}{4A_{n+4}}u_{n+4} - \frac{(n+(3/2))}{2A_{n+2}}u_{n+2} + \frac{3(n^2+n+(1/2))}{2A_n}u_n \\ - \frac{n(n-1)(2n-1)}{A_{n-2}}u_{n-2} \frac{n(n-1)(n-2)(n-3)}{A_{n-4}}u_{n-4}) \end{aligned} \tag{B.16}$$

where,

$$A_n = (2^n n!\sqrt{\pi})^{-1/2} \tag{B.17}$$

In order to evaluate the nonlinear terms, we can introduce an analytical expression providing the definite integral of the product of Hermite functions defined by (Ripa, 1983),

$$I_\beta(J;\mathbf{m};\lambda) = \int_{-\infty}^{+\infty} dx \exp(-\beta^2 x^2) \prod_{j=1}^{J} u_{m_j}(\lambda_j x)$$
$$for \quad \Re e(\beta + \frac{1}{2}\sum_{j=1}^{J} \lambda_j^2) \geq 0 \tag{B.18}$$

where λ and β are arbitrary constants. Then, the result can be given as,

$$I_\beta = \pi^{1/2} \rho \left[\prod_{j=1}^{J} A_{m_j}\right] \sum_{[n_j=0]}^{[m_j/2]} \cdots$$
$$\sum ((-1)^{N+M} (N+1)_N \prod_{j=1}^{J} \mu_j^{m_j-2n_j} \frac{(m_j)!}{(m_j-2n_j)!} (n_j!)^{-1}) \tag{B.19}$$

where,

$$M = \frac{1}{2}\sum_{j=1}^{J} m_j, \quad N = M - \sum_{j=1}^{J} n_j, \quad \mu_j = \lambda_j \rho, \quad \rho = \left[\beta + \frac{1}{2}\sum_{j=1}^{J} \lambda_j^2\right]^{-1/2} \tag{B.20}$$

and with the Pochhammer symbol defined as,

$$(N+1)_N = (N+1)(N+2).....(N+(N-1)) \tag{B.21}$$

It should be noted that the integral vanishes unless M is integer.

APPENDIX C. DERIVATION OF THE DYNAMICAL SYSTEM

We consider the infinite-dimensional scalar streamfunction partial differential equation (2.4) and apply the Galerkin spectral method to reduce it to a finite-dimensional ordinary differential equation system describing the time evolution of the time dependent complex expansion coefficients. We will give in this appendix the necessary spectral integrations to derive this system and make use of the special properties of Chebyshev and Hermite functions cited in the previous appendices.

The first term in the equation (2.4), i. e. the time derivative of the Laplacian of the streamfunction will translate into,

$$\left(M\dot{\mathbf{a}}\right)_{k'm'} = \iint_D \Big(\sum_k \sum_m \dot{a}_{km} \exp(i2\pi kx / L)(\Phi_m'' - (4\pi^2 k^2 / L^2)\Phi_m) \exp(-i2\pi k'x / L)\Phi_{m'} w(y)dxdy \tag{C.1}$$

where D =[0,L]×[-1,1] in the case of channel flow and D =[0,L]×[-∞,∞] in the free shear flow case. The weight function $w(y)$ is the function (3.4) in the channel flow case and the unity function in the free shear layer case. We now introduce some functions to express the result of the integration,

$$delta(m,m') = \begin{cases} \delta_{mm'} & if\ m,m' \neq 0 \\ 2 & if\ m = m' = 0 \end{cases} \tag{C.2}$$

$$g(m,m') = \begin{cases} m(m^2 - m'^2) & if \quad m > m'\ and\ \mathrm{mod}(m,2) = \mathrm{mod}(m',2) \\ 0 & if \quad m \leq m'\ or\ \mathrm{mod}(m,2) \neq \mathrm{mod}(m',2) \end{cases} \tag{C.3}$$

$$\begin{aligned} R(f(m,m')) = {} & \frac{f(m+2,m'-2)}{m(m+1)m'(m'-1)} - \frac{2f(m+2,m')}{m(m+1)(m'^2-1)} + \frac{f(m+2,m'+2)}{m(m+1)m'(m'+1)} - \\ & \frac{2f(m,m'-2)}{(m^2-1)m'(m'-1)} + \frac{4f(m,m')}{(m^2-1)(m'^2-1)} - \frac{2f(m,m'+2)}{(m^2-1)m'(m'+1)} + \\ & \frac{f(m-2,m'-2)}{m(m-1)m'(m'-1)} - \frac{2f(m-2,m')}{m(m-1)(m'^2-1)} + \frac{f(m-2,m'+2)}{m(m-1)m'(m'+1)} \end{aligned} \tag{C.4}$$

Then, we can write the result of (C.1) in the case of channel flow as,

$$\left(M\dot{\mathbf{a}}\right)_{k'm'} = (\frac{\pi}{2}L)\sum_{m}(R(g(m,m'))-(\frac{4\pi^2k'^2}{L^2})R(delta(m,m'))\dot{a}_{k'm} \tag{C.5}$$

and in the case of free shear layer as,

$$\left(M\dot{\mathbf{a}}\right)_{k'm'} = L\sum_{m}(\frac{\sqrt{2^{m'}m'!}}{\sqrt{2^{m}m!}}(\frac{1}{4}\delta_{m+2,m'}-(m+\frac{1}{2})\delta_{m,m'}+m(m-1)\delta_{m-2,m'}) -(\frac{4\pi^2k'^2}{L})\delta_{m,m'})\dot{a}_{k'm} \tag{C.6}$$

The second term in the equation (2.4), i. e. the biharmonic viscous term will translate into,

$$\left(N\mathbf{a}\right)_{k'm'} = \iint_{D}(\sum_{k}\sum_{m}a_{km}\exp(i2\pi kx/L)(\Phi_m^{iv}-(8\pi^2k^2/L^2)\Phi_m''+ (16\pi^4k^4/L^4)\Phi_m)\exp(-i2\pi k'x/L)\Phi_{m'}w(y)dxdy \tag{C.7}$$

We introduce the following function for the channel flow case,

$$h(m,m') = \begin{cases}\frac{1}{24}m(m^2(m^2-4)^2-3m'^2m^4+3m'^4m^2-m'^2(m'^2-4)^2) & if\ \ i>j \\ 0 & if\ \ i\le j\end{cases} \tag{C.8}$$

Then, the integral (C.7) gives, for the channel flow case,

$$\left(N\mathbf{a}\right)_{k'm'} = (\frac{\pi}{2}L)\sum_{m}(R(h(m,m'))-(\frac{8\pi^2k'^2}{L^2})R(g(m,m')) +(\frac{16\pi^4k'^4}{L^4})R(delta(m,m'))a_{k'm} \tag{C.9}$$

The integral (C.7), for the free shear layer flow case, gives,

$$
\begin{aligned}
(N\mathbf{a})_{k'm'} = L\sum_{m}\Big(\frac{\sqrt{2^{m'}m'!}}{\sqrt{2^{m}m!}}\Big(\frac{1}{16}\delta_{m+4,m'} - \frac{1}{2}(m+\frac{3}{2})\delta_{m+2,m'} + \\
\frac{3}{2}(m^2+m+\frac{1}{2})\delta_{m,m'} - m(m-1)(2m-1)\delta_{m-2,m'} + \\
m(m-1)(m-2)(m-3)\delta_{m-4,m'}\Big) - \Big(\frac{8\pi^2 k'^2}{L}\Big)\Big(\frac{1}{4}\delta_{m+2,m'} - \\
(m+\frac{1}{2})\delta_{m,m'} + m(m-1)\delta_{m-2,m'}\Big) + \Big(\frac{16\pi^4 k'^4}{L}\Big)\delta_{m,m'}\Big)a_{k'm}
\end{aligned}
\tag{C.10}
$$

For the nonlinear terms in the formulation (2.4), we have to introduce some other functions which involve the products of the expansion functions as,

$$
phi(m,j,n) = \int_S \Phi'_m \Phi''_j \Phi_n w(y)dy \tag{C.11}
$$

$$
thi(m,j,n) = \int_S \Phi'_m \Phi_j \Phi_n w(y)dy \tag{C.12}
$$

$$
rhi(m,j,n) = \int_S \Phi_m \Phi'''_j \Phi_n w(y)dy \tag{C.13}
$$

where $S = [-1,1]$ in the channel flow case and $S = [-\infty,\infty]$ in the free shear layer case.

To give these functions explicitly, we proceed first for the channel flow case and define new functions,

$$phi = \frac{2(m+2)(j+2)}{m(m+1)j(j+1)} fn(m+2,j,n) - \frac{4(m+2)j}{m(m+1)(j^2-1)} fn(m+2,j-2,n) +$$
$$\frac{2(m+2)(j-2)}{m(m+1)j(j-1)} fn(m+2,j-4,n) - \frac{4m(j+2)}{(m^2-1)j(j+1)} fn(m,j,n) +$$
$$\frac{8mj}{(m^2-1)(j^2-1)} fn(m,j-2,n) - \frac{4m(j-2)}{(m^2-1)j(j-1)} fn(m,j-4,n) + \qquad \text{(C.14)}$$
$$\frac{2(m-2)(j+2)}{m(m-1)j(j+1)} fn(m-2,j,n) - \frac{4j(m-2)}{m(m-1)(j^2-1)} fn(m-2,j-2,n) +$$
$$\frac{2(m-2)(j-2)}{m(m-1)j(j-1)} fn(m-2,j-4,n).$$

where,

$$fn(i,j,k) = \frac{1}{k(k-1)} en(k-2,i-2,j) - \frac{2}{k^2-1} en(k,i-2,j) + \frac{1}{k(k+1)} en(k+2,i-2,j) \qquad \text{(C.15)}$$

where,

$$en(n,m,j) = \begin{cases} 0 & if \quad n > m+j+1 \\ \frac{\pi}{4} \sum_{k=-j,2}^{j} an(n-k,m)bn(k,m) & otherwise \end{cases} \qquad \text{(C.16)}$$

where,

$$an(i,m) = \begin{cases} 1 & if \quad \text{mod}(i,2) \neq \text{mod}(m,2) \; and \; |i| < (m+2) \\ 0 & otherwise \end{cases} \qquad \text{(C.17)}$$

$$bn(j,k) = \begin{cases} (j+2)^2 - k^2 & if \quad \text{mod}(k,2) = \text{mod}(j,2) \; and \; |k| \leq j \\ 0 & otherwise \end{cases} \qquad \text{(C.18)}$$

Similarly, we can write,

$$thi = \frac{2(m+2)}{m(m+1)j(j+1)} fc(m+2,j,n) - \frac{4(m+2)}{m(m+1)(j^2-1)} fc(m+2,j-2,n) + \frac{2(m+2)}{m(m+1)j(j-1)} fc(m+2,j-4,n) - \frac{4m}{(m^2-1)j(j+1)} fc(m,j,n) + \frac{8m}{(m^2-1)(j^2-1)} fc(m,j-2,n) - \frac{4m}{(m^2-1)j(j-1)} fc(m,j-4,n) + \frac{2(m-2)}{m(m-1)j(j+1)} fc(m-2,j,n) - \frac{4(m-2)}{m(m-1)(j^2-1)} fc(m-2,j-2,n) + \frac{2(m-2)}{m(m-1)j(j-1)} fc(m-2,j-4,n). \quad \text{(C.19)}$$

where,

$$fc(i,j,k) = \frac{1}{k(k-1)} ec(k-2,i-2,j) - \frac{2}{k^2-1} ec(k,i-2,j) + \frac{1}{k(k+1)} ec(k+2,i-2,j) \quad \text{(C.20)}$$

where,

$$ec(n,m,j) = \begin{cases} 0 & if \quad n > m+j+3 \\ \frac{\pi}{4}(an(n+j+2,m) + an(n-j-2,m)) & otherwise \end{cases} \quad \text{(C.21)}$$

Similarly, we can write,

$$rhi = \frac{1}{m(m+1)j(j+1)} fr(m+2,j,n) - \frac{2}{m(m+1)(j^2-1)} fr(m+2,j-2,n) + \frac{1}{m(m+1)j(j-1)} fr(m+2,j-4,n) - \frac{2}{(m^2-1)j(j+1)} fr(m,j,n) + \frac{4}{(m^2-1)(j^2-1)} fr(m,j-2,n) - \frac{2}{(m^2-1)j(j-1)} fr(m,j-4,n) + \frac{1}{m(m-1)j(j+1)} fr(m-2,j,n) - \frac{2}{m(m-1)(j^2-1)} fr(m-2,j-2,n) + \frac{1}{m(m-1)j(j-1)} fr(m-2,j-4,n). \quad \text{(C.22)}$$

where,

$$fr(i,j,k) = \frac{1}{k(k-1)} er(k-2,i-2,j) - \frac{2}{k^2-1} er(k,i-2,j) + \frac{1}{k(k+1)} er(k+2,i-2,j) \quad \text{(C.23)}$$

where,

$$er(n,m,j) = \begin{cases} 0 & if \quad n > m+j+2 \\ \frac{\pi}{4}(br(j,n-m-2) + br(j,n+m+2)) & otherwise \end{cases} \quad \text{(C.24)}$$

where,

$$br(j,k) = \begin{cases} \sum_{i=|k|+1,2}^{j} 2i(j+2)((j+2)^2 - i^2) & if \ \mathrm{mod}(k,2) \neq \mathrm{mod}(j,2) \ and \ |k| \leq j-1 \\ 0 & otherwise \end{cases} \quad \text{(C.25)}$$

In the case of free shear layer, the above functions (C.11-13), will be given explicitly in terms of the following function,

$$sh(m,j,n)=\sum_{i_3=0}^{n/2}\sum_{i_2=0}^{j/2}\sum_{i_1=0}^{m/2}(-1)^{(N+M)}(N+1,N)\rho^{(m+j+n-2(i_1+i_2+i_3))}\cdot \frac{m!\,j!\,n!}{i_1!(m-2i_1)!\,i_2!(j-2i_2)!\,i_3!(n-2i_3)!} \tag{C.26}$$

where $(N+1,N)$ is the Pochhammer function as defined in (B.21) and,

$$\rho=\sqrt{2/3},\quad M=(m+j+n)/2,\quad N=M-(i_1+i_2+i_3) \tag{C.27}$$

We should note that *sh(m,j,n)* will vanish if m or $j<0$, or mod$(M, 2)\neq 0$.

Then, we can define the functions (C.11-13), in terms of the above function,

$$\begin{aligned} phi(m,j,n)=&-\frac{1}{A_mA_jA_n}\Big(\frac{1}{8}sh(m+1,j+2,n)-\frac{1}{2}(j+\frac{1}{2})sh(m+1,j,n)+\\ &\frac{1}{2}j(j-1)sh(m+1,j-2,n)-\frac{m}{4}sh(m-1,j+2,n)+\\ &m(j+\frac{1}{2})sh(m-1,j,n)-mj(j-1)sh(m-1,j-2,n)\Big) \end{aligned} \tag{C.28}$$

$$thi(m,j,n)=-\frac{1}{A_mA_jA_n}\Big(\frac{1}{2}sh(m+1,j,n)-m.sh(m-1,j,n)\Big) \tag{C.29}$$

$$\begin{aligned} rhi(m,j,n)=&-\frac{1}{A_mA_jA_n}\Big(\frac{1}{8}sh(m,j+3,n)-\frac{3(j+1)}{4}sh(m,j+1,n)-\\ &\frac{3j^2}{2}sh(m,j-1,n)-j(j-1)(j-2)sh(m,j-3,n)\Big) \end{aligned} \tag{C.30}$$

where A_m's are defined as in (B.17).

We can therefore in both cases express the nonlinear terms in the formulation (2.4) as,

$$\left(F(\mathbf{a})\right)_{k'm'} = iL \sum_{k_1+k_2=k'} \sum_{m,j} \left(\frac{2\pi k_2}{L} phi(m,j,m') - \frac{2\pi k_1}{L} rhi(m,j,m') - \frac{8\pi^3 (k_2^3 - k_1 k_2^2)}{L^3} thi(m,j,m')\right) a_{k_1 m} a_{k_2 j} \tag{C.31}$$

Hence, the dynamical system is given by,

$$M\dot{\mathbf{a}} = N\mathbf{a} + F(\mathbf{a}) \tag{C.32}$$

REFERENCES

Atalık, K. and A. Tezel, "Düzlem Kanal Akışında Türbülans Probleminin Lineer Olmayan Galerkin Yöntemiyle Sayısal Analizi," *X. Ulusal Mekanik Kongresi -Bildiriler-*, pp. 117-127, Maslak, 15 September-19 September 1997, Teorik ve Uygulamalı Mekanik Türk Milli Komitesi, Maslak, 1998.

Atalık, K. and A. Tezel, "Applications of the Nonlinear Galerkin Methods to some Flow Problems," *Proceedings of the Workshop on Industrial and Environmental Applications of Direct and Large Eddy Simulations*, Boğaziçi University, 5 August-7 August 1998, to be published in Lecture Notes in Physics, Springer-Verlag, 1999.

Aubry, N., P. Holmes, J. L. Lumley and E. Stone, "The Dynamics of Coherent Structures in the Wall Region of a Turbulent Boundary Layer," *Journal of Fluid Mechanics*, Vol. 192, pp. 115-173, 1988.

Baldwin, B. S. and H. Lomax, "Thin Layer Approximation and Algebraic Model for Separated Turbulent Flows," *AIAA Paper 78-257*, AIAA 16th Aerospace Sciences Meeting, Huntsville, 1978.

Barkley, D., "Theory and Predictions for Finite-Amplitude Waves in Two-Dimensional Plane Poiseuille Flow," *Phys. Fluids A*, Vol. 2(6), pp. 955-970, 1990.

Batchelor, G. K. and A. A. Townsend, A, "The Nature of Turbulent Motion at High Wave Numbers," *Proc. R. Soc. A*, Vol. 199, pp. 238-255, 1949.

Betchov, R. and W. O. Criminale, Jr., *Stability of Parallel Flows*, Academic Press, New York, 1967.

Billoti, J. E. and J. P. La Salle, "Dissipative Periodic Processes," *Bull. Amer. Math. Soc.*, Vol. 77, pp. 1082-1088, 1971.

Boussinesq, J., "Théorie de l'écolement tourbillant," *Mém. Présentés par Divers Savants Acad. Sci. Inst. Fr.*, Vol. 23, pp. 46-50, 1877.

Boyd, J. P., "The Optimization of Convergence for Chebyshev Polynomials in an Unbounded Domain," *J. of Comp. Physics*, Vol. 45, pp. 43-79, 1982.

Boyd, J. P., "Asymptotic Coefficients of Hermite Function Series," *J. of Comp. Physics*, Vol. 54, pp. 382-410, 1984.

Boyd, J. P., "Spectral Methods Using Rational Basis Functions on an Infinite Interval," *J. of Comp. Physics*, Vol. 69, pp. 112-142, 1987.

Boyd, J. P., "The Orthogonal Rational Functions of Higgins and Christov and Algebraically Mapped Chebyshev Polynomials," *J. of Approximation Theory*, Vol. 61, pp. 98-105, 1990.

Brown, G. L. and A. Roshko, "On Density Effects and Large Structure in Turbulent Mixing Layers," *Journal of Fluid Mechanics*, Vol. 64, pp. 775-816, 1974.

Bushnell, D. M., "Simplex Discussion Regarding "Modeling: Present and Future" with Emphasis Upon High Speeds. Comment 3," in J. L. Lumley (Ed.), *Whither Turbulence? Turbulence at the Crossroads*, pp. 513-516, Springer-Verlag, New York, 1990.

Busse, F. H., "Transition to Turbulence in Rayleigh-Bénard Convection," in H. L. Swinney and J. P. Gollub (Eds.), *Hydrodynamic Instabilites and the Transition to Turbulence*, pp. 97-137, Springer-Verlag, New York, 1981.

Caffarelli, L., R. Kohn and L. Nirenberg, "Partial Regularity of Suitable Weak Solutions of the Navier-Stokes Equations," *Comm. Pure Appl. Math.*, Vol. 35, pp. 771-831, 1982.

Cain, A. B., J. H. Ferziger and W. C. Reynolds, "Discrete Orthogonal Function Expansions for Non-Uniform Grids Using the Fast Fourier Transform," *J. of Comp. Physics*, Vol. 56, pp. 272-286, 1983.

Canuto, C., M. Y. Hussaini, A. Quarteroni and T. A. Zang, *Spectral Methods in Fluid Dynamics*, Springer-Verlag, New York, 1988.

Cebeci, T. and A. M. O. Smith, *Analysis of Turbulent Boundary Layers*, Academic Press, New York, 1974.

Christov, C. I., "A Complete Orthonormal System of Functions in $L^2(-\infty,\infty)$ Space," *SIAM J. Appl. Math.*, Vol. 42, pp. 1337-1344, 1982.

Collatz, L., *Numerical Treatment of Differential Equations*, Springer-Verlag, Berlin, 1960.

Constantin, P., C. Foias, O. Manley and R. Temam, "Connexion entre la Théorie Mathématique des Equations de Navier-Stokes et la Théorie Conventionnelle de la Turbulence," *C. R. Acad. Sc. Paris*, Série I, Vol. 297, pp. 599-602, 1983.

Constantin, P., C. Foias, O. Manley and R. Temam, "Determining Modes and Fractal Dimension of Turbulent Flows," *Journal of Fluid Mechanics*, Vol. 150, pp. 427-440, 1985.

Constantin, P., C. Foias and R. Temam, "On the Dimension of the Attractors in Two-Dimensional Turbulence," *Physica D*, Vol. 30, pp. 284-296, 1988.

Constantin, P., C. Foias, B. Nicolaenko and R. Temam, *Integral Manifolds and Inertial Manifolds for Dissipative Evolution Equations*, Springer-Verlag, 1989.

Dean, R. B., "Reynolds Number Dependence of Skin Friction and Other Bulk Flow Variables in Two-Dimensional Rectangular Duct Flow," *J. of Fluid Eng.*, Vol. 100, pp. 215-223, 1978.

Debussche, A. and T. Dubois, "Approximation of Exponential Order of the Attractor of a Turbulent Flow," *Physica D*, Vol. 72, pp. 372-389., 1994.

Devulder, C. and M. Marion, "A Class of Numerical Algorithms for Large Time integration: the Nonlinear Galerkin Methods," *SIAM J. of Numerical Analysis*, Vol. 29(2), pp. 462-483, 1992.

DiPrima, R. C. and H. L. Swinney, "Instabilities and Transition in Flow Between Concentric Rotating Cylinders," in H. L. Swinney and J. P. Gollub (Eds.), *Hydrodynamic Instabilites and the Transition to Turbulence*, pp. 139-180, Springer-Verlag, New York, 1981.

Eringen, A. C., "Simple Microfluids,", *Int. J. of Eng. Sci.*, vol. 2, pp. 205-217, 1964.

Eringen, A. C., "On Nonlocal Fluid Mechanics," *Int. J. of Eng. Sci.*, vol. 10, pp. 561-575, 1972.

Eringen, A. C., "On Nonlocal Microfluid Mechanics," *Int. J. of Eng. Sci.*, vol. 11, pp. 291-306, 1973.

Eringen, A. C., *Polar and Nonlocal Theories of Continua*, Boğaziçi University Publications, Istanbul, 1974.

Foias, C. and R. Temam, "Some Analytic and Generic Properties of the Evolution Navier-Stokes Equations," *J. Math. Pures Appl.*, Vol. 58, pp. 339-368, 1979.

Foias, C., O. Manley and R. Temam, R., "Self-Similar Invariant Families of Turbulent Flows," *Phys. Fluids*, Vol. 30, pp. 2007-2020, 1987a.

Foias, C., O. Manley and R. Temam, "Sur l'Interaction des Petits et Grands Tourbillons dans les Ecoulements Turbulents," *C. R. Acad. Sci. Paris Sér. I*, Vol. 305, pp. 497-500, 1987b.

Foias, C., G. R. Sell and R. Temam, "Inertial Manifolds for Nonlinear Evolutionary Equations," *J. of Differential Equations*, Vol. 73, pp. 309-353, 1988a.

Foias, C., O. Manley and R. Temam, "Modelling of the Interaction of Small and Large Eddies in Two Dimensional Turbulent Flows," *MMAN*, Vol. 22(1), pp. 93-114, 1988b.

Foias, C., M. S. Jolly, I. G. Kevrekidis, G. R. Sell and E. S. Titi, "On the Computation of Inertial Manifolds," *Physics Letters A*, Vol. 131, pp. 433-436, 1988c.

Gatski, T. B., "Turbulent Flows: Model Equations and Solution Methodology," in R. Peyret (Ed.), *Handbook of Computational Fluid Mechanics*, pp. 339-415, Academic Press, 1996.

Gottlieb, D. and S. A. Orszag, *Numerical Analysis of Spectral Methods*, SIAM-CBMS, Philadelphia, 1977.

Grosch, C. E. and S. A. Orszag, "Numerical Solutions of Problems in Unbounded Regions: Coordinate Transforms," *J. of Comp. Physics*, Vol. 25, pp. 273-296, 1977.

Guckenheimer, J., "Strange Attractors in Fluids," *Annual Review of Fluid Mechanics*, Vol. 18, pp. 15-31, 1986.

Härtel, C., "Turbulent Flows: Direct Numerical Simulation and Large-Eddy Simulation," in in R. Peyret (Ed.), *Handbook of Computational Fluid Mechanics*, pp. 283-338, Academic Press, 1996.

Herring, J., "The Utility and Drawbacks of Traditional Approaches. Comment 3," in J. L. Lumley (Ed.), *Whither Turbulence? Turbulence at the Crossroads*, pp. 70-80, Springer-Verlag, New York, 1990.

Higgins, J. R., *Completeness and Basis Properties of Sets of Special Functions*, Cambridge University Press, New York, 1977.

Hinze, J. O., *Turbulence*, McGraw-Hill, New York, 1959.

Ho, C. M. and L. S. Huang, "Subharmonics and Vortex Merging in Mixing Layers," *Journal of Fluid Mechanics*, Vol. 119, pp. 443-473, 1982.

Holmes, P., "Can Dynamical Systems Approach Turbulence," in J. L. Lumley (Ed.), *Whither Turbulence? Turbulence at the Crossroads*, pp. 195-249, Springer-Verlag, New York, 1990.

Holmes, P., J. L. Lumley and G. Berkooz, *Turbulence, Coherent Structures, Dynamical Systems and Symmetry*, Cambridge University Press, Cambridge, 1996.

Hopf, E., "A Mathematical Example Displaying the Features of Turbulence," *Comm. Pure Appl. Math.*, Vol.1, pp. 303-322, 1948.

Jauberteau, F., C. Rosier and R. Temam, "A Nonlinear Galerkin Method for the Navier-Stokes Equations," *Comp. Meth. In App. Mech. And Eng.*, Vol. 80, pp. 245-260, 1990.

Johnson, D. A and L. S. King, "A Mathematically Simple Turbulence Closure Model for Attached and Separated Boundary Layers," *AIAA Journal*, Vol. 23, pp. 1684-1692, 1985.

Jolly, M. S., "Bifurcation Computations on an Approxiamte Inertial Manifold for the 2D Navier-Stokes Equations," *Physica D*, Vol. 63, pp. 8-20, 1993.

Kantarovich, L. V. and V. I. Krylov, *Approximate Methods of Higher Analysis*, P. Noordhof Ltd., Groningen, 1964.

Kline, S. J., M. V. Morkovin, G. Sovran and D. J. Cockrell (editors), *Computation of Turbulent Boundary Layers*, Stanford University, 1969.

Kolmogorov, A. N., "Local Structure of Turbulence in an Incompressible Fluid at Very High Reynolds Numbers," *Dokl. Akad. Nauk. SSSR*, Vol. 30, 299-303, 1941.

Kolmogorov, A. N., "A Refinement of Previous Hypotheses Concerning the Local Structure of Turbulence in Viscous Incompressible Fluid at High Reynolds Number," *Journal of Fluid Mechanics*, Vol. 13(1), pp. 82-85, 1962.

Kraichnan, R. H., "The Structure of Isotropic Turbulence at Very High Reynolds Numbers," *Journal of Fluid Mechanics*, Vol. 5, pp. 497-543, 1959.

Kraichnan, R. H. and J. R. Herring, "A Strain-Based Lagrangian-History Turbulence Theory," *Journal of Fluid Mechanics*, Vol. 88, pp. 355-367, 1978.

Kraichnan, R. H., "Models of Intermittency in Hydrodynamic Turbulence," *Physical Review Letters*, Vol. 65, pp. 575-578, 1990.

Kwak, M., "Finite-Dimensional Inertial Forms for 2D Navier-Stokes Equations," *Indiana University Mathematics Journal*, Vol. 41(4), pp. 927-981, 1992.

Lanczos, C., *Applied Analysis*, Prentice-Hall, Englewood Cliffs, N. J., 1956.

Landau, L. D. and E. M. Lifschitz, *Fluid Mechanics*, Pergamon Press, Oxford, 1959.

Lanford, O. E., "Strange Attractors and Turbulence," in H. L. Swinney and J. P. Gollub (Eds.), *Hydrodynamic Instabilites and the Transition to Turbulence*, pp. 7-26, Springer-Verlag, New York, 1981.

Lebedev, N. N., *Special Functions and their Applications*, Prentice-Hall, Englewood Cliffs, N. J., 1965.

Leray, J., "Etude de Diverses Intégrales non Linéaires et de quelques Problèmes que Pose l'Hydrodynamique," *J. Math. Pures Appl.*, Vol. 12, pp. 1-82, 1933.

Leray, J., "Essai sur les Mouvements Plans d'un Liquide Visqueux que Limitent des Parois," *J. Math. Pures Appl.*, Vol. 13, pp. 331-418, 1934a.

Leray, J., "Essai sur le Mouvement d'un Liquide Visqueux Emplissant l'Espace," *Acta Mech.*, Vol. 63, pp. 193-248, 1934b.

Lesieur, M., *Turbulence in Fluids*, second revised edition, Kluwer Academic Publishers, the Netherlands, 1993.

Leslie, D. C., *Developments in the Theory of Turbulence*, Clarendon Press, Oxford, 1973.

Liepmann, H. W., "Aspects of the Turbulence Problem, Part II," *Z. Angew. Math. Phys.*, Vol. 3, pp. 407-426, 1952.

Liu, J. T. C., "Contributions to the Understanding of Large-Scale Coherent Structures in Developing Free Turbulent Shear Flows," *Advances in Applied Mechanics*, Vol. 26, pp. 183-309, 1988.

Lorenz, E. N., "Deterministic Non-Periodic Flows," *J. of Atmos. Sciences*, Vol. 20, pp. 130-141, 1963.

Lumley, J. L., *Stochastic Tools in Turbulence*, Academic Press, New York, 1970.

Lumley, J. L., "The Utility and Drawbacks of Traditional Approaches. Comment 1," in J. L. Lumley (Ed.), *Whither Turbulence? Turbulence at the Crossroads*, pp. 49-58, Springer-Verlag, New York, 1990.

Maday Y. and B. Métivet, "Chebyshev Spectral Approximation of Navier-Stokes Equations in a Two Dimensional Domain," *MMAN*, Vol. 21(1), pp. 93-123, 1987.

Mallet-Paret, J., "Negatively Invariant Sets of Compact Maps and an Extension of a Theorem of Cartwright," *J. of Differential Equations*, Vol. 22, pp. 331-348, 1976.

Mandelbrot, B. B., "Intermittent Turbulence in Self-Similar Cascades: Divergence of High Moments and Dimension of the Carrier," *J. of Fluid Mechanics*, Vol. 62, pp. 331-358, 1974.

Mañé, R., "On the Dimension of the Compact Invariant Sets of Certain Nonlinear Maps," in D. Rand (Ed.), *Dynamical Systems and Turbulence*, Springer-Verlag, New York, 1981.

Marion M. and R. Temam, "Nonlinear Galerkin Methods: the Finite Elements Case," *Numer. Math.*, Vol. 57, pp. 205-226, 1990.

McComb, W. D., *The Physics of Fluid Turbulence*, Oxford University Press, New York, 1992.

Meiburg, E., P. K. Newton, N. Raju and G. Ruetsch, "Unsteady Models for the Nonlinear Evolution of the Mixing Layer," *Physical Rev. E*, Vol. 52(2), pp. 1639-1657, 1995.

Metcalfe, R. W., S. A. Orszag, M. E. Brachet, S. Menon and J. J. Riley, "Secondary Instability of a Temporally Growing Mixing Layer," *Journal of Fluid Mechanics*, Vol. 184, pp. 207-243, 1987.

Mohammadi, B. and O. Pironneau, *Analysis of the K-Epsilon Turbulence Model*, Masson, Paris, 1994.

Moin, P. and J. Kim, "On the Numerical Solution of Time-Dependent Viscous Incompressible Flows Involving Solid Boundaries," *J. of Comp. Phys.*, Vol. 35, pp. 381-392, 1980.

Monin, A. S. and A. M. Yaglom, *Statistical Fluid Mechanics*, Vol. 2, MIT Press, Cambridge, 1975.

Moser, R. D., P. Moin and A. Leonard, "A Spectral Numerical Method for the Navier-Stokes Equations with Applications to Taylor-Couette Flow," *J. of Comp. Physics*, Vol. 52, pp. 524-544, 1983.

Nakano, T., "Direct Interaction Approximation of Turbulence in the Wave Packet Representation," *Phys. Fluids*, Vol. 31, pp. 1420-1430, 1988.

Narasimha, R., "The Utility and Drawbacks of Traditional Approaches," in J. L. Lumley (Ed.), *Whither Turbulence? Turbulence at the Crossroads*, pp. 13-48, Springer-Verlag, New York, 1990.

Newhouse, S., D. Ruelle and F. Takens, "Occurrence of strange Axiom A attractors near quasi-periodic flows on T^m, $m \geq 3$," *Commun. Math. Phys.*, Vol. 64, pp. 35-40, 1978.

Oboukhov, A. M., "Some Specific Features of Atmospheric Turbulence," *Journal of Fluid Mechanics*, Vol. 13, pp. 71-81, 1962.

Orszag, S. A., "Accurate Solution of the Orr-Sommerfeld Stability Equation," *Journal of Fluid Mechanics*, Vol. 50, pp. 689-703, 1971.

Orszag, S. A. and Israeli, M., "Numerical Simulation of Viscous Incompressible Flows", *Annual Review of Fluid Mech.*, Vol. 6, pp. 281-318, 1974.

Orszag, S. A., "Statistical Theory of Turbulence," in R. Balian and J. L. Peube (Eds.), *Fluid Dynamics 1973*, Les Houches Summer School of Theoretical Physics, Gordon and Breach, pp. 237-374, 1977.

Orszag, S. A. and L. C. Kells, "Transition to Turbulence in Plane Poiseuille and Plane Couette Flow," *Journal of Fluid Mechanics*, Vol. 96, pp.159-205, 1980.

Orszag, S. A. and A. T. Patera, "Secondary Instability of Wall-Bounded Shear Flows," *Journal of Fluid Mechanics*, Vol. 128, pp. 347-385, 1983.

Pozrikidis, C., *Introduction to Theoretical and Computational Fluid Dynamics*, Oxford University Press, New York, 1997.

Prandtl, L., "Über die ausgebildete Turbulenz," *ZAMM*, Vol. 5, pp. 136-139, 1925.

Procaccia, I. and P. Constantin, "Non-Kolmogorov Scaling Exponents and the Geometry of High Reynolds Number Turbulence," *Physical Review Letters*, Vol. 70, pp. 3416-3419, 1993.

Pugh, J. D. and P. G. Saffman, "Two-Dimensional Superharmonic Stability of Finite-Amplitude Waves in Plane Poiseuille Flow," *Journal of Fluid Mechanics*, Vol. 194, pp. 295-307, 1988.

Reynolds, R. R., L. N. Virgin and E. H. Dowell, "High-Dimensional Chaos Can Lead to Weak Turbulence," *Nonlinear Dynamics*, Vol. 4(6), pp. 531-546, 1993.

Ripa, P., "Definite Integral of the Product of Hermite Functions, with Applications to the Theory of Nonlinear Interactions among Equatorial Waves," *J. of Geophysical Research*, Vol. 88, pp. 9741-9744, 1983.

Robinson, S. K., "Coherent Motions in the Turbulent Boundary Layer," *Annual Review of Fluid Mech.*, Vol. 23, pp. 601-639, 1991.

Roshko, A., "Structure of Turbulent Shear Flows: A New Look," *AIAA J.*, Vol. 14, pp. 1349-1357, 1976.

Ruelle, D. and Takens, F., "On the Nature of Turbulence," *Commun. Math. Phys.*, Vol. 20, pp. 167-192, 1971.

Schlichting, H., *Boundary-Layer Theory*, seventh edition, McGraw-Hill Inc., New York, 1979.

Sell, G. R., "An Optimality Condition for Approximate Inertial Manifolds," in G. R. Sell, C. Foias and R. Temam (Eds.), *Turbulence in Fluid Flows*, pp. 165-186, 1993.

She, Z. S., "Physical Model of Intermittency in Turbulence: Near-Dissipation-Range Non-Gaussian Statistics,", *Physical Review Letters*, Vol. 66, pp. 600-603, 1991.

Shen, J. and R. Temam, "Nonlinear Galerkin Method Using Chebyshev and Legendre Polynomials I. the One-Dimensional Case," *SIAM J. of Numerical Analysis*, Vol. 32, pp. 215-234, 1995.

Smagorinsky, J., "General Circulation Experiments with the Primitive Equations," *Mon. Weather Rev.*, Vol. 91, pp. 99-165, 1963.

Smith, G. F., "On Isotropic Functions of Symmetric Tensors, Skew-Symmetric Tensors and Vectors," *Int. J. Eng. Sci*, Vol. 9, pp. 899-916, 1971.

Snyder, M. A., *Chebyshev Methods in Numerical Approximation*, Prentice-Hall, Englewood Cliffs, N. J., 1966.

Speziale, C. G., "On Nonlinear *K-l* and *K-ε* Models of Turbulence," *Journal of Fluid Mechanics*, Vol. 178, pp. 459-475, 1987.

Speziale, C. G., "Turbulence Modelling: Present and Future. Comment 2," in J. L. Lumley (Ed.), *Whither Turbulence? Turbulence at the Crossroads*, pp. 490-512, Springer-Verlag, New York, 1990.

Speziale, C. G., "Analytical Methods for the Development of Reynolds-Stress Closures in Turbulence," *Annual Review of Fluid Mechanics*, Vol. 23, pp. 107-157, 1991.

Speziale, C. G., "Modeling of Turbulent Transport Equations," in T. B. Gatski, M. Y. Hussaini and J. L. Lumley (Eds.), *Simulation and Modeling of Turbulent Flows*, pp. 185-242, 1996.

Swinney, H. L. and J. P. Gollub (editors), *Hydrodynamic Instabilities and the Transition to Turbulence*, Springer-Verlag, New York, second edition, 1985.

Taylor, G. I., "Diffusion by continuous movements," *Proc. R. Soc.*, Vol. 20, pp. 196-211, 1921.

Temam, R., *Infinite Dimensional Dynamical Systems in Mechanics and Physics*, Springer, Berlin, 1988.

Temam, R., "Stability Analysis of the Nonlinear Galerkin Method," *Math. of Computation*, Vol. 57(146), pp. 477-505, 1991.

Temam, R., "New Emerging Methods in Numerical Analysis: Applications to Fluid Mechanics," in M. D. Gunzburger and R. A. Nicolaides (Eds.), *Incompressible Computational Fluid Dynamics: Trends and Advances*, pp. 409-426, Cambridge University Press, New York, 1993.

Temam, R. and S. Wang, "Inertial Forms of Navier-Stokes Equations on the Sphere," *J. of Functional Analysis*, Vol. 117, pp. 215-242, 1993.

Temam, R., *Navier-Stokes Equations and Nonlinear Functional Analysis*, SIAM, Philadelphia, 1995.

Temam, R., "Multilevel Methods for the Simulation of Turbulence," *J. of Comp. Physics*, Vol. 127, pp. 309-315, 1996.

Tennekes, H. and J. L. Lumley, *A First Course in Turbulence*, the MIT Press, Cambridge, 1972.

Titi, E. S., "Une Variété Approximante de l'Attracteur Universel des Equations de Navier-Stokes, Non Linéaire, de Dimension Finie," *C. R. Acad. Sci. Paris Sér. I*, Vol. 307, pp. 383-385, 1988.

Townsend, A. A., *The Structure of Turbulent Shear Flow*, Cambridge University Press, 1956.

von Karman, T. and L. Howarth, "On the Statistical Theory of Isotropic Turbulence," *Proc. Roy. Soc. London*, Vol. A164, pp. 192-215, 1938.

von Kerczek, C. H., "The Instability of Oscillatory Plane Poiseuille Flow," *Journal of Fluid Mechanics*, Vol. 116, pp. 91-114, 1982.

Weideman, J. A. C. and A. Cloot, "Spectral Methods and Mappings for Evolution Equations on the Infinite Line," *Comp. Meth. in App. Mech. And Eng.*, Vol. 80, pp. 467-481, 1990.

Weideman, J. A. C. and A. Cloot, "An Adaptive Algorithm for Spectral Computations on Unbounded Domains," *J. of Comp. Physics*, Vol. 102, pp. 398-406, 1992.

Yakhot, V. and S. A. Orszag, "Renormalization Group Analysis of Turbulence I. Basic Theory," *J. Sci. Comp.*, Vol 1, pp. 3-51, 1986.

Yorke, J. A. and E. D. Yorke, "Chaotic Behavior and Fluid Dynamics," in H. L. Swinney and J. P. Gollub (Eds.), *Hydrodynamic Instabilites and the Transition to Turbulence*, pp. 77-95, Springer-Verlag, New York, 1981.